D-Theory Formulation of Quantum Field Theories and Application to $CP(N-1)$ Models

Inauguraldissertation
der Philosophisch-naturwissenschaftlichen Fakultät
der Universität Bern

vorgelegt von

Stéphane Jean Riederer

von St. Gallen/SG

Leiter der Arbeit: Prof. Dr. Uwe-Jens Wiese
Institut für theoretische Physik
Universität Bern

D-Theory Formulation of Quantum Field Theories and Application to $CP(N-1)$ Models

Inauguraldissertation
der Philosophisch-naturwissenschaftlichen Fakultät
der Universität Bern

vorgelegt von

Stéphane Jean Riederer

von St. Gallen/SG

Leiter der Arbeit: Prof. Dr. Uwe-Jens Wiese
Institut für theoretische Physik
Universität Bern

Von der Philosophisch-naturwissenschaftlichen Fakultät angenommen.

Der Dekan:

Bern, den 1. Juni 2006 Prof. Dr. P. Messerli

Abstract

D-theory is an alternative non-perturbative approach to quantum field theory formulated in terms of discrete quantized variables instead of classical fields. Classical scalar fields are replaced by generalized quantum spins and classical gauge fields are replaced by quantum links. The classical fields of a d-dimensional quantum field theory reappear as low-energy effective degrees of freedom of the discrete variables, provided the $(d+1)$-dimensional D-theory is massless. When the extent of the extra Euclidean dimension becomes small in units of the correlation length, an ordinary d-dimensional quantum field theory emerges by dimensional reduction. The D-theory formulation of scalar field theories with various global symmetries and of gauge theories with various gauge groups is constructed explicitly and the mechanism of dimensional reduction is investigated. In particular, D-theory provides an alternative lattice regularization of the 2-d $CP(N-1)$ quantum field theory. In this formulation the continuous classical $CP(N-1)$ fields emerge from the dimensional reduction of discrete $SU(N)$ quantum spins. In analogy to Haldane's conjecture, ladders consisting of an even number of transversely coupled spin chains lead to a $CP(N-1)$ model with vacuum angle $\theta = 0$, while an odd number of chains yields $\theta = \pi$. In contrast to Wilson's formulation of lattice field theory, in D-theory no sign problem arises at $\theta = \pi$, and an efficient cluster algorithm is used to investigate the θ-vacuum effects. At $\theta = \pi$ there is a first order phase transition with spontaneous breaking of charge conjugation symmetry for $CP(N-1)$ models with $N > 2$. Despite several attempts, no efficient cluster algorithm has been constructed for $CP(N-1)$ models in the standard Wilson formulation of lattice field theory. In fact, there is a no-go theorem that prevents the construction of an efficient Wolff-type embedding algorithm. In this thesis, we construct an efficient cluster algorithm for ferromagnetic $SU(N)$-symmetric quantum spin systems, which provides a regularization for $CP(N-1)$ models at $\theta = 0$ in the framework of D-theory. We present detailed studies of the autocorrelations and find a dynamical critical exponent that is consistent with $z = 0$. Cluster rules for antiferromagnetic spin chains, which also provide a regularization for $CP(N-1)$ models at $\theta = 0$ and π, are investigated in detail as well.

Contents

Acknowledgments

First and foremost, I would like to thank Professor Uwe-Jens Wiese for giving me the opportunity of undertaking this research project under his supervision. He has always been a source of inspiration and I have largely benefited from his inexhaustible knowledge and support. His enthusiasm and kindness have been extremely precious throughout the last three years. I have often entered his office with a doubtful mind and always got out with a clearer vision. Most of what is included in this thesis would not have been possible without the help of Michele Pepe, who proved very patient and interested in what I was doing. I would like to thank him warmly. The over-sea collaboration with Bernard B. Beard has also been fruitful. I especially thank him for letting me using his "continuous time" computer codes. I also benefited from discussions with Ferenc Niedermayer, Peter Hasenfratz, Peter Minkowski, Richard Brower and Markus Moser. I would like to thank also the sysadmins for the great job they are doing and more largely all members of the institute. Special thanks to Ottilia Hänni for helping me to find my way out of all kind of administrative questions. Thanks to Pascal, Laurent, and Adrian for entertaining me with endless sport or social debates over lunch time. Of course, nothing would have been possible without my parents France and Jürg, who have always supported me through all these years. Sincere thanks as well to the rest of my family and friends for simply being around. Last, but certainly not least, I have no idea what I would become without the sweetest one. Thanks for all Odile.

Chapter 1

Introduction

At a fundamental level, nature is governed by four different interactions. Gravity and electromagnetism which have long range effects and two nuclear forces which act only at short distances. The weak force is implied in all disintegration processes while the strong interaction is responsible for the cohesion of matter. The most successful theories to describe natural phenomena are nowadays general relativity and the standard model of particle physics. They have both been tested intensively and none of them has been ruled out at the moment. However, they are not compatible since a theory of quantum gravity has not yet been formulated. Hence, gravity cannot be included naturally in the standard model of particle physics, which describes all what we know about the three other fundamental forces. The standard model has been investigated in great detail up to energies of about 100 GeV. In particle accelerators, it has so far passed all the tests very well. However, it is almost certain that this model must be replaced at some higher energy scale, where "new physics" may appear. Supersymmetric models, string theories, or grand unification scenarios are among many propositions for describing the ultra-high energy phenomena where unification of forces ultimately occurs. Hopefully, the new LHC experiments at CERN will provide new insights into the next deeper layer of fundamental physics.

The standard model of particle physics is an effective quantum field theory, which is invariant under Lorentz transformations and has an internal gauge symmetry with the corresponding non-abelian gauge group $SU(3)_C \otimes SU(2)_L \otimes U(1)_Y$. One can separate the model into two parts, the electroweak and the strong sectors. In the late 60's, Glashow, Salam, and Weinberg proposed a way to describe electromagnetism and the weak interaction in a common framework. The so-called electroweak theory is a chiral $SU(2)_L \otimes U(1)_Y$ symmetric gauge theory and exists in a Higgs-phase, in which the gauge symmetry breaks down spontaneously to the subgroup $U(1)_{em}$ of electromagnetism. As a result, one obtains massive gauge bosons (the W- and Z-particles), while the photon remains massless. One cannot strictly speak about unification since two coupling constants still describe the interaction strengths, nevertheless it is a weakly coupled theory where a perturbative approach is well adapted. Therefore, one has been able to make very precise theoretical predictions, which agree with experiments to a great precision. The last piece of the puzzle (the Higgs

particle) is hoped to be found with the next generations of particle accelerators — the large hadron collider (LHC) at CERN.

The strong sector of the standard model describes the interactions between quarks via gluons exchange. The fundamental theory believed to describe such interactions is quantum chromodynamics (QCD), a relativistic quantum field theory with a non-Abelian gauge symmetry $SU(3)_C$, where the interacting particles carry a color charge. At high energy, due to asymptotic freedom, the quarks and gluons behave almost like free particles and form a plasma. The coupling constant is then small and a perturbative approach is therefore adapted. On the other hand, at low energy the theory exists in a confined phase; the gauge bosons do not appear in the spectrum. QCD is hence strongly coupled and a perturbative expansion in term of the coupling constant is senseless. Therefore, at low energies, a number of essential questions such as the structure of hadrons, spontaneous chiral symmetry breaking, the non-trivial topology of the vacuum, or the mechanism of confinement (the reason why we never see free quarks), are not accessible to perturbative approaches. In fact, one needs to attack these problems with non-perturbative techniques, the most commonly used nowadays being lattice gauge theory. Let us now briefly review the standard non-perturbative approach to QCD, before turning to an introduction of the alternative D-theory formulation of quantum field theories, which will be presented in detail in this thesis.

1.1 Wilson's Approach to Quantum Field Theory

The standard approach to quantum field theory is to define an action whose degrees of freedom are the field variables. One quantizes the theory by exponentiating the action and obtains a partition function which represents a functional integral over the field configurations. Such generating functional is used to compute observables of the quantum theory. This formal integral is a divergent expression. The theory therefore needs to be regularized and renormalized in order to absorb the infinities. In the perturbative approach, one deals with ultra-violet divergences at any order of the perturbative expansion. In 1974, K. Wilson proposed to define quantum field theory on a space-time lattice [1]. He used the lattice spacing a as a cut-off in the regularization procedure. The theory is thus finite and completely well-defined, because no infinities are present in the reguralized theory. One important technical ingredient in this formulation is the Wick-rotation of the time variable to imaginary values (Euclidean time). This is a well-justified procedure since physical observables in Minkowski or Euclidean space-time can be easily related. As a consequence, Euclidean quantum field theory regularized on a lattice offers a clear equivalence with statistical mechanics. This opens wide new perspectives, since it becomes possible to study quantum field theory with techniques developed in condensed matter physics such as Monte Carlo simulations (for the numerical evaluation of the partition function). Eventually, in order to recover the continuum physics, the lattice spacing a must be sent to zero. The Lorentz-invariance is then restored without fine-tuning of the coupling constant. For

example, in lattice QCD, one reaches the continuum limit by sending the coupling constant g to zero, thus approaching a second order phase transition of the corresponding statistical system with a diverging factor ξ/a, where ξ is the correlation length. In condensed matter problems, the lattice spacing is kept fixed and the correlation length diverges. Here, one reaches a vanishing lattice spacing $a \to 0$, while keeping ξ fixed. Since $\xi = 1/m$, one can hence obtain particles with finite mass. Near their critical points, statistical systems have the remarkable property of universality. Indeed the long range physics of such extreme systems does not depend on the underlying microscopic details. The systems hence fall in a small number of universality classes, distinguished by the symmetries and the number of space dimensions. The members of a class show identical critical exponents. This is of central importance in lattice field theory. The lattice spacing a becomes negligible when the correlation function is large. According to the scaling hypothesis the correlation length is the only relevant length scale near criticality.

Not entering in any details, let us briefly sketch how one can define field theories non-pertubatively from first principles. First, the continuous scalar fields are replaced by lattice fields, which are restricted to the points x of the Euclidean lattice. In the continuum, the gauge fields are given in terms of vector potential (i.e. parallel transporters along infinitesimal distances). Due to the discrete nature of the lattice, the parallel transporters are now associated with the links connected neighboring lattice points. The introduction of fermions implies non-trivial problems and needs special care. The most straightforward way to define fermion fields on a lattice is to replace the continuum Grassmann fields by Grassmann variables that live on the lattice points x. These variables define the so-called Grassmann algebra, which is characterized by anticommutation relations. Considering the naive lattice version of the Dirac action for free fermions and the corresponding fermion propagator, one observes extra states in the spectrum which remain when one takes the continuum limit. This naive lattice regularization does not lead to the correct continuum theory. The single derivative in the action is at the origin of the problem. Modes appear in the fermion propagator at each corner of the Brillouin zone, with the same dispersion relation. This problem is known as fermion doubling and leads to a multiplication of fermion species. The problem is severe since Nielsen and Ninomiya [2] have proven that all chiral invariant free fermion lattice actions, which are local, hermitean and translation invariant imply non-physical copies of fermions. In four dimensions, the naive free fermion lattice action hence describes 16 free fermions in the continuum limit. It is possible to reduce that number to 4 by assigning to each lattice site only a single fermion field component. The remaining species can be interpreted as physical flavors in the continuum. Indeed, the so-called staggered fermions [3] represent 4 flavors of 4 mass-degenerate fermions. It's a good framework to study chiral symmetry breaking for 4 fermion flavors.

To cure the fermion doubling problem, Wilson has proposed to introduce extra terms in the action which decouple the unwanted modes by giving them a mass at the order of the cut-off. These terms vanish in the continuum limit but have the inconvenience to break explicitly the chiral symmetry [4]. Implementing chiral symmetry on a lattice is a

non-trivial task and was for a long time an unsolved problem. In the early 90's, Kaplan realized that it is possible to localize fermionic zero-modes on a four-dimensional domain-wall embedded in a five-dimensional world [5]. This is of central importance for this thesis since an extra dimension naturally arises in the D-theory formulation of quantum field theory described below. In Kaplan's formulation, the doubling problem disappears and the Wilson terms in five dimension do not break the chiral invariance of the 4-d domain wall fermions. At the same time, Narayanan and Neuberger developed another approach which solves the problem by considering an infinite number of flavors [6]. The so-called overlap fermions are closely related to domain-wall fermions since the flavor-space can be considered as an extra dimension. These formulations satisfy the so-called Ginsparg-Wilson relation [7] which guarantees that the lattice action has good chiral properties. In order to do so, the Dirac operator in the action has to anticommute with the generators of the chiral symmetry up to a factor proportional to the lattice spacing. Another approach has been developed by Hasenfratz and Niedermayer, who have constructed a class of actions completely free of cut-off effect. They observed that the fixed points of non-perturbative renormalization group blocking transformations on a lattice correspond to so-called perfect actions [8]. Classical perfect actions for QCD can be approximated in order to satisfy the Ginsparg-Wilson relation with a high accuracy. However, one needs a lot of fine-tuning of the action in order to obtain massless perfect fermions. This poses great challenges in the practical implementation of this formulation.

Recently, Lüscher has finally been able to construct the full standard model beyond perturbation theory [9, 10]. This was a major breakthrough since besides the global chiral symmetry of QCD, the local chiral invariance of the electroweak sector rests now on a solid non-perturbative ground. Of course, it will take many more years before any accurate numerical simulation of the full theory can be performed, but nevertheless the standard model is now defined beyond perturbation theory and that is already a great achievement. In the case of QCD only, the situation is much simpler but still highly non-trivial. The domain wall, overlap, or perfect fermions are dynamically very difficult to treat. They demand a huge amount of computer power. Wilson or staggered fermions are a lot easier to simulate. In order to deal with fermions in the path integral, one has to integrate them out. This results in a non-local action with a large quark matrix which has to be inverted. Computing the determinant of such matrices is computationally very demanding, especially when one wants to simulate small quark masses. In the quenched approximation, one simply puts the determinant of the quark matrix to one, and the simulations can be performed efficiently. However, this is an unphysical situation where the virtual quark loops effects are ignored. Nevertheless, some phenomenological facts in the low energy hadron physics suggest that these loops may have small effects. In the partially quenched approximation, it is possible to include such effects by allowing the quark in the loops to be heavier. These two approximations are mostly used to compute physical quantities for light quarks.

As emphasized earlier, the great advantage of the lattice formulation is the analogy with statistical mechanics where powerful numerical techniques were developed. The Monte

Carlo methods are among them and offer a natural environment to answer the most interesting questions in lattice QCD, which are most of the time not accessible analytically. The idea is to evaluate the partition function numerically. However the path integral is an extremely high dimensional integral, therefore a direct evaluation is hopeless. The solution is to treat the problem statistically. In the partition function, the Boltzmann factor $\exp(-\beta S[s,u,\psi])$ is interpreted as the probability to generate the corresponding field configuration. Here, β is the inverse temperature and $S[s,u,\psi]$ is the lattice action with s,u and ψ the scalar, link, and Grassmann lattice field variables. In a Monte Carlo simulation, the field configurations which give the largest contributions to the path integral are dominant. In order to obtain a new configuration from an initial one, we use an iterative algorithm and thus generate a sequence of configurations, a so-called Markow chain. For example the Metropolis algorithm [11] is a local algorithm which performs local changes in the configuration. After each Monte Carlo step, the new Boltzmann weight is evaluated and the new configuration can be accepted or rejected according to its probability. Usually, local changes of the degrees of freedom imply small fluctuations in the action. Therefore, the step can be accepted and one gets a new field configuration. Due to these small changes in the successive sweeps, we need a large number of iterations in order to get a new statistically independent configuration. The number of sweeps can be determined by considering the autocorrelation time τ, which is obtained from the exponential fall-off of the autocorrelation function.

In lattice field theory, the continuum limit is reached by adjusting the coupling constant to a value at which the theory approaches a second order phase transition where the correlation length ξ diverges. Near such a transition, the autocorrelation time depends on ξ as $\tau \approx a\xi^z$, where z is the dynamical critical exponent. We then face large fluctuations in the physical system and the algorithm has to generate large-scale effects. Being local, the Metropolis algorithm is not efficient in that limit and have a critical exponent $z \approx 2$, which means an increasing number of iterations to get a statistically independent configuration when one approaches the continuum limit. This phenomenon is known as critical slowing down and reflects an impossibility to simulate critical systems. A class of algorithms, for example the Swendsen-Wang cluster algorithm [12], are able to suppress almost completely the critical slowing down in a number of field theory models. These algorithms work with global updates of the system and will be described in more details later in this thesis. However, those techniques are, at the moment, not applicable to gauge theories and critical slowing down occurs in all attempts to simulate QCD on a lattice. Another problem is, of course, the finite nature of the lattice. This implies finite volume effects. Nowadays, the related problems are well-known and can be controlled completely with finite size scaling techniques which allow correspondences with the infinite volume values. Nevertheless, one will have to deal with a simulation cost proportional to $(L/a)^4$. Therefore, one still has to work with sufficiently large lattices to get rid of the finite volume effects, and with sufficiently small lattice spacing a in order to be close to the continuum limit. Together with the critical slowing down, the total simulation cost is hence proportional to L^4/a^{4+z}.

As sketched above, simulation of fermions is a hard problem due to the evaluation of the Dirac operator on the lattice. Moreover, independent from the continuum limit, critical slowing down appears as well for small pion mass — in the chiral limit. At present, most of the simulations use the quenched approximation but algorithmic improvements are required to fully simulate QCD on a lattice, steps in this direction have already been performed [13, 14]. For good textbooks and reviews on lattice field theory and chiral symmetry on a lattice, one can refer to [15, 16, 17, 18, 19].

1.2 The D-theory Approach

In this thesis, we will attack quantization of field theory from a completely different point of view. Indeed, the D-theory formulation is an alternative regularization for quantum field theory which offers a wide new framework for non-perturbative studies. D-theory is formulated in terms of discrete quantum variables which undergo dimensional reduction. D-theory was originally developed in the mid 90's as a discrete approach to $U(1)$ and $SU(2)$ gauge theory [20]. This work was developed independently of earlier studies by Horn [21] and later by Orland and Rohrlich [22], in which was discussed the gauge theory of discrete quantum variables — the so-called quantum links. It was also inspired from quantum statistical mechanics where fundamental degrees of freedom are described by quantum variables acting in a Hilbert space. D-theory was extended to $SU(N)$ gauge theories and full QCD in [23, 24] as well as to a variety of other models in [25, 26, 27, 28].

As emphasized before, a quantum field theory (QFT) is quantized by performing a path integral over configurations of classical fields. However, there is another form of quantization which is well known from quantum mechanics: a classical angular momentum can be replaced by a vector of Pauli matrices. This is a well-known procedure [29]. The angular momentum represents a continuous degree of freedom, while the resulting quantum spin is described by a discrete variable $\pm 1/2$. In our alternative formulation, the same kind of quantization will be applied to field theories. It is, of course, far from obvious that such a procedure is equivalent to the usual one in QFT. Indeed, how can the full Hilbert space of a quantum field theory be recovered when one replaces the classical variables in the partition function by discrete variables? For example, the spin 1/2 has the same symmetry properties as a classical angular momentum, but it operates in a finite Hilbert space. In fact, this requires a specific dynamics that will be described below. Remarkably the D-theory formulation can be constructed for a wide variety of models such as scalar field theories or gauge theories.

In D-theory, the classical fields of d-dimensional quantum field theories reappear as the low-energy collective dynamics of discrete quantum variables of a $(d+1)$-dimensional quantum model. The extra dimension is needed in order to collect a large number of discrete variables. Dimensional reduction occurs when the $(d+1)$-dimensional theory is in a massless phase. Hence, the low-energy dynamics can be described by an effective action in

$(d+1)$ dimensions. Once the finite extent of the extra dimension becomes small in units of the correlation length, which occurs in all asymptotically free theories, the system undergoes dimensional reduction and the target d-dimensional field theory emerges. In this way, the quantum formulation in one more dimension offers another type of regularization for QFT. This means that the D-theory models describe the same physics as the corresponding ones in the standard Wilson formulation of lattice field theory.

In D-theory, the scalar field analogs are quantum spins. They act as operators in a finite Hilbert space. In lattice gauge theories, the gauge fields are represented by link variables, whose elements take values in $\mathbb{C}$. Their analogs in D-theory are quantum links, whose elements are non-commuting operators acting in a Hilbert space. Quantum link QCD is quite different from the standard Wilson's formulation. In the partition function, the classical action is replaced by a Hamilton operator. In standard lattice QCD, the Hilbert space contains all $SU(3)$ representation on a link. The corresponding Hilbert space of an $SU(N)$ quantum link model consists of a single representation of $SU(2N)$. This can be achieved by considering the theory in $(4+1)$ dimensions. Of course, the D-theory formulation of QCD must also include the fermionic degrees of freedom. As emphasized earlier, Kaplan has proposed to represent 4-dimensional chiral fermions by working with a domain-wall in a 5-dimensional world [5]. Although our motivations to include a fifth dimension are different, it is also natural to use this extra dimension in order to protect the chiral symmetry of fermions. Since we actually work with a finite extent in the extra dimension, it is better to use Shamir's variant [30] of Kaplan's proposal which works in a 5-dimensional slab. Remarkably, the correlation length of these fermions is exponentially large in the depth of the slab, which is required in order to survive the dimensional reduction in D-theory. More details about fermions in this framework will be presented below.

D-theory has several interesting features that go beyond the usual Wilson's formulation of lattice field theory. First, since we are using discrete variables, the theory can be completely fermionized. Indeed, all bosonic fields can be written as pairs of fermionic constituents. We call them "*Rishons*", which means "first" in Hebrew and has been used as a name for fermionic constituents of gauge bosons [31]. Using the rishon representation, the quantum link Hamiltonian can be expressed in terms of color-neutral operators. Indeed, the two indices of a bosonic matrix field (for example the two color indices of a gluon field matrix) can be separated because they are carried by two different rishons. This offers new ways to attack the large N limit of QCD and other models [32]. Another great advantage is on the computational side. Discrete variables are indeed well suited for numerical simulations. For example, using efficient cluster algorithms, it has been possible to simulate the D-theory version of the 2-d $O(3)$ model at non-zero chemical potential [28]. This is impossible in the standard formulation due to the severe complex action problem. That type of problem are generally NP-hard to solve [33] and for the same reasons, simulating QCD at non-zero quark density is still not possible. In the context of the 2-d $O(3)$ model, which is a toy model for QCD, the sign problem is solved completely with a meron-cluster algorithm [34]. In this thesis, we will present another achievement of the D-theory formu-

lation. Using our alternative formalism and an efficient cluster algorithm, we have been able to simulate $CP(N-1)$ models directly at non-trivial θ-vacuum angle [26]. This allows us to conclude about the model phase structure for different value of N, which remains impossible with the traditional Wilson approach due once again to a complex action problem.

This thesis is organized as follow. In the next chapter, we first introduce the D-theory formulation with a simple model. Then we turn to a full description of various other models both with global or local symmetries. This detailed presentation is based on the publication [25]. In the third chapter, we give some details on classical $CP(N-1)$ models described in the continuum. There are interesting quantum field theories with non-trivial topological properties. In chapter four, we investigate $CP(N-1)$ models in the D-theory context. This allows us to conclude about non-perturbative problems which were previously inaccessible in the framework of Wilson's lattice field theory. In particular, we have been able to simulate the model directly at non-zero vacuum angle which is normally almost impossible due to a complex term in the classical action. In our alternative picture such problems do not occur. It is therefore possible to conclude about the phase structure of the model. This chapter is based on the work published in [26]. Finally, in chapter five, we turn to the details concerning the numerical simulations. We present the cluster algorithm that we have used and investigate its efficiency close to the continuum limit. We will see that the critical slowing down is almost completely suppressed. The main results regarding the part on algorithms have been published in [35]. Finally, the last chapter contains the conclusions and outlooks.

Chapter 2

D-Theory Formulation of Quantum Field Theory

Usually, one quantizes field theories by performing a path integral over classical fields configurations. The obtained partition function is used as a generating functional for the evaluation of physical observables. This approach is used both in perturbation theory and in Wilson's non-perturbative lattice field theory. In this work, we propose an alternative non-perturbative approach to quantum field theory. The classical fields of the action emerge from the low-energy collective dynamics of discrete quantum variables which undergo dimensional reduction. *Dimensional* reduction of *discrete* variables is a generic phenomenon that occurs in a number of models. This leads to an alternative non-perturbative formulation of quantum field theory which we called *D-theory* [20, 23, 24, 36]. In this chapter, we will construct explicitly the D-theory formulation of different spin models with various global symmetries — $O(N)$ models as well as $U(N)$, $SU(N)$, $SO(N)$ or $Sp(N)$ chiral models. The case of the $CP(N-1)$ model will be treated separately in chapter four. The D-theory constructions for gauge theories with various gauge groups will be presented within this new framework too, thus leading to the full QCD formulation where fermionic degrees of freedom can be naturally added. The dynamics of our D-theory models, in particular the mechanism of dimensional reduction, will be investigated in detail as well. This alternative non-perturbative approach to quantum field theory will eventually allow us to attack unsolved problems with powerful cluster algorithms.

We here focus on the algebraic structure of D-theory. The chapter is organized as follows. In the next section, one presents the original idea of D-theory in the context of the non-linear $O(3)$ model in various dimensions. Section 2.2 contains the construction of the basic blocks that can be used in a number of D-theory models. In particular, we show how real and complex vector and matrix fields can be build in the D-theory context. For example, the discrete analog of a real scalar field which is $O(N)$ symmetric is a generalized quantum spin in the algebra of $SO(N+1)$. On the other hand, the $U(N)$ symmetric complex vector is represented by an $SU(N+1)$ quantum spin. Similarly, a complex $SU(N)$ or real $SO(N)$ matrix, as well as a $Sp(N)$ tensor, are represented in D-theory by

quantum link variables which are naturally embedded into the algebras $SU(2N)$, $SO(2N)$, and $Sp(2N)$, respectively. Symmetric and anti-symmetric tensors are also constructed. In section 2.3 and 2.4, we use these basic building blocks to define quantum spin models. Namely, the D-theory regularizations of the $O(N)$ model and principal chiral models. Their dynamics, in particular the mechanism of dimensional reduction and formulas for the finite correlation length in the dimensionally reduced theory, are also investigated. The generalization of the D-theory construction to gauge theories with various gauge groups is presented in sections 2.5 and 2.6. The dimensional reduction scenario, which is rather different from the one for quantum spin systems, is also described. Eventually, in section 2.7, we carry on with the natural inclusion of fermions using Shamir's version of Kaplan's domain wall fermions. This yields a full D-theory construction of QCD. Some remarks and outlooks then conclude this chapter.

2.1 The $O(3)$ Model from D-theory

2.1.1 The 2-dimensional $O(3)$ model

Let us illustrate the D-theory idea with the most simple example, the 2-dimensional $O(3)$ non-linear σ model, which can be viewed as Euclidean field theory in $(1+1)$ dimensions. This model shares a number of features with QCD such as asymptotic freedom, a non-perturbatively generated mass-gap, instantons, and a θ-vacuum structure. It is therefore a very interesting toy model for quantum chromodynamics. The continuum classical action has the form

$$S[\vec{s}] = \frac{1}{2}\int d^2x\ \partial_\mu \vec{s}\cdot\partial_\mu \vec{s}, \tag{2.1}$$

where $\vec{s}(x)$ is a 3-component unit vector. This action is invariant under $O(3)$ transformation $\vec{s}\,' = O\vec{s}$, where $O^T O = \mathbb{1}$. The theory is non-linear because the fields obey the constraint

$$\vec{s}(x)\cdot\vec{s}(x) = \sum_{i=1}^{3} s^i(x)^2 = 1, \tag{2.2}$$

which prevents the system from being a free field theory. The classical theory is quantized by considering the path integral

$$Z = \int \mathcal{D}\vec{s}\ \exp\left(-\frac{1}{g^2}S[\vec{s}]\right), \tag{2.3}$$

where $\mathcal{D}\vec{s}$ denotes the integration over all field configurations and g^2 is the dimensionless coupling constant. The above formal integral is a divergent expression. In order to regularize and renormalize the theory, let us first follow Wilson's formulation of lattice field theory and introduce a lattice as an ultraviolet cut-off. The partial derivatives are then replaced by finite differences and, neglecting an irrelevant constant, the lattice action is given by

$$S[\vec{s}] = -\sum_{x,\mu} \vec{s}_x\cdot\vec{s}_{x+\hat{\mu}}, \tag{2.4}$$

where the classical 3-component unit vector $\vec{s}_x$ is located on the sites x of a quadratic lattice of spacing a . Here $\hat{\mu}$ represents the unit vector in the μ-direction. One quantizes the theory by considering the classical partition function

$$Z = \prod_x \int_{S^2} d\vec{s}_x \exp\left(-\frac{1}{g^2} S[\vec{s}]\right). \tag{2.5}$$

The integration extends over the sphere S^2, i.e. over all possible orientations $\vec{s}_x$, independently for all lattice points x. In order to extract physical information from this theory, one needs to compute the n-point Green function. For example, the 2-point function

$$\langle \vec{s}_x \cdot \vec{s}_y \rangle = \frac{1}{Z} \prod_z \int d\vec{s}_z \ \vec{s}_x \cdot \vec{s}_y \exp\left(-\frac{1}{g^2} S[\vec{s}]\right) \tag{2.6}$$

decays exponentially at large distance $|x-y|$ of the two lattice points x and y,

$$\langle \vec{s}_x \cdot \vec{s}_y \rangle \sim \exp\left(-\frac{|x-y|}{\xi}\right), \tag{2.7}$$

where $\xi = 1/m$ is the correlation length. The inverse correlation length defines the mass-gap m of the theory, it corresponds to the energy of the first excited state above the vacuum — the mass of the lightest particle in the theory. Due to asymptotic freedom, the continuum limit of the lattice-regularized theory is taken by sending the bare coupling constant $g \to 0$. In this limit, the correlation length diverges exponentially as $\xi \propto \exp(2\pi/g^2)$, where the short distance lattice artifacts disappear. The strength of the exponential increase is given by the 1-loop β-function coefficient $1/2\pi$ of the model.

2.1.2 The 2-dimensional quantum Heisenberg model

Quantization in D-theory is radically different, one does not quantize by integrating over the classical field configuration $[\vec{s}]$. Instead, the classical vectors $\vec{s}_x$ are replaced by quantum spin operators $\vec{S}_x$. These quantum variables are the $SO(3)$ group generators, which obey the usual commutation relations

$$[S_x^i, S_y^j] = i\delta_{xy}\epsilon_{ijk} S_x^k. \tag{2.8}$$

For example, $\vec{S}_x$ may denote a vector of Pauli matrices for a spin 1/2, but actually the generators can be in any representations of $SO(3)$. The classical action of the 2-dimensional $O(3)$ model is thus replaced by the quantum Hamilton operator

$$H = J \sum_{x,\mu} \vec{S}_x \cdot \vec{S}_{x+\hat{\mu}}, \tag{2.9}$$

which is in fact the Hamiltonian of a quantum Heisenberg model in two dimensions where J is the coupling constant. The case $J < 0$ corresponds to ferromagnetic and $J > 0$ to

antiferromagnetic couplings. Like in the classical case, the quantum operator H is invariant under global $SO(3)$ transformations. In a quantum theory, this naturally follows from the relation $[H, \vec{S}] = 0$, where

$$\vec{S} = \sum_x \vec{S}_x \tag{2.10}$$

is the total spin. The quantum partition function for the Heisenberg model is given by

$$Z = \mathrm{Tr} \exp(-\beta H), \tag{2.11}$$

where the trace is taken over the full Hilbert space, which is the direct product of Hilbert spaces of individual quantum spins. In a condensed matter interpretation, β is the inverse temperature of the quantum system and can be viewed as an extent of dimension. For a 2-dimensional quantum spin system, this extra dimension would be Euclidean time. However, in D-theory the Euclidean time is already part of the 2-dimensional lattice. Indeed, as we will see, the additional Euclidean dimension will ultimately disappear via dimensional reduction.

2.1.3 D-theory regularization and dimensional reduction

At this point, we have replaced the 2-d $O(3)$ model, formulated in terms of classical fields, by a 2-dimensional system of quantum spins with the same symmetry and an extent β in a third dimension. Let us now consider a 2-dimensional antiferromagnetic Heisenberg model, i.e. with $J > 0$. In the case of spin 1/2, this model has very interesting properties. It describes the undoped precursor insulators of high-temperature superconductors, for example materials like La_2CuO_4, whose ground states are Néel ordered with a spontaneously generated staggered magnetization. There is indeed overwhelming numerical evidence that the ground state of the 2-dimensional antiferromagnetic spin 1/2 quantum Heisenberg model exhibits long-range order [37, 38, 39]. The same is true for higher spins, and the following discussion applies equally well for higher representations of the $SO(3)$ generators. Nevertheless, the smallest spin 1/2 is in practice the most interesting case, since it allows us to represent the physics of the 2-d $O(3)$ model in the smallest possible Hilbert space.

Formulating this 2-dimensional quantum model as a path integral in Euclidean time results in a 3-d $SO(3)$-symmetric classical model. At zero temperature of the quantum system, we are in the infinite-volume limit of the corresponding 3-dimensional classical model (infinite extent β). The Néel order of the ground state at that temperature implies that the staggered magnetization vector points in a particular direction, thus breaking the $SO(3)$ spin rotational symmetry spontaneously. In other words, this means that the corresponding 3-dimensional classical model is in a broken phase, in which only an $SO(2)$ symmetry remains intact (the rotations around the staggered magnetization direction). As a consequence of the Goldstone theorem [40], a number of Goldstone bosons arises when a global continuous symmetry is spontaneously broken. Here, the $SO(3)$ symmetry is broken

down to $SO(2)$, the full symmetry group has three generators, while the subgroup has only one. Therefore, according to the theorem, there must be $3 - 1 = 2$ massless Goldstone bosons, which are called magnons or spin-waves.

All systems of Goldstone bosons are weakly coupled at low-energy. Hence, one can use a perturbative approach to describe their dynamics. In the context of QCD, Gasser and Leutwyler have developed a perturbative approach to study the low-energy dynamics of pions, which are Goldstone bosons resulting from spontaneous chiral symmetry breaking. The so-called chiral perturbation theory [41, 42] has been designed for QCD, but is universally applicable to any system of Goldstone bosons. In particular, it has been used to investigate the magnon dynamics at low-energies [43]. Indeed, when a global symmetry G is spontaneously broken to a subgroup H, the resulting Goldstone bosons are described by a field in the coset space G/H. The dimension of this space is equal to the number of Goldstone bosons — the difference between the number of generators of G and H. In our case, the coset space is $SO(3)/SO(2) \equiv S^2$, which is simply the 2-dimensional sphere. Consequently, the magnons are described by 3-component unit-vectors $\vec{s}(x)$ — the same fields that appear in the original classical 2-d $O(3)$ model. According to chiral perturbation theory, the low-energy effective Lagrangian must be invariant under the full symmetry group $G = SO(3)$, and the lowest order terms in the effective Lagrangian contain the smallest possible number of derivatives. These terms are sufficient to describe the low-energy physics, while for studies at higher energies one can add terms with more derivatives. To summarize, due to spontaneous symmetry breaking, the collective excitations of many discrete quantum spin variables form an effective classical field $\vec{s}(x)$. This is one of the main dynamical ingredients of D-theory. To lowest order in chiral perturbation theory, the effective action of the magnons take the form

$$S[\vec{s}] = \int_0^\beta dx_3 \int d^2x \; \frac{\rho_s}{2} \left(\partial_\mu \vec{s} \cdot \partial_\mu \vec{s} + \frac{1}{c^2} \partial_3 \vec{s} \cdot \partial_3 \vec{s} \right). \tag{2.12}$$

Where c and ρ_s are the spin-wave velocity and the spin stiffness, ρ_s plays here the same role as F_π in the chiral perturbation theory approach to QCD. Note that μ extends over the physical space-time indices 1 and 2 only. The 2-dimensional quantum system at finite temperature thus corresponds to a 3-dimensional classical model with finite extent β in the third dimension.

Another key ingredient is dimensional reduction, to which we now turn. For massless magnons, which imply the presence of an infinite correlation length ξ, the non-zero temperature system appears dimensionally reduced to two dimensions because the finite extent β in the extra dimension is negligible compared to the infinite correlation length. However, in two dimensions, the Hohenberg-Mermin-Wagner-Coleman theorem prevents the existence of interacting massless Goldstone bosons [44, 45]. Indeed, it is well known that the 2-d $O(3)$ model has a non-perturbatively generated mass-gap. Naturally, one can ask if the finite correlation length at finite temperatures still gives rise to dimensional reduction. One will see that this is still the case, but in contrast to naive expectations,

dimensional reduction occurs in the zero temperature limit — i.e. when the extent β of the extra dimension becomes large.

Hasenfratz and Niedermayer used a block spin renormalization group transformation to map the 3-d continuum $O(3)$ model with finite extent β to a 2-d lattice $O(3)$ model [46]. The 3-dimensional field is averaged over volumes of size β in the third direction and βc in the two space-time directions. This is illustrated in figure 2.1. Due to the large correlation length, the field is essentially constant over these blocks. The average field lives at the block centers, which form a 2-dimensional lattice with lattice spacing $a' = \beta c$ — which is different from the lattice spacing a of the underlying quantum antiferromagnet. The effective action of the averaged field defines a 2-d lattice $O(3)$ model formulated in the standard Wilson framework. The dimensionless bare coupling constant g of this lattice model is the coupling at the scale $a' = \beta c$. Using chiral perturbation theory, Hasenfratz and Niedermayer were able to express this coupling constant in terms of the parameters of the original Heisenberg model. This can be done by computing a physical quantity in both models and then adjust the coefficients until the two values match. In order to do so, they chose to add a chemical potential in both models and then compute the free energy density. They finally expressed the coupling constant as

$$1/g^2 = \beta\rho_s - \frac{3}{16\pi^2\beta\rho_s} + \mathcal{O}(1/\beta^2\rho_s^2). \tag{2.13}$$

In an earlier work, Chakravarty, Halperin, and Nelson were using the 2-loop β-function of the 2-d $O(3)$ model in order to express the correlation length as [47]

$$\xi \propto \frac{c}{\rho_s}\exp(2\pi\beta\rho_s). \tag{2.14}$$

Hasenfratz and Niedermayer then extended this result to a more complete relation. Using the 3-loop β-function and the exact result for the mass-gap of the theory [48, 49], they found

$$\xi = \frac{1}{m} = \frac{e}{8\Lambda_{\overline{MS}}}. \tag{2.15}$$

Here, e is the base of the natural logarithm. This last relation is a remarkable result. If one would find the same type of relation in QCD, one would understand the mass of the proton. Unfortunately, the situation is a lot more complicated in 4-dimensional quantum field theories and an analytic approach seems rather unlikely. The mass-gap of a field theory is a non-perturbatively generated scale that arises quantum mechanically. The classical action (2.1) is scale invariant — it does not contain any dimensionful parameters. This scale invariance is anomalous, it is explicitly broken when a cut-off is introduced in the theory. This can be seen as well in perturbation theory via dimensional transmutation. Hasenfratz, Maggiore, and Niedermayer have used dimensional regularization in the $\overline{MS}$ scheme where the energy scale is $\Lambda_{\overline{MS}}$. With the 3-loop β-function calculation, one obtains

$$\beta c\Lambda_{\overline{MS}} = \frac{2\pi}{g^2}\exp(-2\pi/g^2)\left[1 - \frac{g^2}{8\pi} + \mathcal{O}(g^4)\right]. \tag{2.16}$$

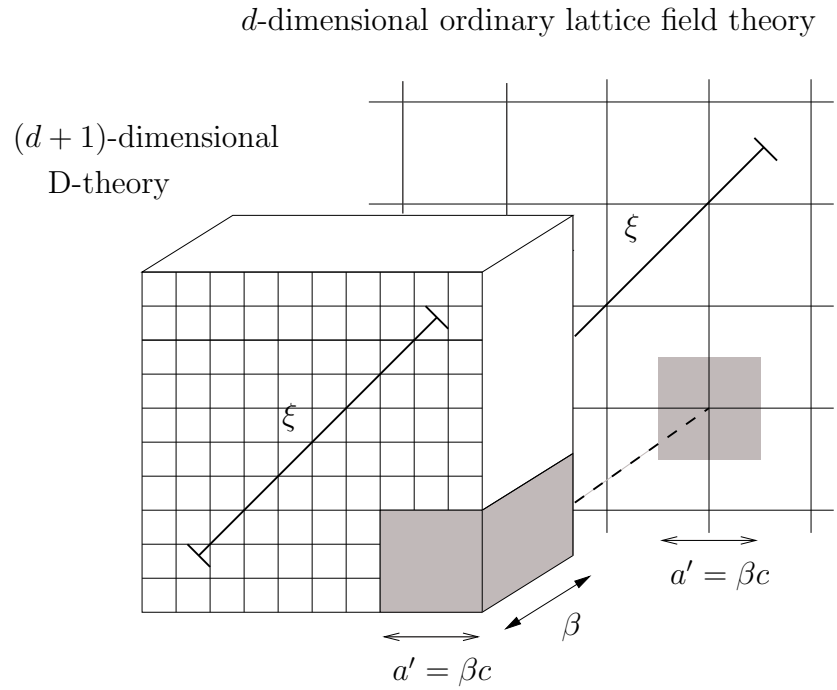

Figure 2.1: *Dimensional reduction of a D-theory model: Averaging the (d+1)-dimensional effective field of the D-theory over blocks of size β in the extra dimension and βc in the space-time directions results in an effective d-dimensional Wilsonian lattice field theory with lattice spacing $a' = \beta c$.*

This yields the following correlation length for the quantum antiferromagnetic Heisenberg model

$$\xi = \frac{ec}{16\pi\rho_s} \exp(2\pi\beta\rho_s) \left[1 - \frac{1}{4\pi\beta\rho_s} + \mathcal{O}(1/\beta^2\rho_s^2)\right]. \tag{2.17}$$

This equation resembles the asymptotic scaling behavior of the 2-d classical $O(3)$ model. Actually, one can view the 2-dimensional antiferromagnetic quantum Heisenberg model in the zero temperature limit as a regularization of the 2-d $O(3)$ field theory. Remarkably, the D-theory formulation is entirely discrete, even though the 2-d $O(3)$ model is usually formulated with a continuous classical configuration space.

The dimensionally reduced theory is an effective 2-dimensional lattice model with lattice spacing βc. The continuum limit of that theory is reached as $g^2 = 1/\beta\rho_s \to 0$, hence as the extent β of the extra dimension becomes large. Still, in physical units of the correlation length the extent β is negligible in that limit. Indeed, from (2.17) one gets $\xi \gg \beta$. Therefore, the system undergoes dimensional reduction to two dimensions once the extent of the third dimension becomes large. This might look rather surprising but this process occurs in all D-theory models. D-theory introduces a discrete substructure underlying Wilson's lattice theory. In the continuum limit, the lattice spacing βc of the effective 2-d

$O(3)$ model becomes large in units of the microscopic lattice spacing of the quantum spin system. In other words, D-theory regularizes quantum fields at a much shorter distance scale then the one considered in the Wilson formulation.

The additional microscopic structure may provide new insight into the long-distance continuum limit. In a condensed matter system such as the quantum Heisenberg model, electrons are hopping on the sites of a physical microscopic crystal lattice. Thus, spin-waves of a quantum antiferromagnet are just collective excitations of the spins of many electrons. In the context of the D-theory formulation for QCD described below, gluons appear as collective excitations of rishons hopping on a microscopic lattice. In that case, the lattice is unphysical and serves just as a regulator. Although rishons propagate only at the cut-off scale and are not directly related to physical particles, they may be still useful to study the physics in the continuum limit. In the quantum Heisenberg model, the rishons can be identified with the physical electrons. One can express the quantum spin operator $\vec{S}_x$ at a lattice site x in terms of a vector of Pauli matrices $\vec{\sigma}$ and electron creation annihilation operators $c_x^{i\dagger}$ and c_x^i

$$\vec{S}_x = \frac{1}{2} \sum_{i,j} c_x^{i\dagger} \vec{\sigma}_{ij} c_x^j. \tag{2.18}$$

Here, i and $j \in \{1, 2\}$ and $c_x^{i\dagger}$ and c_x^i obey the usual anti-commutation relations

$$\{c_x^{i\dagger}, c_y^{j\dagger}\} = \{c_x^i, c_y^j\} = 0, \ \{c_x^i, c_y^{j\dagger}\} = \delta_{xy}\delta_{ij}. \tag{2.19}$$

From this construction, it is straightforward to show that $\vec{S}_x$ satisfies the correct commutation relations (2.8). In fact, those commutation relations are also satisfied when the rishons are quantized as bosons. It should be noted that the total number of rishons is fixed at each lattice site x. It is a conserved quantity because the local rishon number operator

$$\mathcal{N}_x = \sum_i c_x^{i\dagger} c_x^i \tag{2.20}$$

commutes with the Hamiltonian (2.9). In fact, fixing the number of rishons on a site is equivalent to selecting a value for the spin, i.e. a choice of an irreducible representation of $SO(3)$. More details on rishons in the context of various models will be given below.

The discrete nature of the D-theory degrees of freedom is particularly well suited for numerical approaches. Indeed, the quantum Heisenberg model, for example, can be treated with very efficient cluster algorithms such as the so-called loop-cluster algorithm [38, 50]. In addition, Beard and Wiese showed that the path integral for discrete quantum systems does not require discretization of the additional Euclidean dimension. This observation has led to a very efficient loop-cluster algorithm operating directly in the continuum of the extra dimension [39]. This algorithm, combined with finite-size scaling techniques, has been used to study the correlation length of the Heisenberg model up to $\xi \approx 350000$ lattice

spacings [27]. In this way, the analytic prediction (2.17) of Hasenfratz and Niedermayer has been verified to high precision, which proves as well the scenario of dimensional reduction. This shows that the D-theory formulation of field theory can be used to investigate very efficiently the 2-d $O(3)$ model. Simulating the $(2+1)$-d path integral of the 2-dimensional quantum Heisenberg model seems as efficient as the simulation of the 2-d $O(3)$ model directly with the Wolff cluster algorithm [51, 52]. In addition, D-theory allows us to simulate this model even at non-zero chemical potential [28], which has not been possible with traditional methods due to a severe complex action problem.

2.1.4 Generalization to other dimensions $d \neq 2$

The exponential divergence of the correlation length is due to the asymptotic freedom of the 2-d $O(3)$ model. Hence, one might expect that the above scenario of dimensional reduction is specific to $d = 2$. As emphasized before, D-theory has a wide domain of application. As we will see now, dimensional reduction also occurs in higher dimensions but in a slightly different way. Let us consider the antiferromagnetic quantum Heisenberg model on a d-dimensional lattice with $d > 2$, the ground state of the system is again in a broken phase and the low-energy excitations are two massless magnons. From chiral perturbation theory, the effective action is the same as before (2.12) except that one integrates over a higher-dimensional space-time. Again, for an infinite extent β of the extra dimension, at zero temperature of the quantum system, one has an infinite correlation length ξ. Thus, once β becomes finite, the extent of the extra dimension is negligible in comparison to the correlation length and the system undergoes dimensional reduction to d dimensions. Nevertheless, in contrast to the 2-dimensional case, there is no reason why the magnons should pick up a mass after dimensional reduction. Consequently, the correlation length remains infinite and we end up with a d-dimensional theory in a broken phase. Eventually, as one reduces the β extent, the Néel order is removed and one reaches a symmetric phase with a finite correlation length. The transition between the symmetric and the broken phase is expected to be second order. In that case, as one approaches the critical "temperature" from the symmetric phase at low β, where dimensional reduction does not occur, the system eventually goes through the second order phase transition. This implies a divergent correlation length and hence the dimensional reduction scenario. Thus, the universal continuum physics of $O(3)$ models for $d \geq 2$ is naturally contained in the framework of D-theory. Nevertheless if the phase transition is first order, it would mean that the $(d+1)$-dimensional lattice system in the symmetric phase (at low β) would not have a continuum limit and the model will hence not fall in a universality class. In other words, the lattice formulation would not regularize the continuum $O(3)$ model in that case. However, a first order phase transition is unlikely, although this can be shown only via numerical simulations.

The case $d = 1$ implies subtle situations and requires a separate discussion. In contrast to the 2-dimensional quantum antiferromagnetic Heisenberg model, the antiferromagnetic quantum spin chain can be solved analytically. Indeed, using his famous ansatz, Bethe

was able to find the ground state for a spin 1/2 chain [53]. He found a vanishing mass-gap at zero temperature. This was a puzzling result, because if we consider that the quantum partition function can be expressed as a $(1+1)$-d path integral with an extent β in the extra dimension, the quantum spin chain can be reformulated as a 2-dimensional classical system at zero temperature. The low-energy physics can naturally be described by a 2-d $O(3)$ model with the action (2.1). However, from the Hohenberg-Mermin-Wagner-Coleman theorem we know that this theory has a mass-gap which contradicts the Bethe solution. This puzzle was solved by Haldane, who conjectured that half-integer spin chains are gapless, while those with integer spins have a mass-gap [54, 55, 56]. This conjecture has by now been verified in great detail. It has been shown analytically that all half-integer spins are gapless [57, 58, 59, 60]. On the other hand, there is strong numerical evidences for a mass-gap with spins 1 and 2 [61, 62, 63, 64, 65].

Following Haldane's arguments, the $(1+1)$-dimensional D-theory model with an infinite extent β in the second direction — the antiferromagnetic quantum spin chain at zero temperature — has a low-energy dynamics described by

$$S[\vec{s}] = \int_0^\beta dx_1 \int dx_2 \ \left[\frac{1}{2g^2}\left(\partial_1\vec{s}\cdot\partial_1\vec{s} + \frac{1}{c^2}\partial_2\vec{s}\cdot\partial_2\vec{s}\right)\right] + i\theta Q, \tag{2.21}$$

where the last term in the action is a topological θ-vacuum contribution with the topological charge

$$Q = \frac{1}{8\pi}\int_0^\beta dx_1 \int dx_2 \ \epsilon_{\mu\nu}\ \vec{s}\cdot(\partial_\mu\vec{s}\times\partial_\nu\vec{s}). \tag{2.22}$$

Here $\mu,\nu \in \{1,2\}$ and Q is an integer in the second homotopy group $\Pi_2(S^2) = \mathbb{Z}$. It measures the winding number of the field configuration $\vec{s}(x) : S^2 \to S^2$, which can be viewed as a map from the compactified space-time $\mathbb{R}^2(\equiv S^2)$ to the intrinsic space of the spins which is also S^2. More details on topology of field theories will be given in the third chapter of this thesis. Haldane hence argued that the vacuum angle $\theta = 2\pi s$ is determined by the total spin $s \in \{1/2, 1, 3/2, 2, ...\}$. First, in the case of integer spins, the vacuum angle is a multiple of 2π and the additional factor $\exp(i\theta Q)$ in the path integral is equal to 1. We are left with the $O(3)$ model described by (2.21) at $\theta = 0$ which indeed has a mass-gap. For half-integer spin chains, $\theta = \pi$ and $\exp(i\theta Q) = (-1)^Q$. It has been shown numerically in [66] that a second order phase transition with a vanishing mass-gap occurs at $\theta = \pi$, which confirms the Haldane conjecture. The simulation at non-trivial vacuum angle is extremely difficult due to the sign problem in the partition function. Still, Bietenholz, Pochinsky and Wiese used a Wolff cluster algorithm combined with an appropriate improved estimator for the topological charge distribution. Moreover, they also confirmed another conjecture due to Affleck [67], according to which the 2-d $O(3)$ model is in the universality class of a 2-dimensional conformal field theory, the $k = 1$ Wess-Zumino-Novikov-Witten model [68, 69].

In the D-theory formulation, the lattice 1-d $O(3)$ model is obtained by dimensional reduction of the model defined by (2.21) which describes the low-energy dynamics of an

antiferromagnetic quantum spin chain. To make the argument more precise, dimensional reduction occurs when the extent β of the second dimension becomes finite. In that case, the topological term disappears because $\partial_2 \vec{s}$ is negligible due to the large correlation length. Using the same renormalization group argument as before, one obtains the Wilson version of the 1-d $O(3)$ model with an effective coupling constant β/g^2. In the continuum limit $\beta \to \infty$, the model describes the quantum mechanics of a particle moving on a 2-sphere S^2. However, D-theory strictly works only for half-integer spins where the correlation length is infinite. For integer spins, one of the main dynamical ingredients is missing: an infinite correlation length. Therefore dimensional reduction cannot occur. Still, using coherent state path integral techniques [70], one can consider the classical limit of large integer spins S, where the correlation length increases as $\xi \propto \exp(\pi S)$. In that way, one could reach the continuum limit of the 2-d $O(3)$ model with $1/g^2 = S/2$. However, this is not in the spirit of D-theory since one then effectively works with classical fields again.

So far, we have seen that D-theory naturally contains the continuum physics of the $O(3)$ model in any dimension. One will now show that the D-theory formulation is far more general and can be extended to various field theory models with various global or local symmetries in different space-time dimensions. In particular a ferromagnetic Heisenberg model ($J < 0$) provides as well a valid regularization for the 2-d $O(3)$ model. This will be presented below in the context of the $CP(N-1)$ models, which generalizes the previous construction (note that $O(3) = CP(1)$).

2.2 D-Theory Representation of Basic Field Variables

In the context of D-theory, a 3-component unit-vector of a classical configuration is replaced by a vector of Pauli matrices. We hence defined a 2-dimensional quantum Heisenberg model, which provides in the low temperature limit a regularization for the 2-d $O(3)$-symmetric continuum field theory. In the coming chapter, we will show that such a structure is completely general in the framework of D-theory. We will expose how real and complex vector and matrix fields can be represented by quantum operators. Symplectic, symmetric, and anti-symmetric tensors will also be defined. They can then be used as basic building blocks to construct all kind of D-theory models.

2.2.1 Real vectors

At a first sight, it is not obvious how to represent the N-component unit-vectors of a classical $O(N)$ model by a quantum operator. Indeed, one cannot generalize the above D-theory construction for the $O(3)$ model to higher values of N. The $O(3)$ case is special since it is equivalent to a $CP(1)$ model. In fact, a natural generalization of the previous construction will yield the $CP(N-1)$ class of models. For $O(N)$ models, a hint comes from considering the classical $O(2)$ model (which is also known as the XY model) and its D-theory regularization. The action of the system is similar to equation (2.1), with

however a 2-component unit vector $\vec{s} = (s^1, s^2)$. As before, to quantize the theory one replaces $\vec{s}$ by the first two components (S^1, S^2) of a quantum spin $\vec{S}$ which form a vector under $SO(2)$. The corresponding Hamilton operator then has the form

$$H = J \sum_{x,\mu} (S^1_x S^1_{x+\hat{\mu}} + S^2_x S^2_{x+\hat{\mu}}), \tag{2.23}$$

which describes the $SO(2)$-symmetric quantum XY model. In this case, the Hamiltonian does only commute with the third component of the total spin, i.e. $[H, S^3] = 0$.

To summarize, the 2-component unit-vectors of an $O(2)$ model can be represented in D-theory by considering the Lie algebra of $SO(3)$. Indeed, two of its generators transform as a vector under $SO(2)$ transformations, while the third one generates the group $SO(2)$ itself. This has a natural generalization to higher N. If we consider the $(N+1)N/2$ generators of $SO(N+1)$, among them N generators transform as a vector under $SO(N)$ while the $N(N-1)/2$ others generate the subgroup $SO(N)$. In other words, in the subgroup decomposition $SO(N+1) \supset SO(N)$ the adjoint representation decomposes as

$$\left\{ \frac{N(N+1)}{2} \right\} = \left\{ \frac{N(N-1)}{2} \right\} \oplus \{N\}. \tag{2.24}$$

More details on Lie algebras and Lie groups properties can be found in [71]. We can thus define the commutation relations of the group $SO(N+1)$ in the following way

$$\begin{aligned} &[S^i, S^j] = iS^{ij}, \ [S^i, S^{jk}] = i(\delta^{ik} S^j - \delta^{ij} S^k), \\ &[S^{ij}, S^{kl}] = i(\delta^{il} S^{kj} + \delta^{ik} S^{jl} + \delta^{jk} S^{li} + \delta^{jl} S^{ik}), \end{aligned} \tag{2.25}$$

where S^{ij} are the generators of the subgroup $SO(N)$ and $S^i = S^{0i}$ ($i \in \{1, 2, ..., N\}$) the N generators which transform as a vector under $SO(N)$. Note that, just as in the XY model, one works with an $SO(N+1)$ algebra while the D-theory model itself is only $SO(N)$ symmetric. Interestingly and as expected, the case $N = 3$ does not reduce to a quantum Heisenberg model. With this construction one obtains another $SO(3)$-invariant quantum spin model expressed in terms of the six generators of $SO(4)$.

The commutation relations (2.25) of $SO(N+1)$ can be represented with rishon constituents

$$\begin{aligned} S^i &= S^{0i} = -i(c^0 c^i - c^i c^0), \\ S^{ij} &= -i(c^i c^j - c^j c^i). \end{aligned} \tag{2.26}$$

In this case, since we are working with real valued fields, the rishon operators $c^0 = c^{0\dagger}$ and $c^i = c^{i\dagger}$ are Hermitean and obey the following anti-commutation relations

$$\{c^0, c^i\} = 0, \ \{c^i, c^j\} = \delta_{ij}. \tag{2.27}$$

These "Majorana" rishons form a Clifford algebra which can be represented by the usual γ matrices. The "Majorana" representation of spin operators has a long history in particle and condensed matter physics [72]. For example it has been used for the description of disordered spins that occur in frustrated quantum magnets [73].

2.2.2 Real matrices

Chiral spin models with an $SO(N)_L \otimes SO(N)_R$ symmetry are formulated in field theory by classical and real $O(N)$ matrix fields o. In the Wilson formulation of lattice field theory, one deals with real parallel transporter represented by matrices o_x which transform appropriately under $SO(N)_L \otimes SO(N)_R$ global symmetries on the left and and the right. On the other hand, a gauge theory with Lie group $SO(N)$ is formulated in terms of parallel transporters $o_{x,\mu}$, which are defined on the links in the μ-direction. Following the same type of arguments as for the real vectors, the $SO(N)_L \otimes SO(N)_R$ symmetry is generated by $N(N-1)$ Hermitean operators. As one quantizes the theory in the D-theory framework, one replaces the real valued classical matrix o by an $N \times N$ matrix O whose elements are N^2 Hermitean quantum operators. Altogether, this gives $N(N-1)+N^2 = N(2N-1)$, which is exactly the total number of generators of $SO(2N)$. Therefore, one gets the subgroup decomposition $SO(2N) \supset SO(N)_L \otimes SO(N)_R$, which in the adjoint representation gives

$$\{N(2N-1)\} = \left\{\frac{N(N-1)}{2}, 1\right\} \oplus \left\{1, \frac{N(N-1)}{2}\right\} \oplus \{N, N\}. \tag{2.28}$$

The $N(2N-1)$ generators S^{mn} of $SO(2N)$ $(m, n \in (1, ..., 2N))$ can hence be decomposed into $N(N-1)/2$ generators L^{ij} which generate the $SO(N)_L$ symmetry on the left, $N(N-1)/2$ generators R^{ij} which generate the $SO(N)_R$ symmetry on the right, and an $(N \times N)$ matrix O^{ij}, where again $i, j \in (1, ..., N)$. The commutation relations

$$[S^{mn}, S^{op}] = i(\delta^{mp} S^{on} + \delta^{mo} S^{np} + \delta^{no} S^{pm} + \delta^{np} S^{mo}) \tag{2.29}$$

are indeed satisfied $(m, n, o, p \in (1, ..., 2N))$. In particular, it is straightforward to show that the following rishon representation generates the $SO(2N)$ algebra,

$$\begin{aligned} O^{ij} &= -i(c_+^i c_-^j - c_-^j c_+^i), \\ L^{ij} &= -i(c_+^i c_+^j - c_+^i c_+^j), \\ R^{ij} &= -i(c_-^i c_-^j - c_-^i c_-^j). \end{aligned} \tag{2.30}$$

The two sets of Hermitean "Majorana" rishons, $c_+^i = c_+^{i\dagger}$ and $c_-^i = c_-^{i\dagger}$, are associated with the left and right $SO(N)$ symmetries generates by the two vectors $\vec{L}$ and $\vec{R}$, formed with the $N(N-1)/2$ generators L^{ij} and R^{ij}. They obey the anti-commutation relations

$$\{c_+^i, c_+^j\} = \delta_{ij}, \ \{c_-^i, c_-^j\} = \delta_{ij}, \ \{c_+^i, c_-^j\} = 0. \tag{2.31}$$

2.2.3 Complex vectors

We have seen how to represent a real N-component vector $\vec{s}$ in the D-theory context. One simply replaces $\vec{s}$ by an N-component vector $\vec{S}$ of Hermitean operators of the $SO(N+1)$ algebra. Let us now discuss the D-theory representation of classical N-component complex vectors $\vec{z}$. As we will see in chapter 4, $CP(N-1)$ models have different formulations in D-theory. In one of them, complex vectors $\vec{z}$ arise and the symmetry group is then $U(N)$. In that case, there are N^2 generators of the symmetry and $2N$ Hermitean operators which form the quantum complex vector $\vec{Z}$ — N for the real and N for the imaginary parts. Altogether this gives $N^2+2N=(N+1)^2-1$, the total number of generators of $SU(N+1)$. Thus, one obtains the following decomposition $SU(N+1) \supset SU(N) \otimes U(1)$, which in the adjoint representation gives

$$\{(N+1)^2-1\} = \{N^2-1\} \oplus \{1\} \oplus \{N\} \oplus \{\overline{N}\}. \tag{2.32}$$

We hence work with the algebra of $SU(N+1)$, which can be decomposed in the following way: the quantum operators Z^i and $Z^{i\dagger}$, a vector $\vec{G}$ of $SU(N)$ generators obeying

$$[G^a, G^b] = 2if_{abc}G^c, \tag{2.33}$$

and a $U(1)$ generator G. Again, this algebra has a natural rishon representation given by

$$Z^i = c^{0\dagger}c^i,\ \vec{G} = \sum_{ij} c^{i\dagger}\vec{\lambda}_{ij}c^j,\ G = \sum_i c^{i\dagger}c^i. \tag{2.34}$$

In this case, we use "Dirac" rishons $c^0, c^{0\dagger}, c^i, c^{i\dagger}$ with the usual anti-commutation relations (2.19). Here $\vec{\lambda}$ is a vector of generalized Gell-Mann matrices for $SU(N)$, they obey $[\lambda^a, \lambda^b] = 2if_{abc}\lambda^c$ as well as $\mathrm{Tr}(\lambda^a\lambda^b) = 2\delta_{ab}$.

2.2.4 Complex matrices

In the Wilson approach, $U(N)$ or $SU(N)$ gauge theories are described in terms of link variables which are classical complex $U(N)$ matrix fields $u_{x,\mu}$. In the same way, chiral spin models with a global $SU(N)_L \otimes SU(N)_R \otimes U(1)$ symmetry are described with $U(N)$ matrix fields u_x. The corresponding symmetry transformations are generated by $2(N^2-1)+1$ Hermitean operators. In the D-theory formulation, the classical complex valued matrix u is replaced by a matrix U whose elements are non-commuting quantum operators. The matrix U is formed by $2N^2$ Hermitean generators, N^2 representing the real part and N^2 representing the imaginary part of the classical complex matrix u. Hence, altogether we have $2(N^2-1)+1+2N^2 = 4N^2-1$ generators, which is exactly the number of generators of $SU(2N)$. The corresponding subgroup decomposition $SU(2N) \supset SU(N)_L \otimes SU(N)_R \otimes U(1)$ takes the following form in the adjoint representation

$$\{4N^2-1\} = \{N^2-1,1\} \oplus \{1,N^2-1\} \oplus \{1,1\} \oplus \{N,\overline{N}\} \oplus \{\overline{N},N\}. \tag{2.35}$$

As before, one can construct a rishon representation for the $SU(2N)$ algebra

$$\begin{aligned} U^{ij} &= c_+^{i\dagger} c_-^j,\ \vec{L} = \sum_{ij} c_+^{i\dagger} \vec{\lambda}_{ij} c_+^j,\ \vec{R} = \sum_{ij} c_-^{i\dagger} \vec{\lambda}_{ij} c_-^j, \\ T &= \sum_i (c_+^{i\dagger} c_+^i - c_-^{i\dagger} c_-^i). \end{aligned} \tag{2.36}$$

The two sets of "Dirac" rishons, c_+^i and c_-^i, are again associated with the left and right $SU(N)$ symmetries generated by $\vec{R}$ and $\vec{L}$, and they obey the usual anticommutation relations. Here, T is the $U(1)$ generator. As we will see, this structure is used both for $U(N)$ and $SU(N)$ quantum link models.

2.2.5 Symplectic, symmetric, and anti-symmetric complex tensors

Besides $SO(N)$ and $SU(N)$, there is a third sequence of Lie group, the symplectic group $Sp(N)$. The group $Sp(N)$ is a subgroup of $SU(2N)$. Therefore its elements g are unitary and have a determinant equal to one. In addition, they obey the constraint

$$g^* = J g J^\dagger,\ J^2 = \mathbb{1}, \tag{2.37}$$

where J is a skew-symmetric matrix. It is interesting to ask how $Sp(N)$ gauge theories can be formulated in the D-theory framework. Remarkably, this is completely analogous to the $SO(N)$ or $SU(N)$ cases. The $Sp(N)_L \otimes Sp(N)_R$ symmetry transformations are generated by $N(2N+1)$ Hermitean operators on the left and $N(2N+1)$ others on the right. In D-theory, a $Sp(N)$ matrix is $2N$-dimensional and its elements are hence described by $4N^2$ Hermitean operators. Altogether, one thus gets $2N(2N+1)+4N^2 = 2N(4N+1)$ generators, which is the number of generators of $Sp(2N)$. The corresponding subgroup decomposition $Sp(2N) \supset Sp(N)_L \otimes Sp(N)_R$ takes the following form in the adjoint representation

$$\{2N(4N+1)\} = \{N(2N+1), 1\} \oplus \{1, N(2N+1)\} \oplus \{2N, 2N\}. \tag{2.38}$$

Other useful building blocks in D-theory are the symmetric ($S^T = S$) and the anti-symmetric ($A^T = -A$) complex tensors. They transform under $SU(N)$ group transformations as

$$S' = g S g^T,\ A' = g A g^T, \tag{2.39}$$

where $g \in SU(N)$. According to Slansky's branching rules for all maximal subgroups [74], one has the subgroup decomposition $Sp(N) \supset SU(N) \otimes U(1)$. Counting the generators one gets $N(2N+1)$ for $Sp(N)$. Subtracting N^2-1 for $SU(N)$ and one for the $U(1)$ symmetry, one is left with $N(N+1)$ generators, which is exactly the number of Hermitean operators we need to represent the $N(N+1)/2$ elements of a complex symmetric tensors. Therefore, the above subgroup decomposition takes the following form in the adjoint representation

$$\{N(2N+1)\} = \{N^2-1\} \oplus \{1\} \oplus \left\{\frac{N(N+1)}{2}\right\} \oplus \left\{\overline{\frac{N(N+1)}{2}}\right\}. \tag{2.40}$$

Similarly, working with the $SO(2N)$ algebra with the subgroup decomposition $SO(2N) \supset SU(N) \otimes U(1)$ leads naturally to a definition of a complex anti-symmetric tensor. Again, the $N(N-1)/2$ elements of such a tensor are represented by $N(N-1)$ operators. Together with the generators of $SU(N)$ and $U(1)$, it gives $N(N-1)+N^2 = N(2N-1)$ generators — exactly those of $SO(2N)$. Hence, one gets the following subgroup decomposition in the adjoint representation

$$\{N(2N-1)\} = \{N^2-1\} \oplus \{1\} \oplus \left\{\frac{N(N-1)}{2}\right\} \oplus \left\{\overline{\frac{N(N-1)}{2}}\right\}. \tag{2.41}$$

To summarize, in D-theory classical, real, and complex vectors s and z are replaced by quantum Hermitean operators S and Z which are embedded respectively in $SO(N+1)$ and $SU(N+1)$ algebras. In a similar way, the real and complex valued matrices o and u are replaced by matrices O and U whose operator valued elements are embedded in $SO(2N)$ and $SU(2N)$ algebras. This is a general construction since it is also possible to represent $2N \times 2N$ symplectic matrices and $N \times N$ symmetric and anti-symmetric tensors by embedding them in $Sp(2N)$, $Sp(N)$, and $SO(2N)$ algebras, respectively. In the next sections, we use these basic building blocks to construct a large variety of models, both with global or local symmetries, in the context of D-theory.

2.3 D-Theory Formulation of Various Models with a Global Symmetry

In this section, we investigate various field theory models in the D-theory framework. We show that classical field models with a global symmetry are regularized, in our context, by quantum spin systems. For each system, we introduce an action operator H which is defined on a d-dimensional lattice. It replaces the Euclidean action of Wilson's lattice field theory and due to the quantum nature of this Hamiltonian the system propagates in an extra dimension. Hence, in our case, the partition function $Z = \mathrm{Tr}\exp(-\beta H)$ resembles a quantum statistical system. The dynamics of the models, in particular the mechanism of dimensional reduction, and their general properties will be presented in the next section. In the following, we concentrate only on the algebraic structure of those models. Note that the case of the $CP(N-1)$ models is not addressed here. It will be presented in detail in the chapter 4.

2.3.1 $O(N)$ quantum spin models

In the second section of this chapter, we have described the regularization of an $O(3)$-symmetric non-linear σ model with D-theory in detail. As emphasized before, the generalization to $O(N)$ models is not straightforward and demands a specific algebraic structure. The N-component vector in D-theory is embedded in the algebra of $SO(N+1)$. In the

usual Wilson lattice formulation, the $O(N)$ models are defined in terms of classical N-component unit-vectors $\vec{s}_x$, living on the sites. The Euclidean action is given by a sum over scalar products

$$S[s] = -\sum_{x,\mu} \vec{s}_x \cdot \vec{s}_{x+\hat{\mu}}, \tag{2.42}$$

which is clearly invariant under $SO(N)$ rotations. As before, the model is non-linear because the fields obey the constraint

$$\vec{s}_x \cdot \vec{s}_x = \sum_{i=1}^{N} (s_x^i)^2 = 1. \tag{2.43}$$

Using the results of the previous section, one replaces the classical N-component vector of the classical system by a vector $\vec{S}_x$ of Hermitean operators which represent N of the generators of $SO(N+1)$. The corresponding action operator is

$$H = J \sum_{x,\mu} \vec{S}_x \cdot \vec{S}_{x+\hat{\mu}}, \tag{2.44}$$

with the coupling constant J. The quantum spins $S_x^i = S_x^{0i}$ and S_x^{ij} obey the commutation relations (2.25). The global $SO(N)$ symmetry of the system follows from

$$[H, \sum_x S_x^{ij}] = 0. \tag{2.45}$$

Like the Heisenberg model, the $O(N)$ quantum spin system can be formulated using different representations. However, in this case, unlike in the Heisenberg model, we have the freedom to choose representations of $SO(N+1)$. For example, the rishon representation is the fundamental spinorial representation of $SO(N+1)$. It is given on each lattice site by

$$\begin{aligned} S_x^i &= -i(c_x^0 c_x^i - c_x^i c_x^0), \\ S_x^{ij} &= -i(c_x^i c_x^j - c_x^i c_x^j). \end{aligned} \tag{2.46}$$

These "Majorana" rishons obey the following anti-commutation relations

$$\{c_x^0, c_y^0\} = \delta_{xy}, \ \{c_x^0, c_y^i\} = 0, \ \{c_x^i, c_y^j\} = \delta_{xy}\delta_{ij}. \tag{2.47}$$

2.3.2 $SO(N)_L \otimes SO(N)_R$ chiral quantum spin models

In the Wilson formulation, an $SO(N)_L \otimes SO(N)_R$ chiral spin model is formulated in terms of classical orthogonal $SO(N)$ matrices o_x, which are located on the sites of the lattice. The discretized action is hence

$$S[o] = -\sum_{x,\mu} \mathrm{Tr}(o_x^\dagger o_{x+\hat{\mu}} + o_{x+\hat{\mu}}^\dagger o_x). \tag{2.48}$$

Here the dagger reduces to the transpose due to orthogonality. This action is invariant under global $SO(N)_L \otimes SO(N)_R$ transformations

$$o'_x = \exp(i\vec{\alpha}_+ \cdot \vec{\lambda}) o_x \exp(-i\vec{\alpha}_- \cdot \vec{\lambda}), \tag{2.49}$$

where $\vec{\lambda}$ are the anti-Hermitean generators of $SO(N)$. More properties of the model will be described in the next section. Following the D-theory procedure, we replace the classical matrices o_x by matrices O_x consisting of N^2 generators of the embedding algebra $SO(2N)$. The $SO(N)$ chiral quantum spin model is thus defined by the action operator

$$H = J \sum_{x,\mu} \mathrm{Tr}(O_x^\dagger O_{x+\hat{\mu}} + O_{x+\hat{\mu}}^\dagger O_x), \tag{2.50}$$

The $SO(N)$ global symmetry is generated on the left by the operator $\vec{L} = \sum_x \vec{L}_x$ and on the right by $\vec{R} = \sum_x \vec{R}_x$. The group element W, which is a unitary operator generating the global $SO(N)_L \otimes SO(N)_R$ symmetry transformation, then takes the form

$$W = \exp(i\vec{\alpha}_+ \cdot \sum_x \vec{L}_x) \exp(i\vec{\alpha}_- \cdot \sum_x \vec{R}_x). \tag{2.51}$$

The Hamiltonian commutes with the generators of $SO(N)$ on the right and on the left,

$$[H, \sum_x \vec{L}_x] = [H, \sum_x \vec{R}_x] = 0. \tag{2.52}$$

Using the "Majorana" rishon representation of the $SO(2N)$ algebra, one gets

$$\begin{aligned} O_x^{ij} &= -i(c_{x,+}^i c_{x,-}^j - c_{x,-}^j c_{x,+}^i), \\ L_x^{ij} &= -i(c_{x,+}^i c_{x,+}^j - c_{x,+}^j c_{x,+}^i), \\ R_x^{ij} &= -i(c_{x,-}^i c_{x,-}^j - c_{x,-}^j c_{x,-}^i), \end{aligned} \tag{2.53}$$

and the anti-commutation relations take the form

$$\{c_{x,+}^i, c_{y,+}^j\} = \{c_{x,-}^i, c_{y,-}^j\} = \delta_{xy}\delta_{ij}, \ \{c_{x,+}^i, c_{y,-}^j\} = 0. \tag{2.54}$$

It is straightforward to construct an $Sp(N)$ chiral quantum spin model along the same lines. One shall use the embedding algebra $Sp(2N)$ in that case.

2.3.3 $U(N)_L \otimes U(N)_R$ and $SU(N)_L \otimes SU(N)_R$ chiral quantum spin models

Chiral spin models with a global symmetry $SU(N)_L \otimes SU(N)_R \otimes U(1)$ are usually formulated in terms of classical complex $U(N)$ matrices u sitting on the lattice sites. The Wilson action

$$S[u] = -\sum_{x,\mu} \mathrm{Tr}(u_x^\dagger u_{x+\hat{\mu}} + u_{x+\hat{\mu}}^\dagger u_x) \tag{2.55}$$

is invariant under global chiral $SU(N)_L \otimes SU(N)_R$ transformations, i.e.

$$u'_x = \exp(i\vec{\alpha}_+ \cdot \vec{\lambda}) u_x \exp(-i\vec{\alpha}_- \cdot \vec{\lambda}), \tag{2.56}$$

as well as under global $U(1)$ transformations

$$u'_x = \exp(i\alpha) u_x, \tag{2.57}$$

which do not distinguish between left and right. If one restricts the matrices u_x to $SU(N)$ instead of $U(N)$, the symmetry of the model described by (2.55) is reduced to $SU(N)_L \otimes SU(N)_R$.

In D-theory, the $U(N)_L \otimes U(N)_R$ chiral chiral model is described by the action operators

$$H = J \sum_{x,\mu} \mathrm{Tr}(U_x^\dagger U_{x+\hat{\mu}} + U_{x+\hat{\mu}}^\dagger U_x), \tag{2.58}$$

where the matrices U_x consist of $2N^2$ Hermitean generators of $SU(2N)$. The group element W, which is a unitary operator generating the global symmetry transformation in the Hilbert space, then takes the form

$$W = \exp(i\vec{\alpha}_+ \cdot \sum_x \vec{L}_x) \exp(i\vec{\alpha}_- \cdot \sum_x \vec{R}_x) \exp(i\alpha \sum_x T_x). \tag{2.59}$$

The invariance of the model under $SU(N)_L \otimes SU(N)_R \otimes U(1)$ is imposed by the commutation relations

$$[H, \sum_x \vec{L}_x] = [H, \sum_x \vec{R}_x] = [H, \sum_x T_x] = 0. \tag{2.60}$$

Using the construction of complex matrices, one has the following rishon representation of the $SU(2N)$ algebra per local site

$$\begin{aligned} &U_x^{ij} = c_{x,+}^{i\dagger} c_{x,-}^j, \;\; \vec{L}_x = \sum_{ij} c_{x,+}^{i\dagger} \vec{\lambda}_{ij} c_{x,+}^j, \;\; \vec{R}_x = \sum_{ij} c_{x,-}^{i\dagger} \vec{\lambda}_{ij} c_{x,-}^j, \\ &T_x = \sum_i (c_{x,+}^{i\dagger} c_{x,+}^i - c_{x,-}^{i\dagger} c_{x,-}^i). \end{aligned} \tag{2.61}$$

The rishon operators obey canonical anti-commutation relations

$$\begin{aligned} &\{c_{x,+}^i, c_{y,+}^{j\dagger}\} = \{c_{x,-}^i, c_{y,-}^{j\dagger}\} = \delta_{xy}\delta_{ij}, \\ &\{c_{x,+}^i, c_{y,-}^{j\dagger}\} = \{c_{x,-}^i, c_{y,+}^{j\dagger}\} = 0, \\ &\{c_{x,\pm}^i, c_{y,\pm}^j\} = 0, \;\; \{c_{x,\pm}^{i\dagger}, c_{y,\pm}^{j\dagger}\} = 0. \end{aligned} \tag{2.62}$$

Moreover, one can note that the action operator commutes with the local rishon number

$$\mathcal{N}_x = \sum_i (c_{x,+}^{i\dagger} c_{x,+}^i + c_{x,-}^{i\dagger} c_{x,-}^i). \tag{2.63}$$

It is indeed straightforward to show that $[H, \mathcal{N}_x] = 0$. Remarkably, selecting a fixed number of rishons corresponds to choosing a representation of $SU(2N)$.

In order to obtain an $SU(N)_L \otimes SU(N)_R$ chiral model, one needs to break the additional $U(1)$ symmetry explicitly. One does this by adding the real part of the determinant of each matrix to the action operator (2.58),

$$H = J \sum_{x,\mu} \mathrm{Tr}(U_x^\dagger U_{x+\hat{\mu}} + U_{x+\hat{\mu}}^\dagger U_x) + J' \sum_x (\mathrm{det} U_x + \mathrm{det} U_x^\dagger). \tag{2.64}$$

Note that the definition of $\mathrm{det}U_x$ does not suffer from operator ordering ambiguities. In particular, this determinant takes the following form in the rishon representation

$$\begin{aligned} \mathrm{det}U_x &= \frac{1}{N!} \epsilon_{i_1 i_2 \ldots i_N} (U_x)_{i_1 i'_1} (U_x)_{i_2 i'_2} \ldots (U_x)_{i_N i'_N} \epsilon_{i'_1 i'_2 \ldots i'_N} \\ &= \frac{1}{N!} \epsilon_{i_1 i_2 \ldots i_N} c^{i_1}_{x,+} c^{i'_1 \dagger}_{x,-} c^{i_2}_{x,+} c^{i'_2 \dagger}_{x,-} \ldots c^{i_N}_{x,+} c^{i'_N \dagger}_{x,-} \epsilon_{i'_1 i'_2 \ldots i'_N} \\ &= N!\ c^1_{x,+} c^{1\dagger}_{x,-} c^2_{x,+} c^{2\dagger}_{x,-} \ldots c^N_{x,+} c^{N\dagger}_{x,-}. \end{aligned} \tag{2.65}$$

This operator gives a non-vanishing result only when it acts on a state with $\mathcal{N}_x = N$ rishons. Indeed, the $U(1)$ symmetry can be explicitly broken only when one works with $\mathcal{N}_x = N$ rishons on each site. This corresponds to choosing the $(2N)!/(N!)^2$-dimensional representation of $SU(2N)$ with a totally anti-symmetric Young tableau of N boxes

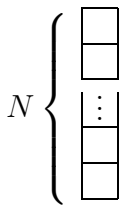

More about the dynamics of rishons will be given below, in the context of quantum link models.

2.4 Classical Scalar Fields from Dimensional Reduction of Quantum Spins

In section 2.2, we have described the regularization of a d-dimensional $O(3)$ spin model in the context of D-theory. In that case, the quantum Heisenberg model provides the regularization framework. In particular, the connection between the two systems can be established using chiral perturbation theory. The Goldstone boson field $\vec{s}$ appears when the global $SO(3)$ symmetry is broken down to $SO(2)$. They describe the low-energy dynamics of the Heisenberg model and can therefore be considered as the collective excitations of the quantum spins. The system is formulated in $(d+1)$ dimensions and by dimensional

reduction the fields $\vec{s}$ become the effective d-dimensional fields of the Wilsonian lattice $O(3)$ model. The key ingredient in all D-theory models relies entirely on the fact that the $(d+1)$-dimensional theory is massless. In case of the quantum Heisenberg model, we are in a broken phase at zero temperature. Thus chiral perturbation theory applies and dimensional reduction occurs. The continuum limit of this lattice model is reached when the extent β of the extra dimension becomes large. This is true for all other D-theory quantum spin models. However, in case of the spin 1/2 quantum Heisenberg model, it requires very precise numerical simulations before one can be sure that spontaneous symmetry breaking occurs.

For other D-theory models, such as chiral principal chiral models or $O(N)$ models, similar simulations have not yet been done. We will show in this thesis that efficient Monte Carlo simulations can be performed in the context of the D-theory version of the $CP(N-1)$ model, where spontaneous symmetry breaking indeed occurs. In the following discussion, we will consider that in the D-theory formulation, the symmetry breaking pattern is identical to the corresponding one in Wilson's lattice description of the theory. This can be shown analytically for sufficiently large representations of the embedding algebra [24]. In numerical simulations, one would like to minimize the number of degrees of freedom of the problem. It is then better to work with smaller representations. For example, in the context of the $CP(N-1)$ presented below, an efficient cluster algorithm can be constructed and it is hence possible to investigate if massless modes exist in the $(d+1)$-dimensional theory. We have been able to perform detailed tests of this dynamical picture. In the following, we will describe the $O(N)$ model and the principal chiral models.

2.4.1 $O(N)$ models

In section 2.1, we have already presented the main physical properties of the $O(3)$ model in d dimensions. The case $d = 2$ is perhaps the most interesting one since it exhibits many of the interesting properties of 4-dimensional gauge theories. Here we investigate the D-theory version, which is defined by the quantum operator (2.44). The quantum statistical partition function

$$Z = \mathrm{Tr}\exp(-\beta H) \tag{2.66}$$

can be represented as a $(2+1)$-dimensional path integral with a finite extent β in the extra Euclidean dimension. At zero-temperature of the quantum system, i.e. at $\beta = \infty$, we have an infinite 3-dimensional system with a global $SO(N)$ symmetry. In Wilson's regularization of quantum field theories, such a model can be in a massless phase in which the symmetry is spontaneously broken down to $SO(N-1)$. In the quantum spin case, we assume that such a symmetry breaking pattern also occurs, this has to be tested numerically for small representations and might well depend on the choice of the representation of the embedding algebra. Let us first consider the case $N > 2$. The abelian $N = 2$ case needs a separate discussion. When an $SO(N)$ symmetry breaks down spontaneously to an $SO(N-1)$ subgroup, $N-1$ Goldstone bosons arise and the low-energy dynamics of the system can

be described using chiral perturbation theory. The Goldstone bosons are represented by fields which live in the coset space $SO(N)/SO(N-1) = S^{N-1}$ — the $(N-1)$-dimensional sphere. Therefore, the Goldstone bosons are N-component unit vector fields $\vec{s}$ and their low-energy effective action (to lowest order) is given by

$$S[\vec{s}] = \int_0^\beta dx_3 \int d^2x \frac{\rho_s}{2} \Big(\partial_\mu \vec{s} \cdot \partial_\mu \vec{s} + \frac{1}{c^2} \partial_3 \vec{s} \cdot \partial_3 \vec{s} \Big), \tag{2.67}$$

where ρ_s and c are the spin stiffness and the spin-wave velocity. The dimensional reduction occurs as in the $O(3)$ Heisenberg model. Once the extent β becomes finite, the correlation length ξ is still much larger than β and the system undergoes dimensional reduction because the fields are essentially constant over the extra dimension. However, we know from the Hohenberg-Mermin-Wagner-Coleman theorem that the Goldstone bosons have to pick up a mass in this slab geometry. The exact mass-gap of the $O(N)$ models has been determined by Hasenfratz and Niedermayer. As a generalization of their earlier result, they obtained the following correlation length

$$\begin{aligned} \xi &= \beta c \left(\frac{e(N-2)}{16\pi\beta\rho_s} \right)^{1/(N-2)} \Gamma\left(1 + \frac{1}{N-2}\right) \exp\left(\frac{2\pi\beta\rho_s}{N-2}\right) \\ &\quad \times \left[1 - \frac{1}{4\pi\beta\rho_s} + \mathcal{O}(1/\beta^2\rho_s^2) \right], \end{aligned} \tag{2.68}$$

where again $1/g^2 = \beta\rho_s$ defines the coupling constant g^2 of the Wilsonian lattice theory with lattice spacing βc. The exponential form of this expression is due to asymptotic freedom. In this case $(N-2)/2\pi$ is the one-loop β function coefficient of the $O(N)$ models. In every asymptotically free theory one reaches the continuum limit by sending the bare coupling constant g to zero. Indeed, in the $g \to 0$ limit the extent β of the extra dimension becomes extremely large. Still, in physical units of ξ, this extent is negligible and the $(2+1)$-dimensional D-theory model indeed reduces to the target 2-d $O(N)$ theory.

The situation for higher dimensions is similar to the one described earlier in the context of the Heisenberg model. If one assumes again spontaneous symmetry breaking and one makes β finite but large enough, we are in a broken phase with an infinite correlation length. Dimensional reduction hence occurs. For small β we might be in the symmetric phase with a finite correlation length. The phase transition between these two phases at a critical β value is believed to be second order. Therefore, the universal continuum behavior, which emerges as one approach the phase transition, is accessible in the framework of D-theory. For $d = 1$, the situation is a bit different. For $N \neq 3$, one does not have instantons or a θ-term. Consequently, we expect the 1-d $O(N)$ quantum spin chain to be always massive. In that case, we would not have an infinite correlation length and dimensional reduction will not occur. That would mean that such quantum models do not have underlying universal continuum physics.

Let's turn now to the abelian $N = 2$ case, the quantum XY model described by the Hamiltonian (2.23). The classical 2-dimensional XY model has a Kosterlitz-Thouless transition at finite temperature separating a massive phase with a vortex condensate from a massless spin-wave phase. Indeed, in the low temperature phase the model describes massless magnons which do not interact. The Hohenberg-Mermin-Wagner-Coleman theorem is hence evaded and no mass-gap is generated. There is numerical evidence for a Kosterlitz-Thouless transition at finite β in the quantum XY model as well [75, 76, 77]. In that case, for a large extent of the third Euclidean dimension, one is in the massless phase with an infinite correlation length already for finite β. One hence has dimensional reduction. The situation is therefore analogous to the $O(N)$ models with $N \geq 3$ in $d \geq 3$ dimensions. The continuum field theory resulting from this dimensional reduction is the 2-dimensional classical XY model — an $SO(2)$-symmetric theory of a free massless scalar field.

2.4.2 $SU(N)$, $Sp(N)$ and $SO(N)$ chiral models

As the $O(N)$ model, the 2-dimensional principal chiral models have very interesting properties such as asymptotic freedom and a non-perturbatively generated mass-gap. Moreover, they have an infinite number of conservation laws at the classical level which survive quantization. An infinite number of conservation laws implies the absence of particle production and allows the determination of the S matrix up to the so-called Castillejo-Dalitz-Dyson factors [78]. Let us be more precise and consider the d-dimensional quantum $SU(N)$ chiral spin model. Its partition function is described by a $(d+1)$-dimensional path integral with an extent β of the extra dimension. At $\beta = \infty$, the $(d+1)$-dimensional system has an $SU(N)_L \otimes SU(N)_R$ chiral symmetry. In [24] it has been shown that the quantum chiral spin model, for a sufficiently large representation of the embedding algebra $SU(2N)$, has the same spontaneous symmetry breaking pattern that occurs in the Wilson formulation. More precisely, the $SU(N)_L \otimes SU(N)_R$ global symmetry breaks down to $SU(N)_{L=R}$ and the N^2-1 Goldstone bosons live in the coset space $SU(N)_L \otimes SU(N)_R / SU(N)_{L=R} = SU(N)$. With $d = 2$ and using chiral perturbation theory one gets the following low-energy effective action

$$S[U] = \int_0^\beta dx_3 \int d^2x \, \frac{\rho_s}{4} \mathrm{Tr} \left(\partial_\mu U^\dagger \partial_\mu U + \frac{1}{c^2} \partial_3 U^\dagger \partial_3 U \right). \tag{2.69}$$

The dimensional reduction is exactly analogous to the $O(N)$ model with $N \geq 3$. In particular, one again has a finite correlation length due to the Hohenberg-Mermin-Wagner-Coleman theorem. Using the result of [78] for the exact mass-gap of the 2-d $SU(N)$ chiral model up to order $1/\beta\rho_s$ corrections, one obtains

$$\xi = \beta c \left(\frac{e}{N \beta \rho_s} \right)^{1/2} \frac{\exp(2\pi\beta\rho_s/N)}{4\sin(\pi/N)} \left[1 + \mathcal{O}(1/\beta\rho_s) \right]. \tag{2.70}$$

Note that this result is consistent with the result of the $O(4)$ model when one considers the case $N = 2$. Again, due to asymptotic freedom, the dimensional reduction and the emergence of universal behavior occurs in the limit $\beta \to \infty$. For higher dimensions, we

have an infinite correlation length already at finite β.

The case of $Sp(N)$ and $SO(N)$ chiral model has been investigated in [79]. In particular, the exact mass-gap of the corresponding 2-dimensional models yields the following expressions for the correlation functions. For the $Sp(N)$ chiral model one gets

$$\xi = \beta c \left(\frac{e}{(N+1)\beta\rho_s} \right)^{1/2} \frac{\exp(2\pi\beta\rho_s/(N+1))}{2^{(3N+1)/(N+1)} \sin(\pi/(N+1))} \left[1 + \mathcal{O}(1/\beta\rho_s) \right]. \tag{2.71}$$

This is consistent with the $SU(2)_L \otimes SU(2)_R$ case for $N = 1$. For $SO(N)_L \otimes SO(N)_R$ with $N \geq 7$ the correlation length is given by

$$\xi = \beta c \left(\frac{e}{(N-2)\beta\rho_s} \right)^{1/2} \frac{\exp(2\pi\beta\rho_s/(N-2))}{2^{(2N-2)/(N-4)} \sin(\pi/(N-2))} \left[1 + \mathcal{O}(1/\beta\rho_s) \right]. \tag{2.72}$$

Since $SO(3) \simeq SU(2) = Sp(1)$, $SO(5) \simeq Sp(2)$, and $SO(6) \simeq SU(4)$, the cases $N = 3$, 5, and 6 are covered by the corresponding $SU(N) \otimes SU(N)$ and $Sp(N) \otimes Sp(N)$ chiral models. The $N = 4$ case corresponds to two decoupled $SU(2) \otimes SU(2)$ chiral models, since $SO(4) \simeq SU(2) \otimes SU(2)$.

2.5 D-Theory Formulation of Various Models with a Gauge Symmetry

We will now turn to gauge theories and to the corresponding D-theory approach — the quantum link models. Quantum link models are related to Wilson's formulation of lattice gauge theory in the same way as quantum spin models are related to their classical counterparts. In lattice gauge theory, the gauge variables are represented by parallel transporter matrices. In D-theory, the corresponding quantum variables are quantum link operators which are matrices whose elements are quantum operators. Similarly, the Wilson Euclidean action corresponds to a quantum Hamiltonian which transports the system in an extra dimension. We will see in the next section that, as for quantum spin models, the extra dimension will ultimately disappear via dimensional reduction. In the following, we construct explicitly various quantum link models which regularize quantum field theories with local symmetries.

2.5.1 $U(N)$ and $SU(N)$ quantum link models

In Wilson's formulation of lattice gauge theory one uses classical complex $SU(N)$ parallel transporters link matrices $u_{x,\mu}$ to form the $SU(N)$ d-dimensional invariant action

$$S[u] = -\sum_{x,\mu\neq\nu} \mathrm{Tr}(u_{x,\mu} u_{x+\hat{\mu},\nu} u^\dagger_{x+\hat{\nu},\mu} u^\dagger_{x,\nu}). \tag{2.73}$$

By construction, this action is invariant under $SU(N)$ gauge transformations

$$u'_{x,\mu} = \exp(i\vec{\alpha}_x \cdot \vec{\lambda}) u_{x,\mu} \exp(-i\vec{\alpha}_{x+\hat{\mu}} \cdot \vec{\lambda}). \tag{2.74}$$

To construct a quantum link representation of $SU(N)$ lattice field theory, we replace the classical action by the quantum operator

$$H = J \sum_{x,\mu\neq\nu} \mathrm{Tr}(U_{x,\mu} U_{x+\hat{\mu},\nu} U^\dagger_{x+\hat{\nu},\mu} U^\dagger_{x,\nu}). \tag{2.75}$$

Here J is the coupling constant and the elements of the $N \times N$ matrices are operators $U_{x,\mu}$ acting in a Hilbert space. The dagger represents Hermitean conjugation in both the Hilbert space and the $N \times N$ matrix space. The trace in this expression is taken only over the $N \times N$ matrix space. Gauge invariance of the quantum link model requires that the above Hamiltonian commutes with the generators $\vec{G}_x$ of the infinitesimal gauge transformations at each lattice sites x. These generators obey the commutation relations

$$[G^a_x, G^b_y] = 2i\delta_{xy} f_{abc} G^c_x. \tag{2.76}$$

The gauge covariance of the quantum link follows by construction if

$$\begin{aligned} U'_{x,\mu} &= \prod_y \exp(-i\vec{\alpha}_y \cdot \vec{G}_y) U_{x,\mu} \prod_z \exp(i\vec{\alpha}_z \cdot \vec{G}_z) \\ &= \exp(i\vec{\alpha}_x \cdot \vec{\lambda}) U_{x,\mu} \exp(-i\vec{\alpha}_{x+\hat{\mu}} \cdot \vec{\lambda}), \end{aligned} \tag{2.77}$$

where the unitary operators which represent a general gauge transformation in Hilbert space is given by

$$W = \prod_x \exp(i\vec{\alpha}_x \cdot \vec{G}_x). \tag{2.78}$$

The above equation implies the following commutation relations between the gauge generators and the link variables

$$[\vec{G}_x, U_{y,\mu}] = \delta_{x,y+\hat{\mu}} U_{y,\mu} \vec{\lambda} - \delta_{x,y} \vec{\lambda} U_{y,\mu}. \tag{2.79}$$

In order to satisfy this relation, we introduce

$$\vec{G}_x = \sum_\mu (\vec{R}_{x-\hat{\mu},\mu} + \vec{L}_{x,\mu}), \tag{2.80}$$

where $\vec{R}_{x,\mu}$ and $\vec{L}_{x,\mu}$ are the generators of right and left gauge transformations of the link variable $U_{x,\mu}$. Expressing these vectors in components, their commutation relations take the form

$$\begin{aligned} &[R^a_{x,\mu}, R^b_{y,\nu}] = \delta_{x,y}\delta_{\mu\nu} 2i f_{abc} R^c_{x,\mu}, \\ &[L^a_{x,\mu}, L^b_{y,\nu}] = \delta_{x,y}\delta_{\mu\nu} 2i f_{abc} L^c_{x,\mu}, \\ &[R^a_{x,\mu}, L^b_{y,\nu}] = 0. \end{aligned} \tag{2.81}$$

In fact, $\vec{L}$ and $\vec{R}$ generate an $SU(N)_L \otimes SU(N)_R$ algebra on each link and they commute with each other when they are associated with different links. The commutation relations (2.79) finally imply

$$\begin{aligned}
[\vec{R}_{x,\mu}, U_{y,\nu}] &= \delta_{x,y}\delta_{\mu\nu} U_{x,\mu}\vec{\lambda}, \\
[\vec{L}_{x,\mu}, U_{y,\nu}] &= -\delta_{x,y}\delta_{\mu\nu}\vec{\lambda} U_{x,\mu}.
\end{aligned} \tag{2.82}$$

One can view the above relations as the canonical commutation relations between the link variables and their canonical conjugate momenta $\vec{L}$ and $\vec{R}$. In Wilson's formulation, similar commutation relations are realized in an infinite-dimensional Hilbert space of square integrable wave functionals. For quantum link models, the situation is different since the Hilbert space becomes finite dimensional by allowing the elements of the link variables to have non-zero commutators.

For each link, the above relations (2.82) can be realized by using the generators of an $SU(2N)$ algebra with the $SU(N)_L \otimes SU(N)_R$ algebra embedded in it. We will give two examples, the fundamental and the spinorial representation of $SU(2N)$. In the fundamental representation one can write

$$\begin{aligned}
&U^{ij}_{x,\mu} = \mathrm{Re}U^{ij}_{x,\mu} + i\ \mathrm{Im}U^{ij}_{x,\mu},\ (U^{\dagger}_{x,\mu})^{ij} = \mathrm{Re}U^{ji}_{x,\mu} - i\ \mathrm{Im}U^{ji}_{x,\mu}, \\
&\mathrm{Re}U^{ij}_{x,\mu} = \begin{pmatrix} 0 & M^{(ij)}_{x,\mu} \\ M^{(ji)}_{x,\mu} & 0 \end{pmatrix}, \\
&\mathrm{Im}U^{ij}_{x,\mu} = \begin{pmatrix} 0 & -iM^{(ij)}_{x,\mu} \\ iM^{(ji)}_{x,\mu} & 0 \end{pmatrix}, \\
&R^{a}_{x,\mu} = \begin{pmatrix} \lambda^{a}_{x.\mu} & 0 \\ 0 & 0 \end{pmatrix},\ L^{a}_{x,\mu} = \begin{pmatrix} 0 & 0 \\ 0 & \lambda^{a}_{x.\mu} \end{pmatrix}.
\end{aligned} \tag{2.83}$$

With $M^{(ij)}$ a set of N^2 matrices (one for each pair (ij)) of size $N \times N$ with $M^{(ij)}_{kl} = \delta_{il}\delta_{jk}$. Suppressing the link index (x, μ) one gets the following local commutation relations between the real and imaginary parts of quantum link elements

$$\begin{aligned}
&[\mathrm{Re}U_{ij}, \mathrm{Re}U_{kl}] = [\mathrm{Im}U_{ij}, \mathrm{Im}U_{kl}] = -i(\delta_{ik}\mathrm{Im}\lambda^{a}_{jl}R^{a} + \delta_{jl}\mathrm{Im}\lambda^{a}_{ik}L^{a}), \\
&[\mathrm{Re}U_{ij}, \mathrm{Im}U_{kl}] = i\left(\delta_{ik}\mathrm{Re}\lambda^{a}_{jl}R^{a} - \delta_{jl}\mathrm{Re}\lambda^{a}_{ik}L^{a} + \frac{2}{N}\delta_{ik}\delta_{jl}T\right).
\end{aligned} \tag{2.84}$$

In particular, one has $[U_{ij}, U_{kl}] = [U^{\dagger}_{ij}, U^{\dagger}_{kl}] = 0$ and the additional generator $T_{x,\mu}$ on a link is given by

$$T_{x,\mu} = \begin{pmatrix} \mathbb{1} & 0 \\ 0 & -\mathbb{1} \end{pmatrix}. \tag{2.85}$$

These operators form the algebra of $SU(2N)$ on each link. The real and imaginary parts of the N^2 matrix elements $U^{ij}_{x,\mu}$ are represented by $2N^2$ Hermitean generators. Together

with the $2(N^2-1)$ generators $R^a_{x,\mu}$ and $L^a_{x,\mu}$ of right and left gauge transformations and with the generator $T_{x,\mu}$, one obtains the $4N^2-1$ generators of $SU(2N)$.

Another representation of the $SU(2N)$ algebra is the rishon representation

$$U^{ij}_{x,\mu} = c^{i\dagger}_{x,+\mu} c^{j}_{x+\hat{\mu},-\mu},\ \vec{L}_{x,\mu} = \sum_{ij} c^{i\dagger}_{x,+\mu} \vec{\lambda}_{ij} c^{j}_{x,+\mu},$$
$$\vec{R}_{x,\mu} = \sum_{ij} c^{i\dagger}_{x+\hat{\mu},-\mu} \vec{\lambda}_{ij} c^{j}_{x+\hat{\mu},-\mu}, \tag{2.86}$$

with the canonical anti-commutation relations for the rishon operators

$$\{c^{i}_{x,\pm\mu}, c^{j\dagger}_{y,\pm\nu}\} = \delta_{xy}\delta_{\pm\mu,\pm\nu}\delta_{ij},\ \{c^{i}_{x,\pm\mu}, c^{j}_{y,\pm\nu}\} = 0,$$
$$\{c^{i\dagger}_{x,\pm\mu}, c^{j\dagger}_{y,\pm\nu}\} = 0. \tag{2.87}$$

Together with the generator

$$T_{x,\mu} = \sum_i (c^{i\dagger}_{x,+\mu} c^{i}_{x,+\mu} - c^{i\dagger}_{x+\hat{\mu},-\mu} c^{i}_{x+\hat{\mu},-\mu}), \tag{2.88}$$

one gets again a complete decomposition of the $SU(2N)$ algebra. Moreover, it is easy to show that this whole algebra commutes with the rishon number operator

$$\mathcal{N}_{x,\mu} = \sum_i (c^{i\dagger}_{x,+\mu} c^{i}_{x,+\mu} + c^{i\dagger}_{x+\hat{\mu},-\mu} c^{i}_{x+\hat{\mu},-\mu}). \tag{2.89}$$

In both cases, one has the following commutation relations between $T_{x,\mu}$ and the link variables

$$[T_{x,\mu}, U_{y,\nu}] = 2\delta_{x,y}\delta_{\mu\nu} U_{x,\mu}, \tag{2.90}$$

which implies that the generator

$$G_x = \frac{1}{2}\sum_\mu (T_{x-\hat{\mu},\mu} - T_{x,\mu}) \tag{2.91}$$

generates an additional $U(1)$ gauge transformation, i.e.

$$\begin{aligned} U'_{x,\mu} &= \prod_y \exp(-i\alpha_y G_y) U_{x,\mu} \prod_z \exp(i\alpha_z G_z) \\ &= \exp(i\alpha_x) U_{x,\mu} \exp(-i\alpha_{x+\mu}). \end{aligned} \tag{2.92}$$

It is easy to show that the Hamilton operator (2.75) is invariant under the extra $U(1)$ symmetry and thus describes a $U(N)$ gauge theory.

It is non-trivial to understand how quantum links can describe QCD. Chandrasekharan and Wiese have constructed an $SU(2)$ quantum link model [20] with link matrices represented by $O(4)$-vectors. This leads to the embedding algebra $SO(5)$ instead of $SU(4)$.

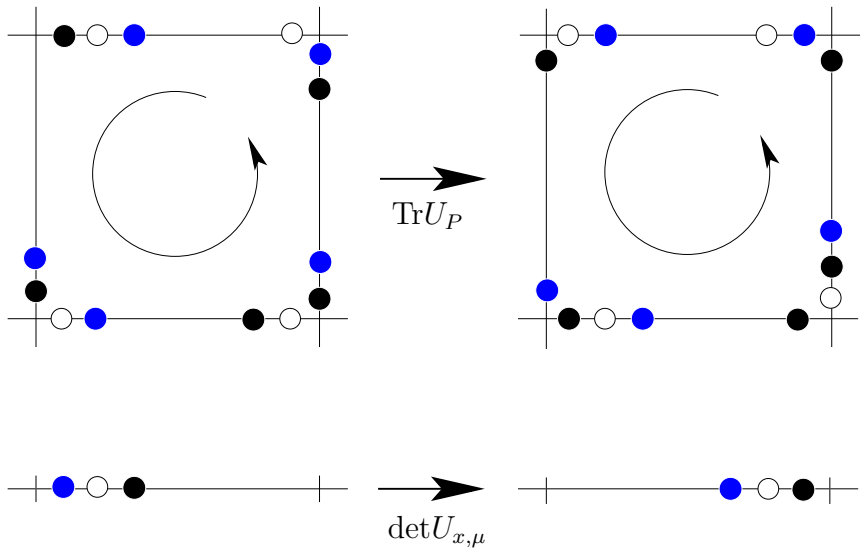

Figure 2.2: *The rishon dynamics: The trace part of the Hamiltonian induces hopping of colored rishons around the plaquette. The determinant part shifts a color-neutral combination of N rishons from one end of a link to the other.*

This construction does not contain the additional $U(1)$ gauge symmetry, but it cannot be generalized to other $SU(N)$ quantum link models. In fact, $SO(5) = Sp(2)$ and the generalization to higher N leads naturally to $Sp(N)$ quantum link models which are embedded in the algebraic structure of $Sp(2N)$. The solution for $SU(N)$ quantum link models is surprisingly simple, one just needs to break the additional $U(1)$ gauge symmetry by adding the real part of the determinant of each link matrix to the Hamilton operator

$$H = J \sum_{x,\mu\neq\nu} \mathrm{Tr}(U_{x,\mu} U_{x+\hat{\mu},\nu} U^{\dagger}_{x+\hat{\nu},\mu} U^{\dagger}_{x,\nu}) + J' \sum_{x,\mu} (\mathrm{det} U_{x,\mu} + \mathrm{det} U^{\dagger}_{x,\mu}). \qquad (2.93)$$

In analogy to the quantum $SU(N)$ chiral spin model, the $U(N)$ symmetry can be reduced to $SU(N)$ via the determinant only when one works with $\mathcal{N}_{x,\mu} = N$ rishons on each link. Again, this corresponds to choosing the $(2N)!/(N!)^2$-dimensional representation of $SU(2N)$ and corresponds to a totally anti-symmetric Young tableau with N boxes. The rishons dynamics is illustrated in figure 2.2. Note, for example, that the fundamental representation of $SU(2N)$ defined by (2.83) will not lead to an $SU(N)$ quantum link model because in that case the determinant in (2.93) is simply zero. Nevertheless, it is clear that the lattice photon, which comes from the extra $U(1)$ symmetry, and the $SU(N)$ lattice gluons will decouple in the continuum limit. Indeed, if one considers the low-energy effective action, the interaction terms scale as a^4 and vanish in the continuum limit as $a \to 0$. However, as long as one simulates the $SU(N) \otimes U(1)$ system on a lattice, one would have to deal with this extra lattice photon and with the interaction term.

2.5.2 $SO(N)$ quantum link models

Gauge theory can be formulated with various gauge groups. Let us now consider a lattice $SO(N)$ gauge theory. The classical Wilson action takes the form

$$S[o] = -\sum_{x,\mu\neq\nu} \mathrm{Tr}(o_{x,\mu} o_{x+\hat{\mu},\nu} o^{\dagger}_{x+\hat{\nu},\mu} o^{\dagger}_{x,\nu}), \tag{2.94}$$

where $o_{x,\mu}$ are real-valued classical orthogonal parallel transporter link matrices. The dagger in this expression reduces to a transpose. In D-theory, this classical action corresponds to the quantum operator

$$H = J \sum_{x,\mu\neq\nu} \mathrm{Tr}(O_{x,\mu} O_{x+\hat{\mu},\nu} O^{\dagger}_{x+\hat{\nu},\mu} O^{\dagger}_{x,\nu}). \tag{2.95}$$

The elements of the $N \times N$ quantum link variables $O_{x,\mu}$ consist of generators of $SO(2N)$. Again, gauge invariance implies that H commutes with the local generators G_x of gauge transformations which are given by

$$G^{ij}_x = \sum_{\mu} (R^{ij}_{x-\hat{\mu},\mu} + L^{ij}_{x,\mu}). \tag{2.96}$$

The rishon representation takes the form

$$\begin{aligned} O^{ij}_{x,\mu} &= -i(c^i_{x,+\mu} c^j_{x+\hat{\mu},-\mu} - c^j_{x+\hat{\mu},-\mu} c^i_{x,+\mu}), \\ L^{ij}_{x,\mu} &= -i(c^i_{x,+\mu} c^j_{x,+\mu} - c^j_{x,+\mu} c^i_{x,+\mu}), \\ R^{ij}_{x,\mu} &= -i(c^i_{x+\hat{\mu},-\mu} c^j_{x+\hat{\mu},-\mu} - c^j_{x+\hat{\mu},-\mu} c^i_{x+\hat{\mu},-\mu}). \end{aligned} \tag{2.97}$$

The "Majorana" rishon operators obey the anti-commutation relations

$$\{c^i_{x,\pm\mu}, c^j_{y,\pm\nu}\} = \delta_{xy}\delta_{\pm\mu,\pm\nu}\delta_{ij}. \tag{2.98}$$

2.5.3 Quantum link models with other gauge groups

Besides $SU(N)$ or $SO(N)$ gauge groups, there is a third main sequence, the symplectic gauge groups $Sp(N)$. One can indeed construct $Sp(N)$ quantum link models in complete analogy to the $SU(N)$ or $SO(N)$ cases. In section 2.3.5, we have constructed the D-theory representation of symplectic matrices. Similarly to the two other main Lie group sequences, one uses the embedding algebra of $Sp(2N)$. Indeed, a $Sp(N)$ matrix appears naturally considering the subgroup decomposition $Sp(2N) \supset Sp(N)_L \otimes Sp(N)_R$. In particular, the $Sp(1) = SU(2)$ quantum link model uses the embedding algebra $Sp(2) = SO(5)$, this case was discussed in detail in [20].

In fact, there are four infinite series of simple Lie algebra, generating what are called the classical groups. Strictly speaking, there is a difference between the sequence $SO(2N)$ and

$SO(2N+1)$ [71]. Cartan, who first discussed the classification of the Lie algebras, called the algebra $SU(n+1)$, $SO(2n+1)$, $Sp(n)$ and $SO(2n)$, A_n, B_n, C_n and D_n, respectively. Here, n denotes the rank of the group. Besides these series, there are the exceptional Lie groups G_2, F_4, E_6, E_7 and E_8, again the index denotes the rank. These groups have very interesting properties. In particular, the study of G_2 Yang-Mills theory has recently lead to interesting results [80, 81]. On the other hand, the search for a grand unified theory, based for example on groups $SU(5)$ or $SO(10)$, leads naturally to an interesting scenario with the E_6 algebra — the E_6 unification [71]. In the D-theory framework, these groups have to be treated on a case by case basis. Let us consider only the simplest of them, the group G_2 which is a subgroup of $SO(7)$. G_2 has rank 2 and 14 generators, it contains the $SO(7)$ generators o which satisfy the cubic constraint

$$T_{ijk} = T_{lmn} o^{li} o^{mj} o^{nk}. \tag{2.99}$$

T is a totally anti-symmetric tensor whose non-zero elements follow by anti-symmetrization from

$$T_{127} = T_{154} = T_{163} = T_{235} = T_{264} = T_{374} = T_{576} = 1. \tag{2.100}$$

These relations implies that (2.99) represents 7 non-trivial constraints which reduce the 21 generators of $SO(7)$ to the 14 of G_2. Therefore, in D-theory one needs 49 Hermitean generators to represent the 7×7 real matrix elements of the link variable. In addition, the embedding algebra must contain the $14 + 14 = 28$ generators of the $G_{2L} \otimes G_{2R}$ gauge symmetry at the two ends of the link. Altogether, this gives $49 + 28 = 77$ generators. It is tempting to try to embed this structure in E_6, which has 78 generators. However, this would not work since, according to Slansky's branching rules for all maximal subgroups [74], E_6 does not even contain $G_{2L} \otimes G_{2R}$ as a subgroup. Instead, one can use the embedding algebra of $SO(14)$, which is already used for $SO(7)$ quantum link model. $SO(14)$ has 91 generators and has the subgroup decomposition $SO(14) \supset G_{2L} \otimes G_{2R}$, which in the adjoint representation gives

$$\{91\} = \{14, 1\} \oplus \{7, 1\} \oplus \{1, 14\} \oplus \{1, 7\} \oplus \{7, 7\}. \tag{2.101}$$

Again, one cannot simply use the Hamiltonian operator of the $SO(7)$ quantum link model, but one has to add a term to the action operator (2.94) in order to explicitly break the $SO(7)$ symmetry down to G_2. This can be done in the following way

$$H = J \sum_{x,\mu\neq\nu} \mathrm{Tr}(O_{x,\mu} O_{x+\hat{\mu},\nu} O^{\dagger}_{x+\hat{\nu},\mu} O^{\dagger}_{x,\nu}) + J' \sum_{x,\mu} T_{ijk} T_{lmn} O^{li}_{x,\mu} O^{mj}_{x,\mu} O^{nk}_{x,\mu}. \tag{2.102}$$

Indeed, the additional term is G_2 but not $SO(7)$ invariant. This procedure is similar to the case of the $U(N)$ quantum link model, which can be reduced to the $SU(N)$ quantum link model.

2.6 Classical Gauge Fields from Dimensional Reduction of Quantum Links

In section 2.4, we have seen that, in the context of quantum spin models, dimensional reduction occurs naturally when one has spontaneous symmetry breaking of a global continuous symmetry. This yields massless Goldstone modes in the spectrum and an infinite correlation length. The situation is different when one deals with local symmetries. Indeed, as a gauge symmetry breaks down spontaneously, the Higgs mechanism prevents massless modes in the spectrum. Thus dimensional reduction cannot occur. Nevertheless, in this section we show that D-theory is completely general and can still be applied to abelian and non-abelian gauge theories.

2.6.1 $SU(N)$ gauge theories

Let us first consider $SU(N)$ non-abelian gauge theory in four dimensions. The action operator H of the corresponding quantum link model, defined on a 4-dimensional lattice, evolves the system in a fifth Euclidean dimension. The partition function of this quantum link model can be written as

$$Z = \mathrm{Tr}\exp(-\beta H), \tag{2.103}$$

and can be represented as a $(4+1)$-dimensional path integral. Note that the trace extends over all states propagating in the fifth dimension. As emphasized before, the spontaneous breaking of a gauge symmetry in four dimensions leads to massive gauge bosons in the spectrum. An essential ingredient, an infinite correlation length, is missing and therefore dimensional reduction cannot occur. Besides the Higgs phase, non-abelian gauge theory can also exist in a confined phase where the correlation length is also finite. Fortunately, non-abelian gauge theories formulated in five dimensions can also be in a Coulomb phase [82]. This has been verified in detail for 5-dimensional $SU(2)$ and $SU(3)$ gauge theory using the Wilson formulation [83]. The same is true for quantum link models if one considers sufficiently large representations of the embedding algebra $SU(2N)$ [24]. Whether the $(4+1)$-d $SU(N)$ quantum link model with a small representation of $SU(2N)$ still is in a Coulomb phase can only be checked with numerical simulations.

When a gauge theory is dimensionally reduced (we will describe the exact mechanism below), usually the Polyakov loop in the extra dimension appears as an adjoint scalar field in the 4-dimensional target theory. Here we want to obtain a 4-dimensional pure Yang-Mills theory after dimensional reduction. Therefore, we have to get rid of these extra charged scalar fields. This can be done if one does not impose Gauss' law for the state propagating in the extra unphysical dimension because the Polyakov loop is a Lagrange multiplier field that enforces the Gauss law. Therefore, we have not included a projection operator on an unphysical 5-dimensional Gauss law, such that gauge-variant states also propagate in the extra dimension. In the path integral, this implies that the fifth component of the gauge

field vanishes

$$A_5 = 0. \tag{2.104}$$

The physical 4-dimensional Gauss law is properly imposed, because the model contains non-trivial Polyakov loops in the Euclidean time direction which is part of the 4-dimensional lattice.

The leading terms in the low-energy effective action of 5-dimensional Coulombic gluons take the form

$$S[A] = \int_0^\beta dx_5 \int d^4x \, \frac{1}{2e^2} \left(\mathrm{Tr}\ F_{\mu\nu} F_{\mu\nu} + \frac{1}{c^2} \mathrm{Tr}\ \partial_5 A_\mu \partial_5 A_\mu \right), \tag{2.105}$$

which is just the standard 5-dimensional Yang-Mills action with $A_5 = 0$. Note that μ and ν run over the 4-dimensional indices only. The quantum link model leads to a 5-dimensional effective gauge theory characterized by the "velocity of light" c. The 5-dimensional gauge coupling $1/e^2$ is the analog of the spin stiffness ρ_s in the spin models. When $\beta = \infty$, we are in the Coulomb phase with massless gluons, and hence with an infinite correlation length ξ. At finite β with periodic boundary conditions in the extra-dimension, this theory has a 4-dimensional gauge invariance only because $A_5 = 0$. The extent of the extra dimension then becomes negligible compared with ξ and the theory appears to be dimensionally reduced to four dimensions.

In the $(2+1)$-dimensional quantum spin models with a finite extent in the extra dimension, the Hohenberg-Mermin-Wagner-Coleman theorem implies that the Goldstone bosons pick up a mass non-pertubatively. On the other hand, when the $(4+1)$-dimensional quantum link model is reduced dimensionally, the confinement hypothesis suggests that gluons are no longer massless. Indeed, as it was argued in [20], a glueball mass

$$\xi \propto \beta c \left(\frac{11 e^2 N}{48 \pi^2 \beta} \right)^{51/121} \exp\left(\frac{24 \pi^2 \beta}{11 N e^2} \right) \tag{2.106}$$

is expected to be generated non-pertubatively. Here $11N/48\pi^2$ is the one-loop β-function coefficient of $SU(N)$ gauge theory. In contrast to the spin models presented earlier in this thesis, the prefactor in the exponential is not known analytically. Finding this number would mean understanding deeply the origin of mass in nature. To leading order (for large β), the coupling constant g^2 of the 4-d $SU(N)$ Yang-Mills theory is related to the $SU(N)$ quantum link model by

$$\frac{1}{g^2} = \frac{\beta}{e^2}. \tag{2.107}$$

Thus, the continuum limit $g^2 \to 0$ of the 4-dimensional Wilson theory corresponds to sending the extent β of the fifth dimension to infinity. This is in complete analogy with what has been described for spin models. This should be no surprise since asymptotic freedom is at the center of this process. Indeed, thanks to that property, the correlation

length grows exponentially with β. To push further the analogy with spin models, one can again refer to figure 2.1, where the reduced theory is nothing else than a 4-dimensional Wilsonian lattice field theory with lattice spacing βc. Again, βc has nothing to do with the original lattice spacing of the quantum model. In fact, one could perform a block renormalization group transformation that averages the 5-dimensional field over cubic blocks of size β in the fifth direction in βc in the four physical other directions. The block centers would then form a 4-dimensional space-time lattice of spacing βc and the effective theory of the block average 5-dimensional field would indeed be a 4-dimensional lattice gauge theory.

Let us now consider the $d = 3$ case. Using D-theory, one can define a quantum link model in (3+1) dimensions. However, due to confinement, there is no massless mode in four dimensions and thus no infinite correlation length. Since we do not expect any universal behavior, the quantum system does not regularize a continuum field theory. However, it is known that QCD in four dimensions has a non-trivial topological vacuum structure and hence a θ-vacuum angle. The situation is analogous to the case of a 1-dimensional quantum spin chain discussed in section 2.1.4. In accordance with Haldane's conjecture, the $O(3) = CP(1)$ quantum spin chain displays an universal behavior because half-integer spins correspond to the massless 2-d $O(3) = CP(1)$ model at $\theta = \pi$. Similarly, it is possible that the 3-d $SU(N)$ quantum link model, with an appropriate representation of the embedding algebra $SU(2N)$, corresponds to the 4-dimensional Yang-Mills theory at $\theta \neq 0$. Again, such a theory may be massless. Simulating a model at non-trivial θ-vacuum angle with traditional approaches is an impossible task due to a complex action problem. This may perhaps be solved with the D-theory formulation, if the corresponding quantum model does not suffer from this problem. It might become possible to use powerful cluster algorithms to investigate numerically the non-trivial topological structure of field theories vacua.

2.6.2 $SO(N)$, $Sp(N)$ and $U(1)$ gauge theories

$SO(N)$ and $Sp(N)$ gauge theories are similar to the previous case. Using the 1- and 2-loop β function coefficients, it is straightforward to derive formulas for the asymptotic behavior of the correlation length of $SO(N)$ and $Sp(N)$ quantum link models. In the $Sp(N)$ case, one gets

$$\xi \propto \beta c \left(\frac{11e^2(N+1)}{48\pi^2\beta} \right)^{51/121} \exp\left(\frac{24\pi^2\beta}{11(N+1)e^2} \right), \tag{2.108}$$

while for $SO(N)$ with $N \geq 4$

$$\xi \propto \beta c \left(\frac{11e^2(N-2)}{48\pi^2\beta} \right)^{51/121} \exp\left(\frac{24\pi^2\beta}{11(N-2)e^2} \right). \tag{2.109}$$

The case $N = 3$ is already covered by (2.106), since $SO(3) \simeq SU(2)$.

The situation for 4-d abelian $U(1)$ gauge theory is analogous to the 2-dimensional XY model. Indeed, in contrast to non-abelian gauge theory, when one has dimensional reduction from five to four dimensions, there is no reason for the photons to pick up a mass. They can naturally exist in a Coulomb phase because they are not confined. Therefore, one has an infinite correlation length already at finite β, which implies dimensional reduction for sufficiently large β — not only in the $\beta \to \infty$ limit. Nevertheless, when β becomes too small, one enters the strong coupling phase which has a finite correlation length. If the phase transition is second order, one can reach a continuum limit and thus universal behavior by approaching the critical point β_c from below $\beta \to \beta_c$.

A $U(1)$ quantum link model in four dimensions can undergo dimensional reduction to three dimension because the 4-d $U(1)$ gauge fields can exist in a massless Coulomb phase. However, it is known that 3-d $U(1)$ gauge theories are always in a confined phase [84, 85]. Therefore the correlation length becomes finite after dimensional reduction. In fact, exactly as in non-abelian gauge theories in four dimensions, one has an exponentially large correlation length. Therefore, dimensional reduction occurs again only in the $\beta \to \infty$ limit. Hence, the universal behavior of $U(1)$ gauge theories both in three or four dimensions, is naturally contained in the framework of D-theory.

2.7 QCD as a Quantum Link Model: The Inclusion of Fermions

In order to describe a realistic quantum field theory such as QCD in the framework of D-theory, it is essential to include fermionic variables. This has been done in detail in [23] and will be reviewed here. Before discussing the full quantum link QCD with quarks, let us introduce the standard Wilson action with quarks

$$\begin{aligned} S[\bar{\psi},\psi,u] &= -\sum_{x,\mu\neq\nu} \mathrm{Tr}[u_{x,\mu}u_{x+\hat{\mu},\nu}u^{\dagger}_{x+\hat{\nu},\mu}u^{\dagger}_{x,\nu}] \\ &+ \frac{1}{2}\sum_{x,\mu}[\bar{\psi}_x\gamma_\mu u_{x,\mu}\psi_{x+\hat{\mu}} - \bar{\psi}_{x+\hat{\mu}}\gamma_\mu u^{\dagger}_{x,\mu}\psi_x] + M\sum_x \bar{\psi}_x\psi_x \\ &+ \frac{r}{2}\sum_{x,\mu}[2\bar{\psi}_x\psi_x - \bar{\psi}_x u_{x,\mu}\psi_{x+\hat{\mu}} - \bar{\psi}_{x+\hat{\mu}}u^{\dagger}_{x,\mu}\psi_x]. \end{aligned} \tag{2.110}$$

The variables $\bar{\psi}_x$ and ψ_x are independent Grassmann valued spinors associated with the lattice site x which obey canonical anti-commutation relations, γ_u are the Dirac matrices and M is the bare quark mass. The term proportional to r is the Wilson term which removes the unwanted lattice fermion doublers. As emphasized in the introduction, it breaks chiral symmetry explicitly. Normally, in Wilson's formulation, the bare quark bare mass must be fine-tuned appropriately in order to reach the continuum limit.

To obtain an $SU(N)$ quantum link model with quarks, we have to consider the Hamiltonian (2.93) and add the spinor part as well. In particular one has to replace $\bar{\psi}_x$ by the quantum operator $\Psi_x^\dagger \gamma_5$. The Hamilton operator which describes the evolution of the system in a fifth direction is given by

$$\begin{aligned} H &= J \sum_{x,\mu\neq\nu} \mathrm{Tr}[U_{x,\mu} U_{x+\hat{\mu},\nu} U_{x+\hat{\nu},\mu}^\dagger U_{x,\nu}^\dagger] + J' \sum_{x,\mu} [\mathrm{det} U_{x,\mu} + \mathrm{det} U_{x,\mu}^\dagger] \\ &+ \frac{1}{2} \sum_{x,\mu} [\Psi_x^\dagger \gamma_5 \gamma_\mu U_{x,\mu} \Psi_{x+\hat{\mu}} - \Psi_{x+\hat{\mu}}^\dagger \gamma_5 \gamma_\mu U_{x,\mu}^\dagger \Psi_x] + M \sum_x \Psi_x^\dagger \gamma_5 \Psi_x \\ &+ \frac{r}{2} \sum_{x,\mu} [2\Psi_x^\dagger \gamma_5 \Psi_x - \Psi_x^\dagger \gamma_5 U_{x,\mu} \Psi_{x+\hat{\mu}} - \Psi_{x+\hat{\mu}}^\dagger \gamma_5 U_{x,\mu}^\dagger \Psi_x]. \end{aligned} \tag{2.111}$$

In this expression, $\Psi_x^\dagger$ and Ψ_x are creation and annihilation operators with canonical anticommutation relations

$$\{\Psi_x^{ia\alpha}, \Psi_y^{jb\beta\dagger}\} = \delta_{xy}\delta_{ij}\delta_{ab}\delta_{\alpha\beta}, \ \{\Psi_x^{ia\alpha}, \Psi_y^{jb\beta}\} = \{\Psi_x^{ia\alpha\dagger}, \Psi_y^{jb\beta\dagger}\} = 0, \tag{2.112}$$

where (i,j), (a,b) and (α,β) are the color, flavor and Dirac indices, respectively. They have not been made explicit in (2.111). Since we have added fermions, the generator of an $SU(N)$ gauge transformation now takes the form

$$\vec{G}_x = \sum_\mu (\vec{R}_{x-\hat{\mu},\mu} + \vec{L}_{x,\mu}) + \Psi_x^\dagger \vec{\lambda} \Psi_x. \tag{2.113}$$

One can easily show that the Hamiltonian (2.111) commutes with G_x^a for all x. The dimensional reduction of fermions is a rather subtle issue. Following earlier work of Rubakov and Shaposhnikov [86], Kaplan studied the physics of a 5-dimensional system of fermions, which is always vector like, coupled to a 4-dimensional domain wall which is a topological defects in the 5-dimensional world [5]. The key observation is that a zero-mode of the 5-dimensional Dirac operator appears as a bound state localized on the the domain wall. From the point of view of the 4-dimensional domain wall, the zero mode represents a massless chiral fermion. The original idea of Kaplan was to construct lattice chiral gauge theory in that way. In D-theory, we also work with one more dimension, but for reasons totally unrelated to the chiral properties of fermions. We will see that this construction is completely natural for D-theory as well.

The Wilson formulation of lattice gauge theory suffers from a so-called fine tuning problem. Indeed, the bare quark mass has to be tuned very carefully in order to reach the chiral limit (where chiral symmetry is restored). In practice this is a problem in numerical simulations. Using Kaplan's proposal, Shamir solved this fine-tuning problem in a very elegant way [30]. The essential difference compared to Kaplan's original model is that one works with a 5-dimensional slab with a finite extent β of the fifth dimension and open boundary conditions for fermions at the two sides. Within this geometry, there are two

zero modes, one at each boundary, which correspond to one left- and one right-handed fermion in four dimensions. In fact, Shamir's method concentrates on the essential topological aspects which are encoded in the open boundary conditions.

This set-up fits naturally with the D-theory construction. In particular, the Hamiltonian (2.111) governs the evolution of the system in the extra dimension. In Shamir's construction, one also sets $A_5 = 0$. However, there are some minor differences between the implementation of this method in the standard formulation of lattice theory and in our quantum link models. In the standard formulation, one works with 4-dimensional gauge fields which are constant in the fifth dimension. In the D-theory formulation this is not the case. The non-trivial dynamics in the fifth dimension turns the discrete variables of quantum links into the continuous degrees of freedom of physical gluons. However, it is still correct to consider the physical gluon field as practically constant in the fifth dimension, because, due to asymptotic freedom, its correlation length grows exponentially with β.

If one considers open boundary conditions for the quarks and usual periodic boundary conditions for the gluons, one has to modify the D-theory partition function. It takes the form

$$Z = \mathrm{Tr}\langle 0| \exp(-\beta H)|0\rangle. \tag{2.114}$$

Note that in Shamir's formulation $r < 0$. The trace extends over the gluonic Hilbert space in order to implement periodic boundary conditions. We decompose the quark spinor operator into left and right components

$$\Psi_x = \begin{pmatrix} \Psi_{Rx} \\ \Psi^\dagger_{Lx} \end{pmatrix}. \tag{2.115}$$

The open boundary condition are realized by letting $\exp(-\beta H)$ act on the Fock state $|0\rangle$, which is annihilated by all right-handed Ψ_{Rx} and left-handed Ψ_{Lx}. Therefore, there are no left-handed quarks at the boundary $x_5 = 0$ and no right-handed quarks at the boundary $x_5 = \beta$ [87]. In that way, both quarks and gluons have zero modes localized on the brane.

In the presence of fermions, the low-energy effective action is modified to

$$\begin{aligned} S[\bar{\psi}, \psi, A_\mu] &= \int_0^\beta dx_5 \int d^4x \left[\frac{1}{2e^2} \left(\mathrm{Tr}(F_{\mu\nu} F_{\mu\nu}) + \frac{1}{c^2} \mathrm{Tr}(\partial_5 A_\mu \partial_5 A_\mu) \right) \right. \\ &+ \left. \bar{\psi} \left(\gamma_\mu (A_\mu + \partial_\mu) + m_q + \frac{1}{c'} \gamma_5 \partial_5 \right) \psi \right]. \end{aligned} \tag{2.116}$$

With $A_5 = 0$ and c' is the "velocity of light" of the quarks in the fifth direction. It is expected to be different from the velocity c of the gluons because in D-theory there is no symmetry between the 4-dimensional space-time and the extra dimension. This is, however, not a problem since we are only interested in the physics in four dimension.

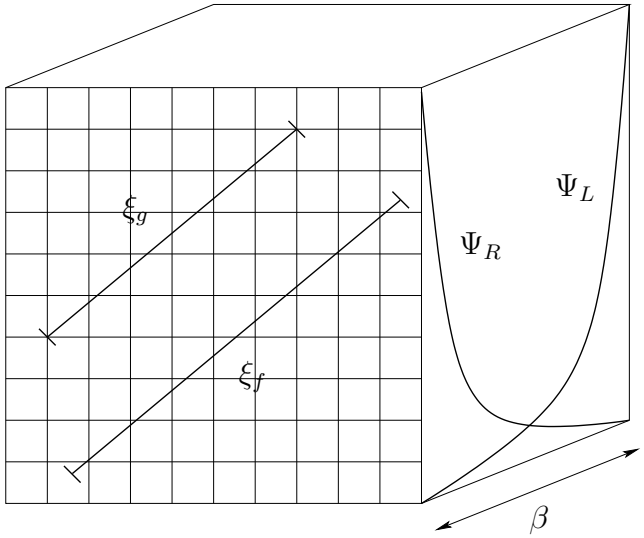

Figure 2.3: *Dimensional reduction of fermions in a 5-dimensional slab geometry: The gluonic correlation length ξ_g is exponentially large in β. The overlap of the fermionic wave-functions Ψ_L and Ψ_R generates a finite correlation length ξ_f which is exponentially large in the depth of the slab.*

Let us now be more precise. The confinement hypothesis prevents an infinite gluonic correlation length ξ_g as long as β remains finite. We know that, due to asymptotic freedom, ξ_g is exponentially large. We will now see that this is the case as well with quarks but for completely different reasons. Indeed, quarks cannot be massless because they pick up non-perturbatively a small mass $\mu = 1/\xi_f$ due to the tunneling process between the two boundaries. This has the effect to mix the left- and right-handed states and thus breaks the chiral symmetry explicitly. To make this argument more obvious, let us consider the Hamiltonian $\mathcal{H}(\vec{p})$, which describes the evolution of free quarks with spatial lattice momentum $\vec{p}$ in the time direction of the space-time lattice.

$$\mathcal{H}(\vec{p}) = \gamma_4 \left(\gamma_5 \partial_5 + M + \frac{r}{2} \sum_i \left(2 \sin \frac{p_i}{2} \right)^2 - i \sum_i \gamma_i \sin p_i \right). \tag{2.117}$$

Note the difference with H, which describes the evolution of the whole system in the extra dimension. The wave function of a stationary quark state with energy $E(\vec{p})$ is determined by the Dirac equation

$$\mathcal{H}(\vec{p})\Psi(\vec{p}, x_5) = E(\vec{p})\Psi(\vec{p}, x_5). \tag{2.118}$$

Let us consider states with lattice momenta $p_i = 0, \pi$. The state with $\vec{p} = \vec{0}$ describes a physical quark at rest, while the other states correspond to doubler fermions. Denoting the number of non-zero momentum components $p_i = \pi$ by

$$n = \sum_i \sin^2 \frac{p_i}{2}, \tag{2.119}$$

the above equation (2.118) then takes the form

$$\begin{aligned} -\partial_5 \Psi_L(\vec{p}, x_5) + (M + 2nr)\Psi_L(\vec{p}, x_5) &= E(\vec{p})\Psi_R(\vec{p}, x_5), \\ \partial_5 \Psi_R(\vec{p}, x_5) + (M + 2nr)\Psi_R(\vec{p}, x_5) &= E(\vec{p})\Psi_L(\vec{p}, x_5). \end{aligned} \tag{2.120}$$

Due to the open boundary conditions introduced before, we must solve these equations with $\Psi_L(\vec{p}, 0) = \Psi_R(\vec{p}, \beta) = 0$. Inserting the following ansatz in the Dirac equation

$$\Psi_L(\vec{p}, x_5) = A \sinh \alpha x_5, \;\; \Psi_R(\vec{p}, x_5) = \pm A \sinh \alpha(x_5 - \beta), \tag{2.121}$$

one immediately has

$$\alpha = (M + 2nr) \tanh \alpha\beta, \;\; M + 2nr = \pm E(\vec{p}) \cosh \alpha\beta. \tag{2.122}$$

This equation has a normalizable solution, and therefore a localized zero-mode, only if $M + 2nr > 0$. In that case, this implies $\alpha = \pm(M + 2nr)$ for large β and hence

$$E(\vec{p}) = \pm 2(M + 2nr) \exp(-(M + 2nr)\beta). \tag{2.123}$$

The important observation is that the bare mass parameter M is not the physical quark mass although we have considered an unrenormalized free theory. Let us first consider the doubler fermions which are characterized by $n > 0$. It is then possible to choose r such that $M + 2nr < 0$ for which no normalizable solution exists. Thus, for $r < -M/2$, i.e. for a sufficiently strong Wilson-term with an unconventional sign $r < 0$, the doubler fermions are removed from the physical spectrum. Their zero-modes cannot be localized on the brane. Thus, the mass of the physical fermion (characterized by $n = 0$) is

$$1/\xi_f = \mu = |E(\vec{0})| = 2M \exp(-M\beta), \tag{2.124}$$

which is exponentially small in β. This situation is illustrated in figure 2.3. The above result suggests how the fine-tuning problem of the fermion mass can be avoided. The confinement physics of quantum link QCD in the chiral limit takes place at a length scale

$$\xi_g = \frac{1}{m} \propto \exp\left(\frac{24\pi^2\beta}{(11N - 2N_f)e^2}\right), \tag{2.125}$$

which is determined by the 1-loop coefficient of the β-function of QCD with N_f massless quarks and by the 5-dimensional gauge coupling e. As long as one chooses

$$M > \frac{24\pi^2}{(11N - 2N_f)e^2}, \tag{2.126}$$

the chiral limit is reached automatically when one approaches the continuum limit by making β large. For a given value of r, one is limited by $M < -2r$ (note that $r < 0$). On the other hand, one can always choose J (and thus e^2) such that the above inequality is satisfied.

2.8 Conclusions and Comments

The D-theory framework provides a rich structure which allows us to formulate quantum field theory in an alternative non-perturbative way — in terms of discrete variables, the quantum spins and quantum links. The essential ingredients in D-theory are the existence of a massless phase in the $(d+1)$-dimensional quantum theory and the mechanism of dimensional reduction to the target d-dimensional field theory. In fact, dimensional reduction of discrete variables is a general phenomenon. In a $(d+1)$-dimensional quantum spin model with $d > 1$, it occurs because of spontaneous symmetry breaking, while in $(4+1)$-dimensional non-abelian quantum link models, it is due to the massless Coulomb phase in the 5-dimensional theory.

Remarkably, the inclusion of fermions is very natural in D-theory. One just follows Shamir's version of Kaplan's domain wall fermion proposal. Working in five dimensions allows us to solve the fine-tuning problem of Wilson fermions in a very elegant way. Moreover, it is important to note that D-theory treats bosons and fermions on an equal footing. Both are formulated in a finite Hilbert space per site, both require an extra dimension, and both have an exponentially large correlation length after dimensional reduction. Here, we have presented the theoretical picture in detail. D-theory is attractive both from a numerical and from an analytic point of view. This formulation has been used to treat unsolved problems in quantum field theory. On the analytic side, the discrete variables and the finite Hilbert space allow us to express the theory in terms of fermionic rishon constituents of bosonic fields. As in an antiferromagnet, where magnons can be viewed as composites of electrons that are hopping on a lattice, gluons in quantum link models can be viewed as composites of rishons. The rishons are lattice artifacts and hence have only a mathematical meaning. However, this formulation may be very useful when one studies the large N limit of various models [32]. From a computational point of view, one can investigate different field theory problems with powerful numerical methods developed for condensed matter systems (like the Heisenberg model). In particular, as will be presented in the next chapters, powerful cluster algorithms can be used to study the vacuum structure of the $CP(N-1)$ models [26, 35]. Recently, using D-theory, a new type of cluster algorithm was developed for the Ising model [88]. Although until now no efficient cluster algorithm has been found for quantum link models, these recent results seem promising for the future of the D-theory formulation.

To summarize, in D-theory the classical fields of ordinary quantum field theory arise via dimensional reduction of discrete variables. This requires a massless theory in one more dimension. It is a general structure which can be applied both to spin models and gauge theories. The dynamical picture in D-theory can be investigated analytically in the large N limit or for a large representation of the embedding algebra [24]. Numerical simulations are also essential to test the theory. The connection to ordinary field theory methods, such as perturbation theory, is rather unclear. Indeed, it seems hopeless to perform perturbative calculation in the D-theory framework. This can be viewed as a

potential weakness, but the large separation from perturbative methods may be a major strength of D-theory. Indeed, the fact that perturbative calculations are difficult may imply that the corresponding non-perturbative calculations are easier. After all, D-theory provides an additional non-perturbative structure underlying Wilson's lattice theory. In the next chapters, we will show that such a construction allows us to better understand $CP(N-1)$ models.

Chapter 3

The $CP(N-1)$ Model and Topology

Before turning to the D-theory version of the model in the next chapter, one would like to present in detail the usual formulation of the $CP(N-1)$ non-linear σ model. Like QCD, this type of model shows very interesting non-perturbative aspects. Among them are the non-trivial topology of the vacuum structure. Indeed, one of the characteristic features of these field theories is the existence of an integer-valued topological charge Q. This gives rise to an additional complex term $i\theta Q$ in the action, where θ is, a priori, a free parameter. The physical implications of a non trivial topology are numerous. For example in QCD, the existence of the topological charge offers an explanation of the notorious $U(1)$-problem — the question why the η' meson is not a Goldstone boson of the spontaneous chiral symmetry breaking. Unfortunately, it implies also some difficulties such as the strong CP problem — the question why θ seems to be zero in Nature.

In this thesis, we aim to study the $CP(N-1)$ model numerically at non-trivial θ-vacuum angle. As for QCD, one has to go beyond perturbation theory to investigate such situations. Wilson's lattice field theory offers a very rich non-perturbative framework which is already well established. However, this formulation has its own limits. In particular, adding a topological term to the action gives rise to complex Boltzmann weights. This is known as the complex action problem and has dramatic consequences in Monte Carlo simulations. It yields an exponential growth of the statistical error and the simulation time becomes unacceptably large. In the next chapter, we will show that this type of problem is completely avoided in the D-theory context. Here, we give a precise description of the $CP(N-1)$ model and show explicitly why it can be considered as a toy-model for QCD. In particular, we concentrate on the topological aspects and use some mathematical concepts such as homotopy theory. Dynamical consequences such as instanton configurations and the generation of a θ-vacuum structure are also investigated. Finally, we close this chapter with some remarks on the topological implications in QCD, the physical theory describing the strong interactions.

3.1 The 2-Dimensional $CP(N-1)$ Model

3.1.1 Introduction

Solving problems in a complicated quantum field theory like QCD implies a lot of technical difficulties and complex issues. Sometimes, it is easier to consider simpler models, which share some properties with the physical theory. For example, 2-dimensional non-linear σ models present a number of similarities with an $SU(N)$ Yang-Mills theory in four space-time dimensions. Indeed, as emphasized in the previous chapter, the $O(N)$-invariant non-linear σ model in two dimensions has a lot in common with QCD. However, this type of model is topologically trivial for $N \geq 4$ and stable instanton solutions are absent in contrary to the physical theory. In the late 70's, D'Adda, Di Vecchia and Lüscher considered and analyzed "a new series of $SU(N)$-symmetric non-linear σ models" [89] — the so-called $CP(N-1)$ models in two dimensions. They found topologically non-trivial configurations for all values of N. This offers a new framework to study QCD topological properties in the context of a simpler situation. Originally, this type of model was proposed by Eichenherr [90] (and independently by Golo and Perelomov [91] and also by Witten [92]), who showed for example that the case $N = 2$ is equivalent to the $O(3)$ model.

The $CP(N-1)$ model in two dimensions is a renormalizable field theory whose fields take values in the corresponding complex projective space. As introduced earlier in the context of the 2-d $O(3)$ model, which is equivalent to $CP(1)$, it displays dimensional transmutation. Although the classical theory does not contain any scale and is therefore scale-invariant, the renormalization procedure introduces a scale into the quantized theory. This occurs as well in non-abelian gauge theory and can be seen already with the perturbative approach. Moreover, the theory contains particles which are massless in perturbation theory but which acquire a mass in the leading $1/N$ approximation. In fact, these massive particles are confined. There is a linear potential between a particle-antiparticle pair which prevents an infinite separation of the two components. Remarkably, this happens without any fundamental gauge field in the theory. Historically, the $1/N$ expansion was envisaged because families of field theories become simpler as N gets larger. For a number of models, very interesting phenomena such as asymptotic freedom, spontaneous symmetry breaking, dimensional transmutation, or confinement show up in the large N expansion. In particular, this has been studied and reviewed in [93] for ϕ^4 theory, as well as for the Gross-Neveu and the $CP(N-1)$ models. The situation in QCD is less simple. One can apply a $1/N$ expansion (with N being the number of colors) but one does not know how to deal even with the leading term of the expansion. Of course, in the real world we have only three colors and an expansion in powers of $1/3$ may seem rather useless. However, one may argue as follows: in the perturbative approach to quantum electrodynamics, one expands in powers of the coupling e, which takes the value $e^2/4\pi = 1/137 \Leftrightarrow e \approx 0.3$. Therefore, a $1/N$ expansion for QCD cannot be rejected a priori and breakthroughs may well occur in that direction. For a review on QCD at large N see [94].

In general, the $CP(N-1)$ fields are massless Goldstone bosons resulting from the spontaneous symmetry breaking $SU(N) \to U(N-1)$. They live in the coset space $SU(N)/U(N-1)$. However, in two space-time dimensions, there is no spontaneous symmetry breaking of continuous global symmetries and hence no massless modes. Instead, the corresponding particles acquires a small mass non-pertubatively. Another important property is asymptotic freedom. As for QCD, the effective coupling constant falls when the energy scale grows. The $CP(N-1)$ model is also non-trivial topologically. It has an instanton topological charge leading to a non-trivial θ-vacuum structure for all N. In the coming sections, we will present further details about that structure. First, let us introduce the model a bit more precisely. Here, we will not describe the $1/N$ expansion of the model. For a good review on this subject one can refer once again to [93].

3.1.2 Classical formulation

The $CP(N-1)$ model has been intensively studied both analytically and numerically since its first formulation in 1978. It has been considered in the $1/N$ expansion [89, 95, 96] as well as within the lattice approach [97, 98, 99]. In the early 90's, the algorithmic improvements and the increasing power of computers have allowed new results on different aspects [100, 101, 102, 103, 104]. There are also different ways to define the model in the continuum. Here, we will try to be as complete as possible, following the seminal work done in [89].

Let us consider a general Lie group G and a subgroup $H \subset G$. By definition, the non-linear σ model is a theory of fields which take values in the coset space G/H. These fields can be defined on an arbitrarily curved two-dimensional space-time. Here we consider the case of a 2-dimensional Euclidean space. The coset space G/H can be identified with the $(N-1)$-dimensional complex projective space $CP(N-1)$ if we choose

$$G = SU(N),\ H = U(N-1). \tag{3.1}$$

This is the space of all equivalence classes $[z]$ of complex vectors $\vec{z} = (z_1, ..., z_N) \neq 0$. Two elements $\vec{z}$ and $\vec{z}\,'$ of a class are equivalent if

$$\vec{z}\,' = \lambda \vec{z}, \tag{3.2}$$

with $\lambda \in \mathbb{C}$. In order to write down the most general action for the $CP(N-1)$ model, let us consider fields of complex unit vectors $\vec{z}(x)$

$$\vec{z}(x) = (z_1(x), ..., z_N(x)), \quad z_\alpha \bar{z}_\alpha = |z_1|^2 + ... + |z_N|^2 = 1. \tag{3.3}$$

The equivalence relation (3.2) is reflected by a $U(1)$ gauge transformation

$$z'_\alpha(x) = e^{i\Lambda(x)} z_\alpha(x), \quad \alpha \in \{1, ..., N\}, \tag{3.4}$$

where the fields $z_\alpha(x)$ and $z'_\alpha(x)$ have to be considered as equivalent. One can now build an action which is invariant under the global transformation

$$\vec{z}\,'(x) = g\vec{z}(x), \tag{3.5}$$

where $g \in SU(N)$, and under the above $U(1)$ gauge transformation. As a necessary prerequisite, we introduce the following auxiliary gauge field

$$A_\mu = \frac{i}{2}(\bar{z}_\alpha \partial_\mu z_\alpha - z_\alpha \partial_\mu \bar{z}_\alpha). \tag{3.6}$$

Here, μ denotes the two space-time indices and A_μ transforms as an abelian gauge field

$$A'_\mu = A_\mu + \partial_\mu \Lambda. \tag{3.7}$$

Hence, the general action for the 2-dimensional $CP(N-1)$ model has the form

$$S[z] = \frac{1}{g^2}\int d^2x\ D_\mu z_\alpha \overline{D_\mu z_\alpha}, \quad D_\mu = \partial_\mu + iA_\mu. \tag{3.8}$$

As emphasized in the previous chapter, the $CP(1)$ model is equivalent to the $O(3)$ non-linear σ model. This latter is expressed in terms of spin fields $s^a(x)$, $a = 1, 2, 3$ of unit length $s^a(x)s^a(x) = 1$. Indeed, the $CP(1)$ model is locally isomorphic to the $O(3)$ model with the identification

$$s^a(x) = \bar{z}_\alpha(x)\sigma^a_{\alpha\beta} z_\beta(x), \tag{3.9}$$

where σ^a are the three Pauli matrices. This relation defines a map between the spin fields $s^a(x)$ onto gauge-equivalence classes of $CP(1)$ fields $z_\alpha(x)$.

For later convenience, it is useful to express the action (3.8) in a slightly different way. Using (3.6), one can write it as

$$S[z] = \frac{1}{g^2}\int d^2x\ (\partial_\mu z_\alpha \partial_\nu z_\alpha + (z\partial_\mu \bar{z}_\alpha)(z\partial_\nu \bar{z}_\alpha)). \tag{3.10}$$

Then, we introduce the projection matrix $P(x)$, which is related to the complex vector fields by

$$P_{\alpha\beta}(x) = z_\alpha(x)\bar{z}_\beta(x), \tag{3.11}$$

and has the following properties

$$P^\dagger(x) = P(x),\ P^2(x) = P(x),\ \mathrm{Tr}P(x) = 1. \tag{3.12}$$

Now expressing (3.10) with this projection matrix, we get the following action

$$S[P] = \frac{1}{2g^2}\int d^2x\ \mathrm{Tr}[\partial_\mu P \partial_\mu P]. \tag{3.13}$$

This formulation will be used later, when we will define the model in the D-theory framework. Note that the auxiliary field A_μ disappears in this notation. Of course, the action still has a global $SU(N)$ symmetry since the matrix field now transforms as

$$P'(x) = gP(x)g^\dagger, \tag{3.14}$$

where $g \in SU(N)$. Moreover, this model is invariant under charge conjugation C, which acts on P as

$$^C P(x) = P(x)^*. \tag{3.15}$$

3.2 Non-trivial Topological Structure of the $CP(N-1)$ Model

In this section, we will investigate the topological vacuum structure of the 2-dimensional $CP(N-1)$ model. In particular, we will show that instantons describe tunneling transitions between topologically distinct vacua for all values of N. This has the effect to lift the degeneracy of the classical vacuum and implies that the true quantum vacuum becomes a θ-state (a linear superposition of classical vacua), characterized by the vacuum angle $\theta \in [-\pi, \pi]$. This phenomenon occurs as well in non-abelian gauge theories and is completely inaccessible to perturbative methods. Before presenting the dynamical implications, let us first introduce the mathematical framework.

3.2.1 Topological aspects

The field configurations defined on a coset space G/H do not need to be continuously deformed into each other. In fact, they fall into equivalence classes, the so-called homotopy classes which represent distinct topological sectors. The elements of a class are fields which can be deformed continuously one into another. The homotopy group displays properties of the fields under continuous deformations and thereby describes their topological characteristics. In the 2-dimensional Euclidean space, the relevant group is the second homotopy group $\pi_2(G/H)$. It collects all the different homotopy classes, i.e. the classes of topologically equivalent field configurations. The index 2 indicates that we consider maps of the 2-dimensional space time $\mathbb{R}^2$ compactified to the sphere S^2, to the manifold G/H. Using homotopy theory and a theorem proved in [105, 106], one can identify the second homotopy group $\pi_2(G/H)$ to a simpler group, i.e.

$$\pi_2(G/H) = \pi_1(H). \tag{3.16}$$

Here, $\pi_1(H)$ denotes the fundamental homotopy group. Therefore, the topological structure of non-linear G/H σ models depends crucially on the stability group H. Note that the role of the fundamental homotopy group is to detect defects (such as a hole in a plane) as obstruction against letting loops in the manifold shrink to a point. For $SU(N)/U(N-1) =$

$CP(N-1)$ models, we have $G = SU(N)$ and $H = U(N-1)$. The above theorem naturally applies and one gets

$$\pi_2(CP(N-1)) = \pi_1(U(N-1)). \tag{3.17}$$

One can then locally identify the $SU(N)$ space as a direct product of spheres, this yields the following decompositions

$$\begin{aligned} SU(N) &\sim S^3 \otimes S^5 \otimes ... \otimes S^{2N-1}, \\ U(N) = SU(N) \otimes U(1) &\sim S^1 \otimes S^3 \otimes S^5 \otimes ... \otimes S^{2N-1}, \end{aligned} \tag{3.18}$$

where $U(1) \equiv S^1$. Therefore, we can locally identify the $CP(N-1)$ manifold with a $(2N-1)$-dimensional sphere to which all points in circles S^1 are identified with single points in S^{2N-1}, i.e.

$$CP(N-1) = \frac{SU(N)}{U(N-1)} \sim \frac{S^{2N-1}}{S^1}, \tag{3.19}$$

where S^N denotes the N-dimensional sphere. Using (3.17), it is clear that the relevant homotopy group of the model is $\pi_1(S^1)$. This group classifies maps from the one-dimensional sphere S^1 to the space $U(1)$, which is also S^1. Let us now investigate the topological implications of such map. We define an arbitrary phase χ on S^1, with the properties

$$\chi(0) = 0, \quad \chi(2\pi) = 2\pi m. \tag{3.20}$$

This can be deformed continuously into the linear function $\chi(\vartheta) = m\vartheta$. Indeed, one can define a homotopy (or deformation) of the map $g : S^1 \to U(1)$ with the parametrization

$$F(\vartheta, t) = (1-t)\chi(\vartheta) + t\vartheta\frac{\chi(2\pi)}{2\pi} \tag{3.21}$$

and with the boundary conditions

$$F(0,t) = (1-t)\chi(0) = 0, \quad F(2\pi, t) = \chi(2\pi) = 2\pi m. \tag{3.22}$$

The equivalence classes are hence characterized by the winding number $m \in \mathbb{Z}$. Since they are additive as one traverses two loops, we obtain the corresponding fundamental homotopy group

$$\pi_1(S^1) = \pi_1(U(1)) = \mathbb{Z}, \tag{3.23}$$

which is non-trivial. This means that going around the circle S^1, the map may cover the group space $U(1)$ any number of times $m \in \mathbb{Z}$. For each integer, there is an equivalence class of maps that can be continuously deformed into one another. This result can be generalized to higher dimensional spheres S^N, for which the corresponding fundamental homotopy groups are trivial for $N \geq 2$. This is illustrated by the following example. Let us consider the 2-dimensional sphere. Each closed curve on a ordinary sphere can be constricted to the north pole. The corresponding map is hence topologically trivial, i.e.

$$\pi_1(S^2) = \{0\}. \tag{3.24}$$

Also, for general $N \geq 2$ one has

$$\pi_1(S^N) = \{0\}. \tag{3.25}$$

To be complete, let us now turn to the $SU(N-1)$ case and its fundamental homotopy group. We start with the $SU(2)$ topological space. As usual, any element U of $SU(2)$ can be parametrized as

$$U = e^{i\vec{\tau}\cdot\vec{\varphi}} = \cos(\varphi) + i\vec{\tau}\cdot\vec{\varphi}\sin(\varphi) = a + i\vec{\tau}\cdot\vec{b}, \tag{3.26}$$

where $\vec{\tau}$ is a vector of Pauli matrices and $\vec{\varphi}$ an arbitrary vector. Unitarity implies the following restriction on a and b

$$UU^\dagger = (a + i\vec{\tau}\cdot\vec{b})(a - i\vec{\tau}\cdot\vec{b}) = a^2 + b^2 = 1. \tag{3.27}$$

This shows the topological equivalence (homeomorphism) between the $SU(2)$ group space and the 3-dimensional sphere,

$$SU(2) \sim S^3. \tag{3.28}$$

The spaces can be mapped continuously and bijectively onto each other and they possess the same connectedness properties. This confirms also the relations (3.18). According to (3.25), the corresponding fundamental homotopy group is trivial and so are the homotopy groups for higher N.

To summarize, the topological properties of the $CP(N-1)$ models are determined by the second homotopy group

$$\pi_2(CP(N-1)) = \pi_1(SU(N-1)\otimes U(1)) = \pi_1(S^1) = \mathbb{Z}. \tag{3.29}$$

Again, this means that for each integer in $\mathbb{Z}$ there is an equivalence class of maps that can be deformed continuously into one another. The distinct topological sectors are labeled by the topological charge Q. Thus, for any field configuration $\vec{z}(x)$, the topological charge Q is an integer. It labels the homotopy classes in a one to one fashion, which means that two fields with the same charge can be deformed continuously into one another. For any integer m, there exist fields with $Q = m$. In the $CP(N-1)$ model we consider maps of the form

$$g : S^2 \to CP(N-1), \tag{3.30}$$

One has shown that this map is topologically identical to

$$g : S^1 \to S^1, \tag{3.31}$$

where the corresponding topological charge counts how many times g covers the circle as one covers S^1 once. This number is an integer and, in our case, is defined as

$$Q[z] = -\frac{i}{2\pi}\epsilon_{\mu\nu}\int d^2x\ D_\mu z_\alpha \overline{D_\nu z_\alpha} = \frac{i}{2\pi}\int d^2x\ \epsilon_{\mu\nu}\bar{z}_\alpha D_\nu D_\mu z_\alpha, \tag{3.32}$$

with $\epsilon_{\mu\nu}$ the usual antisymmetric tensor and $\epsilon_{12}=1$. Let us prove that Q expressed in that form is indeed an integer. One first constructs a field strength from the gauge composite field A_μ

$$F_{\mu\nu}=\partial_\mu A_\nu-\partial_\nu A_\mu. \tag{3.33}$$

This yields

$$F_{\mu\nu}=i\epsilon_{\mu\nu}[D_\nu,D_\mu]=2i\epsilon_{\mu\nu}D_\mu D_\nu. \tag{3.34}$$

Therefore, using (3.3), one gets

$$Q(z)=\frac{1}{4\pi}\int d^2x\ \epsilon_{\mu\nu}F_{\mu\nu}. \tag{3.35}$$

The integrand in this integral is a total divergence, i.e.

$$\frac{1}{2}\epsilon_{\mu\nu}F_{\mu\nu}=\partial_\mu\epsilon_{\mu\nu}A_\nu. \tag{3.36}$$

Substituting this result in (3.35) and using the Gauss law, one integrates over a large disc of radius R and obtains

$$Q[z]=\frac{1}{2\pi}\lim_{R\to\infty}\oint_{|x|=R}dx_\mu\ A_\mu(x). \tag{3.37}$$

The topological charge hence depends only on the behavior of the solution for large $|x|$. If we want to have a finite action, at large distances $D_\mu\vec{z}$ vanishes, therefore

$$D_\mu\vec{z}=0\ \Rightarrow\ [D_\nu,D_\mu]\vec{z}=F_{\mu\nu}\vec{z}=0. \tag{3.38}$$

Of course, $\vec{z}\neq 0$ and this relation implies that the tensor $F_{\mu\nu}$ vanishes. Thus A_μ has to be in a pure gauge, i.e.

$$A_\mu=\partial_\mu\Lambda(x)\ \Rightarrow\ Q(z)=\frac{1}{2\pi}\lim_{R\to\infty}\oint_{|x|=R}dx_\mu\ \partial_\mu\Lambda(x)\in\mathbb{Z}. \tag{3.39}$$

As a consequence, the topological charge measures the variation of the angle $\Lambda(x)$ on a large circle, which is a multiple of 2π because $\vec{z}$ is regular. Hence, once we divide by 2π, Q is indeed an integer $m\in\mathbb{Z}$. To summarize, the homotopy classes of the maps from S^1 to S^1 are characterized by an integer winding number m.

3.2.2 Instantons and θ-vacuum structure

We have demonstrated mathematically that the field configurations of the $CP(N-1)$ model fall into topologically different classes, the homotopy classes. Now, one would like to construct a concrete example of topologically non-trivial field configurations. Here we consider instantons solution of the classical Euclidean field equations. They describe tunneling processes between degenerate classical vacuum states and occur at a given instant in Euclidean time. We will see that their existence gives rise to the θ-vacuum structure

of the $CP(N-1)$ model. Instantons are field configurations with a non-zero topological charge $Q \neq 0$ that are solutions of the Euclidean classical equation of motion. Therefore, they are minima of the Euclidean action (3.8). Let us consider the following integral

$$\int d^2x \; |D_\mu z_\alpha \pm i\epsilon_{\mu\nu} D_\nu z_\alpha|^2 \geq 0. \tag{3.40}$$

We integrate a square, therefore the integral is positive. Expanding the integrand, one gets

$$\begin{aligned}
&\int d^2x \; [D_\mu z_\alpha \pm i\epsilon_{\mu\nu} D_\nu z_\alpha][\overline{D_\mu z_\alpha} \mp i\epsilon_{\mu\rho}\overline{D_\rho z_\alpha}] = \\
&\int d^2x \; [D_\mu z_\alpha \overline{D_\mu z_\alpha} \pm i\epsilon_{\mu\nu} D_\nu z_\alpha \overline{D_\mu z_\alpha} \mp i\epsilon_{\mu\nu} D_\mu z_\alpha \overline{D_\nu z_\alpha} + \epsilon_{\mu\nu}\epsilon_{\mu\rho} D_\nu z_\alpha \overline{D_\rho z_\alpha}] = \\
&\int d^2x \; [D_\mu z_\alpha \overline{D_\mu z_\alpha} \pm 2i\epsilon_{\mu\nu} D_\nu z_\alpha \overline{D_\mu z_\alpha} + D_\mu z_\alpha \overline{D_\mu z_\alpha}] = \\
&\int d^2x \; 2[D_\mu z_\alpha \overline{D_\mu z_\alpha} \pm 2i\epsilon_{\mu\nu} D_\nu z_\alpha \overline{D_\mu z_\alpha}] = 2g^2 S[z] \pm 4\pi Q[z] \geq 0.
\end{aligned} \tag{3.41}$$

From the positivity of the integral, it is clear that

$$S[z] \geq \frac{2\pi}{g^2}|Q[z]|. \tag{3.42}$$

The topologically non-trivial field configurations hence costs a minimum action proportional to the topological charge. Instantons are configurations with absolute minimum action in a sector with definite topological charge. Therefore, for them one has

$$S[z] = \frac{2\pi}{g^2}|Q[z]|. \tag{3.43}$$

This equality corresponds to a minimum and implies that the classical solutions satisfy the equation

$$D_\mu \vec{z} = \pm i\epsilon_{\mu\nu} D_\nu \vec{z}. \tag{3.44}$$

Instantons (and anti-instantons) are the solutions of this first order differential equation. One can solve it by expressing the spatial coordinates in terms of complex variables $w = x_1 + ix_2$ and $\bar{w} = x_1 - ix_2$, and write the previous relation as [107]

$$\begin{aligned}
\partial_w \vec{z}(w,\bar{w}) &= -iA_w(w,\bar{w})\vec{z}(w,\bar{w}) \\
\partial_{\bar{w}} \vec{z}(w,\bar{w}) &= -iA_{\bar{w}}(w,\bar{w})\vec{z}(w,\bar{w}).
\end{aligned} \tag{3.45}$$

Solving the second equation (the first one can be solved in the same way exchanging z_α and $\bar{z}_\alpha$), one can write

$$z_\alpha(w,\bar{w}) = \kappa(w,\bar{w})P_\alpha(w), \tag{3.46}$$

where $\kappa(w,\bar{w})$ is a particular solution of

$$\partial_{\bar{w}}\kappa(w,\bar{w}) = -iA_{\bar{w}}(w,\bar{w})\kappa(w,\bar{w}). \tag{3.47}$$

The gauge invariance allows us to take $\kappa(w,\bar{w})$ real and (3.3) also implies

$$\kappa^2(w,\bar{w})P_\alpha\bar{P}_\alpha = 1. \tag{3.48}$$

The functions $P_\alpha(w)$ have nothing to do with the matrix field variable introduced in section 3.1.2. For reasons related to the asymptotic conditions of the fields $z_\alpha(x)$ (finiteness of the action), the $P_\alpha(w)$ have to be polynomial and one has, asymptotically,

$$P_\alpha(w) \sim c_\alpha w^m. \tag{3.49}$$

With this relation and (3.48) one gets an instanton configuration which takes the form

$$z_\alpha(w,\bar{w}) \sim \frac{c_\alpha}{|\vec{c}|}(w/\bar{w})^{m/2}. \tag{3.50}$$

As expected, once we vary the phase of w by 2π, the phase of z_α varies by $2m\pi$, where m is the corresponding winding number.

Instanton solutions have drastic effects on the vacuum structure of the $CP(N-1)$ model. Classically, there is a ground state for each topological winding number. The tunneling transitions between these distinct vacua, described by instantons, lift the degeneracy of the classical vacuum and the true quantum vacuum turns out to be a θ-state in which configurations with different winding numbers are mixed. Let us be a bit more precise. In the following, we consider the temporal gauge $A_2 = 0$ which leaves space-dependent gauge transformations unfixed. A classical vacuum state is given by

$$z_\alpha(x_1) = e^{i\Lambda(x_1)}v_\alpha, \quad v_\alpha\bar{v}_\alpha = 1, \tag{3.51}$$

where $\vec{v}$ is a constant vector and x_1 the space variable. Again, the classical vacua are classified by their winding number

$$n \in \pi_1(S^1) = \mathbb{Z}, \tag{3.52}$$

and one has a periodic structure. Moreover if the ground state is invariant under space reflection, one has $z_\alpha(-\infty) = z_\alpha(\infty)$ and therefore from (3.39)

$$\Lambda(-\infty) - \Lambda(\infty) = 2\pi n. \tag{3.53}$$

Let us now construct the quantum vacuum state. We first consider small quantum fluctuations around a classical vacuum with given n, which defines a quantum state $|n\rangle$. However, quantum tunneling induces transitions between the various classical vacua, so not only small fluctuations have to be considered. Instead, let us take a large rectangle with extent R in the space dimension and $T = |t_1 - t_0|$ in the Euclidean time direction. Imagine the system in a vacuum state with winding number n at an early time t_0. By a smooth gauge transformation, one puts the instanton solution in the temporal gauge and finally at a time

t_1, it returns to a classical state with winding number m. Then the variation of the pure gauge ($A_\mu = \partial_\mu \Lambda(x)$) comes entirely from the sides at fixed time. For $R \to \infty$, one gets

$$Q \propto \frac{1}{2\pi} \left[\Lambda(\infty, t_0) - \Lambda(-\infty, t_0)\right] - \left[\Lambda(\infty, t_1) - \Lambda(-\infty, t_1)\right] = (n - m). \tag{3.54}$$

As $t_0 \to -\infty$ and $t_1 \to \infty$, the time evolution corresponds to a specific path in the Feynman path integral. The instantons interpolate between different classical vacua. Hence, an instanton configuration with topological charge $Q = m - n$ induces a transition from a classical vacuum with winding number n to one with winding number $m = n + Q$. Writing it as a Feynman path integral that describes the amplitude from one classical vacuum to another with a field configuration restricted to a topological sector Q, one has

$$\langle m|U(-\infty, \infty)|n\rangle = \int \mathcal{D}z^{(m-n)} \exp(-S[z]), \tag{3.55}$$

where $U(t_1, t_0)$ is the time evolution operator and $z^{(Q)}$ the instanton field configuration with topological charge Q. A gauge transformation thus relates the different classical vacua of the model. In the quantum theory, such a transformation can be implemented by a unitary operator T, which acts on a wave functional $\Psi[z]$ as

$$T\Psi[z] = \Psi[gz], \tag{3.56}$$

where g denotes a $U(1)$ gauge transformation. Acting on a state describing small quantum fluctuations around a classical ground state, one finds

$$T|n\rangle = |n + 1\rangle. \tag{3.57}$$

Since the ladder operator T implements a gauge transformation in a gauge-invariant model, it has to commute with the Hamiltonian H. This implies

$$[H, T] = 0, \tag{3.58}$$

and each eigenstate of the Hamiltonian can be labeled by an eigenvalue of T. Eigenvalues of a unitary operator are complex phases $\exp(i\theta)$, for example, for the vacuum state $|\theta\rangle$ one has

$$T|\theta\rangle = \exp(i\theta)|\theta\rangle. \tag{3.59}$$

On the other hand, one can build the θ-vacuum state as a linear combination of states $|n\rangle$

$$|\theta\rangle = \sum_n c_n |n\rangle. \tag{3.60}$$

Using the following argument, one can easily specify the coefficients c_n

$$\begin{aligned} T|\theta\rangle &= \sum_n c_n T|n\rangle = \sum_n c_n |n+1\rangle \\ &= \sum_n c_{n-1}|n\rangle = \exp(i\theta) \sum_n c_n |n\rangle. \end{aligned} \tag{3.61}$$

This clearly implies

$$c_{n-1} = \exp(i\theta)c_n \;\Rightarrow\; c_n = \exp(-in\theta), \tag{3.62}$$

and the vacuum state can be finally expressed as

$$|\theta\rangle = \sum_n \exp(-in\theta)|n\rangle. \tag{3.63}$$

As expected, the true vacuum of the quantum $CP(N-1)$ model is a linear combination of classical ground states with different winding numbers. To each value of θ corresponds a vacuum state. This is analogous to the energy band in a solid, where as a consequence of the discrete translation symmetry a state is labeled by a Bloch momentum. Let us see whether one can have transitions between two θ-vacua,

$$\begin{aligned}
&\langle\theta|U(\infty,-\infty)|\theta'\rangle = \sum_{n,m} \exp(im\theta)\exp(-in\theta')\langle m|U(\infty,-\infty)|n\rangle \\
&= \sum_{m,Q=m-n} \exp(im\theta - i(m-Q)\theta') \int \mathcal{D}z^{(Q)} \exp(-S[z]) \\
&= \delta(\theta-\theta')\sum_Q \int \mathcal{D}z^{(Q)} \exp(-S[z])\exp(i\theta Q[z]) = \int \mathcal{D}z \exp(-S_\theta[z]).
\end{aligned} \tag{3.64}$$

This confirms that there are no possible transitions between different θ-vacua, which means that they are eigenstates. It is now possible to express the action in a non-trivial topological sector ($\theta \neq 0$) as

$$S_\theta[z] = S[z] - i\theta Q[z], \tag{3.65}$$

where $S[z]$ and $Q[z]$ are given by (3.8) and (3.32). This is an important result, since in the next chapter we will investigate the model at the non-trivial angle $\theta = \pi$. Finally, in terms of the matrix variable $P(x)$ (3.11), the topological charge takes the form

$$Q[P] = \frac{1}{2\pi i}\int d^2x\ \epsilon_{\mu\nu}\ \mathrm{Tr}[P(x)\partial_\mu P(x)\partial_\nu P(x)]. \tag{3.66}$$

The factor i is needed here to obtain a real answer because the integral is purely imaginary.

3.3 Topological Consequences in QCD

There has been considerable interest in the subject of topology in field theory, especially also on the lattice. In particular, the $CP(N-1)$ model offers a perfect framework to analyze different mechanisms that can occur as well in QCD. Indeed, in the physical theory classical vacuum field configurations are characterized by an integer winding number from the homotopy group $\pi_3(SU(N)) = \mathbb{Z}$. Hence, one has as well instantons with topological charge Q that describe tunneling between topologically distinct vacua. Again, a θ-vacuum

structure and the vacuum angle manifests itself as an additional term $i\theta Q$ in the Euclidean action with

$$Q = -\frac{1}{32\pi^2}\int d^4x\ \epsilon_{\mu\nu\rho\sigma}\mathrm{Tr}[F_{\mu\nu}(x)F_{\rho\sigma}(x)]. \tag{3.67}$$

The gluon field strength $F_{\mu\nu}$ is defined for non-abelian gauge theories as

$$F_{\mu\nu}(x) = \partial_\mu A_\nu(x) - \partial_\nu A_\mu(x) + g^2[A_\mu(x), A_\nu(x)], \tag{3.68}$$

where g^2 is the dimensionless coupling constant of the 4-d $SU(3)$ Yang-Mills theory already introduced in section 2.6.1 for $SU(N)$ pure gauge theory. Adding such a topological term in the action has an influence on the symmetries both in QCD and in the $CP(N-1)$ model. In the first case, this term explicitly breaks the CP symmetry for $\theta \neq 0, \pi$. As a physical consequence, the electric dipole moment of the neutron would have a value proportional to θ, while without a θ-term (and thus without CP violation), such a dipole moment vanishes. In fact, the observed dipole moment of the neutron is indistinguishable from zero, which puts a strong bound on the vacuum angle, i.e. $|\theta| < 10^{-9}$. Understanding why in nature θ seems to be zero is known as the "strong CP-problem".

The non-trivial topology of the gauge fields offers a nice explanation of another puzzling problem, the so-called "$U(1)$-problem". In the standard model of particle physics, the non-trivial topology in $SU(2)_L$ gauge fields gives rise to a violation of the baryon number conservation law. Similarly, the non-trivial topology of gluons fields in QCD leads to the explicit breaking of the flavor-singlet axial symmetry. This observation allowed 't Hooft to understand the so-called $U(1)$-problem of QCD — the question why the η' meson is not a Goldstone boson of spontaneous chiral symmetry breaking. The chiral symmetry of the classical massless QCD Lagrangian is $SU(N_f)_L \otimes SU(N_f)_R \otimes U(1)_L \otimes U(1)_R$, while in the spectrum only the flavor and baryon number symmetries $SU(N_f)_{L+R} \otimes U(1)_{L=R}$ are manifest. According to the Goldstone theorem, one might expect N_f^2 Goldstone bosons, while one has only $N^2 - 1$ Goldstone bosons in QCD. The candidate for the missing particle is the meson η'. However, its mass is far too heavy to be a Goldstone boson. The clue is then to understand why the $U(1)$ axial symmetry is not spontaneously broken, although it is not manifest in the spectrum. 't Hooft realized that this $U(1)$ axial symmetry does not survive quantization and is therefore not a symmetry of QCD. In fact, it is explicitly broken by the Adler-Bell-Jackiw anomaly [108], the corresponding current is not conserved after quantization. More precisely, the topologically non-trivial gauge configurations of the gluon fields (for example the instantons) give mass to the η'-meson. More on the chiral anomaly and on topological concepts in gauge theories can be found in [107, 109].

The strong CP and $U(1)$ problems are in fact closely related. Naively one can hope to solve the strong CP problem by considering that gluon fields with $Q \neq 0$ are very much suppressed. However, this would not work because one needs frequent gluon configurations with $Q \neq 0$ in order to solve the $U(1)$-problem. Thus, solving the strong CP problem in that way will not help much since we will immediately face again the $U(1)$-problem.

A nice solution of both questions was proposed by Peccei and Quinn in [110, 111]. They suggested to go beyond the standard model and introduce a model with two Higgs doublets instead of one. The second Higgs field allows to rotate θ away and implies an extra global $U(1)_{PQ}$ symmetry which breaks down spontaneously. Later Weinberg and Wilczek pointed out that this leads to the creation of a new pseudo-Goldstone boson called the axion. This particle has so far not been detected by experiments, hence it is still unclear whether this scenario is the right solution of the strong CP problem. Nevertheless, the spontaneous symmetry breaking scale can be shifted to higher energies, making the axion at the moment impossible to detect. If axions exist, they could well play a major role in the Universe. Although weakly coupled to ordinary matter, they are massive and could be a dark matter candidate. Moreover, the spontaneous breakdown of a $U(1)$ symmetry is always accompanied by the generation of topological defects, in our case, the generation of cosmic strings. Therefore, if the axion exists, axionic cosmic strings should be present as well. These topological excitations could then radiate energy by emitting axions.

Chapter 4

Study of $CP(N-1)$ θ-Vacua Using D-Theory

4.1 Introduction

In this chapter, we will illustrate the efficiency of the D-theory formulation in the case of $CP(N-1)$ model. Previously, we have described the algebraic structure of various D-theory models both with global and gauge symmetries. This was already some achievement, but it is also important to show explicitly that our alternative regularization allows us to solve problems which are not accessible with the Wilson traditional non-perturbative approach. Typically, the topological structure of the vacuum and hence the non-trivial topology of field theories is among that type of problems. In the previous chapter, we have presented the classical continuum formulation of the $CP(N-1)$ model. In particular, we have seen that this model is topologically non-trivial, and hence has a θ-vacuum structure.

As emphasized before, the 2-dimensional $CP(N-1)$ model and its topological vacuum structure have been intensively studied on the lattice. First, for large values of N, the theory is linearly confining at $\theta = 0$ with particle-anti-particle bound states [89, 92]. Further more, at $\theta = \pi$ it has been conjectured that the model has a phase transition. In the large N limit, the charge conjugation C and the parity P are spontaneously broken and the phase transition is known to be first order [112, 113]. The mass-gap reduces by approximately a factor of two but remains finite. In the strong coupling region, Seiberg showed that C and P are spontaneously broken for all N [113]. However, for $N = 2$, the model corresponds to the 2-dimensional $O(3)$ model and the phase transition is known to be second order at $\theta = \pi$. Indeed, following Haldane's arguments, the $CP(1)$ model can be obtained from the large spin s limit of a quantum antiferromagnetic spin chain [54, 55, 56]. The consequence is a second order phase transition with a vanishing mass-gap. This has been verified numerically with a meron-cluster algorithm by Bietenholz, Pochinsky, and Wiese in [66]. Nevertheless, Seiberg's statement is still correct, since at strong coupling one indeed has spontaneously broken C and P symmetries for all N. In the weak coupling

phase, C and P are unbroken for $N = 2$ with a diverging correlation length. Based on these results, Affleck has later conjectured that the situation is so for $N = 2$ but not for larger values of N where the phase transition should be first order at $\theta = \pi$ for $N \geq 3$ [114, 115].

The only way to decide the validity of this conjecture is to perform reliable numerical simulations. However, Monte Carlo simulations at $\theta = \pi$ in the usual Wilson framework are extremely difficult. Indeed, there is a severe sign problem due to the complex topological term in the action. As emphasized before, the complex Boltzmann weights imply an increasing statistical error for $\theta \neq 0$. Nevertheless, many attempts have been made in that direction. It turns out that none of them was able to get rid of the sign problem and thus to give a clear answer concerning the above conjecture. Studies have been performed for moderate volumes and in the strong coupling region in [116, 117] or they rely on additional extra assumptions [118, 119, 120]. Other more direct studies, which also suffer from the sign problem can be found in [121, 122]. Numerical investigations of the $CP(N-1)$ models are far from being straightforward even at $\theta = 0$. In the case of the $O(N)$ non-linear σ model, one can construct an efficient Wolff-cluster algorithm [51, 52], which almost completely eliminates the critical slowing down in the continuum limit. We are hence in an ideal situation and the model can be solved numerically with very high precision. In case of the lattice $CP(N-1)$ models, a no-go theorem forbids the existence of such an efficient algorithm [123]. Therefore, most of the simulations near the continuum limit suffer from severe critical slowing down. Still, at $\theta = 0$ a rather efficient multigrid algorithm was developed in [101, 102]. As emphasize before, the situation is worst at $\theta = \pi$. Simulations are simply impossible due to the sign problem. Unfortunately, in this case, the results obtained in [66] for $CP(1)$ cannot be extended to higher N due to the no-go theorem. The efficiency of the D-theory cluster algorithms will be discussed in the next chapter. There, we will present our cluster algorithms in more details.

In the present chapter, we demonstrate that it is possible to draw a clear conclusion on the Seiberg-Affleck conjecture using the D-theory formulation of the model. Indeed, we found a first order phase transition at $\theta = \pi$ for $N \geq 3$, with spontaneous charge conjugation symmetry breaking. This confirms the previous hypothesis and provides a final answer to this difficult problem. Our method is based on the D-theory formulation of field theory in which continuous classical fields emerge from dimensional reduction of discrete variables. This framework has been detailed in the second chapter of this thesis, except for $CP(N-1)$ models. Here, we show that, although the D-theory regularization has a completely different structure than the Wilsonian formulation, it yields the same universal continuum theory. As for the other field theories described in chapter 2, the $CP(N-1)$ fields emerge from dimensional reduction of discrete quantum variables.

There are different ways to formulate $CP(N-1)$ models in the D-theory context. As we will see, some of them are better suited for numerical simulations. First, we can work in complete analogy with what has been described in the second chapter, i.e. working with

the embedding algebras $SU(N+1)$ for the quantum spin variables and $SU(2)$ for the quantum links. However, we will see that in this framework, it is far from obvious how to define an efficient cluster algorithm. This is due to the extra $U(1)$ gauge symmetry of the model. Hence, we looked for another type of regularization. Indeed, we noticed that the $CP(N-1)$ fields can emerge from dimensional reduction of $SU(N)$ quantum spins systems. This was a major breakthrough in this research project and most of the following results are based on this observation. In particular, we will see that one way to regularize d-dimensional $CP(N-1)$ models at $\theta = 0$ is to consider a $(d+1)$-dimensional $SU(N)$-symmetric quantum ferromagnet. In that context, we will demonstrate the equivalence between the D-theory and the Wilson regularizations. In order to investigate the θ-vacuum structure, we will need to consider $SU(N)$-symmetric quantum spin ladders with ferromagnetic coupling along a spacial axis and an antiferromagnetic coupling in the other direction. We will see that an even number of transversely coupled spin chains leads to $CP(N-1)$ models with vacuum angle $\theta = 0$, while an odd number of chains yields $\theta = \pi$. Eventually, we will show that 1-dimensional quantum spin chains, with various representations of the algebra on each site, regularizes as the 2-dimensional model both at $\theta = 0$ and $\theta = \pi$. However, this formulation is less in the spirit of D-theory since one does not have dimensional reduction.

In contrast to the Wilson formulation, one does not face the sign problem at $\theta = \pi$ with the D-theory formulation. We use very efficient cluster algorithms to investigate our D-theory models. In the next chapter, we will describe the algorithmic framework in detail. In particular, no critical slowing down occurs as one approaches the continuum limit. In this way, one evades the no-go theorem which prevents the construction of efficient cluster algorithms in the Wilson context. What follows is based on the published work [25, 26].

4.2 D-Theory Formulation of $CP(N-1)$ Models

In this section, we present $CP(N-1)$ models in the framework of D-theory using the same type of arguments as in chapter 2. Hence, we construct a quantum Hamiltonian which regularizes the model on the lattice and illustrate a possible choice for the representation of the embedding algebras. Let us begin by considering the 2-dimensional $CP(N-1)$ action (3.8) in the Wilson framework. This can be formulated in terms of classical unit vectors $\vec{z}_x$ and complex link variables $u_{x,\mu} \in U(1)$. Omitting the vector and matrix indices this yields

$$S[z,u] = -\frac{1}{g^2}\sum_{x,\mu}(z_x^\dagger u_{x,\mu} z_{x+\hat{\mu}} + z_{x+\hat{\mu}}^\dagger u_{x,\mu}^\dagger z_x). \tag{4.1}$$

As in the continuum formulation, where we do not have a field strength tensor for A_μ, there is no plaquette term for the auxiliary gauge field. Consequently, the gauge field can be integrated out and acts therefore only as an auxiliary field. In D-theory, quantization is performed by replacing the classical variables by quantum operators. The corresponding

Hamiltonian operator hence takes the form

$$H = -J \sum_{x,\mu} (Z_x^\dagger U_{x,\mu} Z_{x+\hat{\mu}} + Z_{x+\hat{\mu}}^\dagger U_{x,\mu}^\dagger Z_x). \tag{4.2}$$

Indeed, in section 2.2.3 we have seen that a complex vector $\vec{z}$ is represented in D-theory by a vector of $2N$ Hermitean operators $\vec{Z}$ embedded in the algebra of $SU(N+1)$. On the other side, a classical $U(1)$ link variable is represented in D-theory by the quantum link operator

$$U_{x,\mu} = S_{x,\mu}^1 + iS_{x,\mu}^2 = S_{x,\mu}^+, \tag{4.3}$$

which is the raising operator of an $SU(2)$ algebra on each link. As before, one can express these operators in terms of fermionic constituents. Indeed, in the rishon representation we get

$$Z_x^i = c_x^{0\dagger} c_x^i, \quad U_{x,\mu} = c_{x,+\mu}^\dagger c_{x+\hat{\mu},-\mu}. \tag{4.4}$$

Again, the creation and annihilation operators c^i and $c^\dagger$ obey the usual anticommutation relations. The dimension of the representation is determined by the number of rishons on each site, respectively links. The global $SU(N)$ transformations are generated by

$$\vec{G} = \sum_x \sum_{ij} c_x^{i\dagger} \vec{\lambda}_{ij} c_x^j, \tag{4.5}$$

where $\vec{G}$ is a vector of $SU(N)$ generators obeying $[G^a, G^b] = 2if_{abc}G^c$. Here $\vec{\lambda}$ is a vector of Gell-Mann matrices for $SU(N)$ which obeys $[\lambda^a, \lambda^b] = 2if_{abc}\lambda^c$ and $\mathrm{Tr}(\lambda^a\lambda^b) = 2\delta_{ab}$. The generator of the $U(1)$ gauge transformation takes the form

$$G_x = \frac{1}{2} \sum_\mu (T_{x-\hat{\mu},\mu} - T_{x,\mu}) + \sum_i c_x^{i\dagger} c_x^i, \tag{4.6}$$

where we have

$$T_{x,\mu} = c_{x,+\mu}^\dagger c_{x,+\mu} - c_{x+\hat{\mu},-\mu}^\dagger c_{x+\hat{\mu},-\mu}. \tag{4.7}$$

The invariance properties of the model follow from the commutation relations

$$[H, \vec{G}] = [H, G_x] = 0. \tag{4.8}$$

The quantum Hamiltonian (4.2) describes the evolution of the system in an extra dimension. Consequently, in D-theory, the partition function of a 2-dimensional $CP(N-1)$ model is given by a $(2+1)$-dimensional path integral with a finite extent β in the extra dimension. In complete analogy with other 2-dimensional models described in chapter 2, in the $\beta \to \infty$ limit we have a 3-dimensional system with a global $SU(N)$ and a local $U(1)$ symmetry, according to (4.8). If one assumes the same symmetry breaking as in Wilson's theory, one has a broken phase where only a global $U(N-1)$ symmetry is left intact. Hence, one gets Goldstone bosons which live in the coset manifold

$$SU(N)/U(N-1) = CP(N-1) \sim S^{2N-1}/S^1. \tag{4.9}$$

In fact, they are just the N-component complex unit-vector fields $\vec{z}(x)$ of a $CP(N-1)$ model with a $U(1)$ gauge symmetry. Therefore, one can write the low-energy effective action of the quantum system described by (4.2) as

$$S[z,A] = \int_0^\beta dx_3 \int d^2x \, \frac{\rho_s}{2} \left[|(\partial_\mu + A_\mu)\vec{z}|^2 + \frac{1}{c^2}|\partial_3 \vec{z}|^2 \right]. \tag{4.10}$$

As expected, there is no kinetic term for the gauge field A_μ. Since we have not imposed Gauss' law for the states propagating in the extra dimension, the third component A_3 of the gauge field vanishes. Consequently, an ordinary (non-covariant) derivative arises in the last term. The dimensional reduction of the 3-dimensional model to the 2-dimensional target theory is exactly as in $O(N)$ or chiral models. When the extent β of the extra dimension becomes finite, the Hohenberg-Mermin-Wagner-Coleman implies the generation of an exponentially large (but finite) correlation length

$$\xi/a' \propto \left(\frac{N}{4\pi\beta\rho_s} \right)^{2/N} \exp\left(\frac{4\pi\beta\rho_s}{N} \right). \tag{4.11}$$

This exponential divergence is due to asymptotic freedom. Again, $1/g^2 = \beta\rho_s$ defines the coupling constant g^2 of an effective Wilsonian lattice $CP(N-1)$ model with lattice spacing a'. Here, the 1-loop β-function coefficient is $N/4\pi$. In that case, the exact mass-gap of the theory is not known analytically. The continuum limit of this effective lattice model is reached as $g^2 \to 0$, which corresponds to an increasing extent $\beta \to \infty$ in the extra dimension. Still, in physical units of ξ, it is clear from the relation (4.11) that the extent β is negligible. Therefore, the $(2+1)$-dimensional D-theory model is reduced to the 2-d $CP(N-1)$ model. In higher dimensions, the reduction is as in $O(N)$ models with $N \geq 3$ or in chiral models (sections 2.4.1 and 2.4.2). One-dimensional $CP(N-1)$ quantum spin chains with the Hamiltonian (4.2) could be interesting because of its similarities with a quantum Heisenberg model. Formulating the quantum $CP(N-1)$ models with appropriate representations of the embedding algebra $SU(N+1)$ may correspond to a 2-dimensional classical $CP(N-1)$ model with a θ-term. However, as we will see, other D-theory formulations offer an easier way to describe and simulate the θ-physics.

Of course, the dynamics of spontaneous symmetry breaking and dimensional reduction described above have to be checked numerically. Unfortunately, this D-theory formulation for $CP(N-1)$ models is not so well suited for numerical simulations. Originally, one has expected to construct efficient cluster algorithms to simulate the D-theory model described by (4.2). However, this seems to be really difficult in this framework. The major difficulties are related to the $U(1)$ gauge symmetry of the model. Indeed, although efficient cluster algorithms exist for different classical or quantum spin systems, so far none have been developed for gauge theories, neither with the Wilson formulation nor with D-theory. A cluster algorithm for $U(1)$ quantum link models was investigated in [83, 124] but turns out to be inefficient close to the continuum limit. Remarkably, one can evade this problem by considering different quantum systems whose low-energy effective theories are described

by $CP(N-1)$ models. This has allowed us to simulate $CP(N-1)$ models both at $\theta = 0$ and $\theta = \pi$. However, with these formulations, we lost the gauge theory aspect of the model. Therefore, finding efficient cluster algorithms for quantum link models, and hence for gauge theories, is still an open problem.

4.3 $CP(N-1)$ Model at $\theta = 0$ as an $SU(N)$ Quantum Ferromagnet

In what follows, we construct a ferromagnetic $SU(N)$-symmetric quantum spin system which provides a regularization for $CP(N-1)$ models at $\theta = 0$ in the framework of D-theory. The model emerges as the low-energy effective theory of the quantum system. The $SU(N)$ symmetry is spontaneously broken to $U(N-1)$ and the corresponding Goldstone bosons live in the coset space $CP(N-1)$. More precisely, the d-dimensional $CP(N-1)$ variables emerge from dimensional reduction of discrete $SU(N)$ quantum spins in $(d+1)$ space-time dimensions.

4.3.1 $SU(N)$ quantum ferromagnet

Ferromagnetic systems have been intensively studied both from a condensed matter and from a field theoretical point of view. In particular, the low-temperature behavior of 2-d quantum ferromagnets has been investigated in [125]. Let us first describe in some detail the theoretical structure of an $SU(N)$-symmetric ferromagnetic quantum system. The $SU(N)$ quantum spin variables are located on the sites x of a d-dimensional periodic hypercubic lattice of size L^d. They are represented by Hermitean operators T_x^a that generate the group $SU(N)$ on each site and obey

$$\begin{aligned} [T_x^a, T_y^b] &= i\delta_{xy} f_{abc} T_x^c, \\ \mathrm{Tr}(T_x^a T_y^b) &= \frac{1}{2}\delta_{xy}\delta_{ab}. \end{aligned} \tag{4.12}$$

Here, f_{abc} are the structure constants of $SU(N)$ and $a = 1, ..., N^2-1$. In particular, they are Gell-Mann matrices for the triplet representation of $SU(3)$, i.e. $T_x^a = \frac{1}{2}\lambda_x^a$. In principle, these generators can be chosen in any irreducible representation of $SU(N)$. However, as we will see, the choice of the representation is essential since not all of them lead to spontaneous symmetry breaking from $SU(N)$ to $U(N-1)$. The Hamilton operator of an $SU(N)$-symmetric ferromagnet has the form

$$H = -J \sum_{x,\mu} T_x^a T_{x+\hat{\mu}}^a, \tag{4.13}$$

where $J > 0$ is the exchange coupling. Here, we have nearest neighbor interactions. By construction, this Hamilton operator is invariant under global $SU(N)$ transformations

because it commutes with the total spin T^a, which is given by

$$T^a = \sum_x T^a_x. \tag{4.14}$$

The Hamiltonian (4.13) describes the evolution of the quantum system in an extra dimension of finite extent β. Note that this extra dimension is not the Euclidean time of the target $CP(N-1)$ theory which is already part of the d-dimensional lattice. Instead, it is an additional compactified dimension which will ultimately disappear via dimensional reduction. Hence, one has the following quantum partition function

$$Z = \mathrm{Tr}\exp(-\beta H), \tag{4.15}$$

where the trace extends over the physical Hilbert space which implies periodic boundary conditions in the extra dimension.

4.3.2 Low-energy effective theory

Let us now investigate the low-energy sector of this $(d+1)$-dimensional quantum ferromagnet. For $d \geq 2$, the ground state of the quantum spin system has a broken global $SU(N)$ symmetry. Remarkably, the choice of the representation determines the symmetry breaking pattern. Here, we want a spontaneous symmetry breaking from $SU(N)$ to $U(N-1)$ in order to obtain Goldstone bosons that live in the coset space $CP(N-1)$. We found that the corresponding $SU(N)$ representation is completely symmetric and can be represented by a Young tableau with a single row containing n boxes.

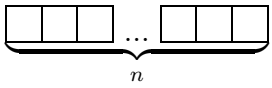

(4.16)

Let us illustrate this with the case of $SU(3)$. For simplicity, we place the fundamental triplet representation $\{3\}$ of $SU(3)$ on each site, which consists of a Young tableau with a single box. Coupling a number of spins results in a direct sum of $SU(3)$ representations. For example, when coupling three spins, one gets

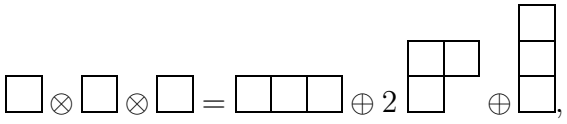

(4.17)

which is equivalent to

$$\{3\} \otimes \{3\} \otimes \{3\} = \{10\} \oplus 2\{8\} \oplus \{1\}. \tag{4.18}$$

In $SU(3)$, one has three spin flavors $q \in \{u, d, s\}$. We choose the symmetric ground state $|uuu\rangle$ transforming in the decuplet representation. This ground state breaks $SU(3)$ but is invariant under the $SU(2)$ transformations which mix the spins d and s. Moreover, it is

clear that a global $U(1)$ transformation, which is just a phase acting on the ground state, leaves this vacuum unchanged. Hence, this yields the correct $SU(3) \to SU(2) \otimes U(1) = U(2)$ spontaneous symmetry breaking. On the other hand, if one chooses a ground state which transforms in the adjoint representation (the octet representation), one finds that only a $U(1) \otimes U(1)$ symmetry is left intact. This, of course, implies a different low-energy physics. For L^2 spins, we choose the corresponding symmetric $\{(L^2+1)(L^2+2)/2\}$-dimensional representation consisting of a Young tableau (4.16) with $n = L^2$ boxes. This yields the correct $SU(3) \to SU(2) \otimes U(1) = U(2)$ spontaneous symmetry breaking.

Generalization to $SU(N)$ is straightforward. We couple L^2 $SU(N)$-spins with a symmetric representation with n boxes on each site. One then chooses the completely symmetric representation which consists of a multiplet of dimension $(N+nL^d-1)!/(N-1)!(NL^d)!$. It is then easy to build the ground state. We can choose, for example, to put $SU(N)$-spins $q \in \{u, d, s, \ldots\}$ of type u on each site. The L^d-dimensional vacuum vector $|0\rangle$ is then defined by the symmetric combination $|uu\ldots u\rangle = |0\rangle$. As a consequence, one generates a uniform magnetization $\vec{\mathcal{M}}$ and the ground state is no longer invariant under $SU(N)$ but only under $SU(N-1) \otimes U(1) = U(N-1)$. Indeed, an $SU(N-1)$ transformation, which mixes all the spins but u, leaves the vacuum state invariant. As before, $U(1)$ acts on $|0\rangle$ as a phase and has no effect on the vacuum. According to the Goldstone theorem, there are therefore $(N^2-1)-(N-1)^2 = 2N-2$ massless particles which govern the low-energy physics. They are represented by the previously introduced matrix field $P(x)$ and live in the coset space $SU(N)/U(N-1) = CP(N-1)$. The uniform magnetization is an order parameter which is a conserved quantity. It is defined as the sum over all spins

$$\mathcal{M}^a = \sum_x T_x^a. \tag{4.19}$$

At zero temperature, the mean value $\langle\vec{\mathcal{M}}\rangle$ does not vanish. This has important consequences for the low-energy physics of the ferromagnetic Goldstone bosons which are also called magnons or spin-waves. In particular, their energy-momentum dispersion relation

$$E = \frac{\rho_s}{m}|\vec{p}|^2, \tag{4.20}$$

is non-relativistic. This was investigated by Leutwyler in [126]. Again, ρ_s is the spin stiffness and $m = |\vec{m}|$ is the magnetization density where we have

$$\langle\vec{\mathcal{M}}\rangle = \int_0^\beta dt \int d^dx\ \vec{m}. \tag{4.21}$$

Note that in a relativistic theory, e.g. an antiferromagnet, the ground state is Lorentz invariant and the charges of an internal symmetry are integrals over the time components of the corresponding currents. Therefore, they cannot pick up an expectation value and appear to vanish for dynamical reasons.

The low-energy effective Lagrangian for $SU(N)$ ferromagnets can then be constructed using chiral perturbation theory. As always, the expansion is ordered according to the number of derivatives of the matrix field $P(x)$. To leading order, the Euclidean action is given by

$$S[P] = \int_0^\beta dt \int d^d x \left[\rho_s \mathrm{Tr}(\partial_\mu P \partial_\mu P) - 2m \int_0^1 d\tau \ \mathrm{Tr}(P\partial_\tau P \partial_t P - P\partial_t P \partial_\tau P) \right]. \quad (4.22)$$

In this effective Lagrangian, the order parameter $\langle \vec{\mathcal{M}} \rangle$ manifests itself through a topological term, the so-called Novikov-Wess-Zumino-Witten term which involves an integral over an interpolation parameter $\tau \in [0,1]$. It is also manifestly $SU(N)$ invariant. Again, for an antiferromagnet, this term does not show up because the uniform magnetization vanishes. Remarkably, for a ferromagnet this contribution is relevant already at leading order and modifies strongly the low-energy structure of the system. The interpolation parameter τ is an unphysical extra dimension which has only a mathematical meaning. Let us show now that the topological term

$$S_{WZW}[P] \propto \int_0^\beta dt \int_0^1 d\tau \ \mathrm{Tr}(P\partial_\tau P \partial_t P - P\partial_t P \partial_\tau P) \quad (4.23)$$

is an integer winding number. Since one has periodic boundary conditions in the β direction, the extra dimension is topologically equivalent to a circle S^1. Therefore, introducing an interpolation parameter τ, the magnon field $P(x,t)$ defined on $\mathbb{R}^d \times S^1$ is extended to a field $P(x,t,\tau)$ in the higher-dimensional space-time $\mathbb{R}^d \times H^2$. Here, H^2 is the 2-dimensional hemisphere with the compactified extra dimension as its boundary. The field obeys the boundary conditions $P(x,t,1) = P(x,t)$ and $P(x,t,0) = diag(1,0,...,0)$. At intermediate values of τ the field is smoothly interpoled between these two limiting cases. There is no topological obstruction against such interpolation because $\pi_1[CP(N-1)]$ is trivial. Of course, the $(d+1)$-dimensional physics has to be independent of how the field is deformed into the bulk of the $(d+2)$ dimensions. There is, in fact, an integer ambiguity due to the choice of the interpolation. This can be illustrated by the following example. Let us choose an integration domain $H^{2\prime}$, which is another 2-dimensional hemisphere as shown in figure 4.1. We hence consider also the corresponding interpolated field $P'(x,t,\tau)$. The difference between the two choices is an integer. Indeed, one has

$$\begin{aligned} &\int_{H^2} dt \ d\tau \ \mathrm{Tr}(P\partial_\tau P \partial_t P - P\partial_t P \partial_\tau P)) - \int_{H^{2\prime}} dt \ d\tau \ \mathrm{Tr}(P'\partial_\tau P' \partial_t P' - P\partial_t P \partial_\tau P)) \\ &= \int_{H^2 \cup H^{2\prime} = S^2} dt \ d\tau \ \mathrm{Tr}(P\partial_\tau P \partial_t P - P\partial_t P \partial_\tau P)) = k \in \mathbb{Z}. \end{aligned} \quad (4.24)$$

The last identity is due to the fact that $\pi_2[CP(N-1)] = \mathbb{Z}$ and we refer to chapter 3 for more details on the topological structure of $CP(N-1)$ models. Of course, such mathematical ambiguity should not affect the physics. Therefore, the prefactor m of the Novikov-Wess-Zumino-Witten term in (4.22) has to be quantized. This ensures that the

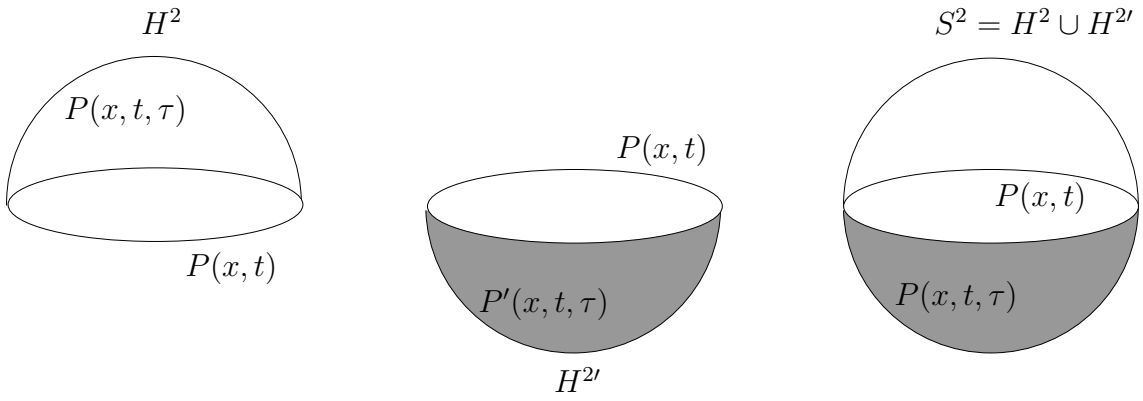

Figure 4.1: *Examples of two different interpolations of $P(x,t,\tau)$ on H^2 and $H^{2\prime}$. The difference of these two interpolations results in an integer ambiguity.*

integer contribution k from the $(d+2)$-dimensional bulk cancels in the path integral. Remarkably, one can prove that the prefactor m is just determined by the number of boxes n of the chosen representation. This can be done by computing the energy-momentum dispersion relation of the ferromagnetic magnons directly in the microscopic theory. One can then match the result with the one obtained using chiral perturbation theory. The details of the calculation are presented in appendix A and on finds

$$m = \frac{n}{2}. \tag{4.25}$$

Moreover, it is also possible to determine the spin stiffness ρ_s in terms of the microscopic parameters J and n. We found that

$$\rho_s = \frac{Jn^2}{4}, \tag{4.26}$$

and we refer again to appendix A for more details.

4.3.3 Dimensional reduction

To summarize, the low-energy effective theory of an $SU(N)$ quantum ferromagnet with a symmetric representation of the symmetry group results in a $(d+1)$-dimensional model described by the effective action (4.22). Let us show now that after dimensional reduction one obtains the d-dimensional $CP(N-1)$ model at vacuum angle $\theta = 0$. First, we consider the case $d = 2$. At $\beta = \infty$, we know that the system has a broken $SU(N)$ symmetry and thus massless Goldstone bosons. Again, as soon as β becomes finite, the Hohenberg-Mermin-Wagner-Coleman theorem forbids a spontaneously broken global symmetry and, consequently, the magnons pick up a small mass non-pertubatively. The corresponding correlation length hence becomes finite and the $SU(N)$ symmetry is restored over that length. The question then arises if ξ is bigger or smaller than the extent β of the extra

dimension. As it will be argued below, $\xi \gg \beta$ and the Goldstone boson fields are essentially constant along the extra dimension . The system hence undergoes dimensional reduction to the 2-dimensional target theory. Indeed, the Novikov-Wess-Zumino-Witten term contains $\partial_t P$ and simply vanishes after dimensional reduction. The action therefore reduces to

$$S[P] = \beta\rho_s \int d^2x \ \mathrm{Tr}[\partial_\mu P \partial_\mu P], \tag{4.27}$$

which is just the action of the 2-d $CP(N-1)$ model at $\theta = 0$. As before, g^2 is the coupling constant of the continuous field theory. It is determined by the extent of the extra dimension and is given by

$$\frac{1}{g^2} = \beta\rho_s. \tag{4.28}$$

Since the 2-dimensional $CP(N-1)$ model is asymptotically free, one can use the universal asymptotic formula for the correlation length [15]

$$a'/\xi = C \ (\beta_1 g^2)^{-\beta_2/\beta_1^2} \exp\left(-\frac{1}{\beta_1 g^2}\right) \{1 + \mathcal{O}(g^2)\}. \tag{4.29}$$

Here, β_1, β_2 are, respectively, the 1- and 2-loop β-function coefficients and C is an unknown coefficient. Like in the 2-d $O(3)$ model, one averages the $(d+1)$-dimensional field over blocks of size β in the extra dimension and a' in the space-time dimensions (see figure 2.1). For an antiferromagnetic system, the energy-momentum dispersion relation is relativistic (i.e. $E = pc$) and we have

$$E = \frac{1}{\beta} = pc = \frac{c}{a'} \Rightarrow a' = \beta c. \tag{4.30}$$

In the case of a ferromagnet, on the other hand, the dispersion relation is non-relativistic and is determined by (4.20). Hence the lattice spacing a' is determined as

$$E = \frac{1}{\beta} = \frac{\rho_s}{m} p^2 = \frac{\rho_s}{m a'^2} \Rightarrow a' = \sqrt{\frac{\beta\rho_s}{m}}. \tag{4.31}$$

Using the universal 1- and 2-loop β-function coefficients of the $CP(N-1)$ model, $\beta_1 = N/4\pi$ and $\beta_2 = 8\pi/N^2$, one finds the following correlation length. At leading order, it is exponentially large in β

$$\xi = C \ \sqrt{\frac{\beta\rho_s}{m}} \left(\frac{N}{4\pi\beta\rho_s}\right)^{2/N} \exp\left(\frac{4\pi\beta\rho_s}{N}\right). \tag{4.32}$$

One sees that $\xi \gg \beta$ as long as β itself is sufficiently large. As in all asymptotically free D-theory models, dimensional reduction happens in the large β limit because ξ then grows exponentially. One then approaches the continuum limit not by adjusting a bare coupling constant but by increasing the extent β of the extra dimension. It should be noted that no fine-tuning is needed to approach this limit.

Unfortunately, the parameter C is not known analytically in the case of the $CP(N-1)$ models. Therefore, as in QCD, one cannot determine the exact mass-gap of the model. In fact, analytic techniques developed to solve 2-dimensional $O(N)$ models or chiral models, happen to fail for $CP(N-1)$ models. Using techniques specific to two dimensions, the brothers Zamolodchikov have derived the exact S-matrix of certain quantum field models [127]. Based on this, Hasenfratz and Niedermayer were able to extract analytically the mass-gap of the theories [49, 78]. However, with the D-theory formulation, it may be possible to determine this mass-gap numerically. Ideas in that direction are given in the conclusion.

Let us say a word about the situation for $d > 2$. In that case, dimensional reduction still occurs but the Goldstone bosons remain massless even at finite β. Similarly, as in the case of the $CP(1) = O(3)$ model (see section 2.1.4), if β is decreased sufficiently, the $SU(N)$ symmetry is restored and the massless modes are replaced by massive excitations. By fine-tuning the extent β to the critical value from below, one can reach a continuum limit of the target theory provided that the corresponding phase transition is second order. Whether the phase transition between the massive and massless phase is first or second order has to be checked numerically. Nevertheless, once we are in a massless phase, D-theory applies naturally.

4.3.4 Equivalence with Wilson's regularization

In order to verify that the $SU(N)$ quantum ferromagnet indeed defines $CP(N-1)$ models in the continuum limit, we can compare physical results obtained from the D-theory formulation and from Wilson's lattice field theory. Let us consider the $d = 2$ case and the following standard lattice action

$$S[P] = -\frac{2}{g^2} \sum_{x,\mu} \mathrm{Tr}[P_x P_{x+\hat{\mu}}]. \tag{4.33}$$

The continuum limit is reached as $g \to 0$. A convenient physical quantity characteristic for a given model is the universal step scaling function. Indeed, it can be considered as a model's finger print and can be defined as

$$F(z) = \frac{\xi(2L)}{\xi(L)}, \tag{4.34}$$

where $\xi(L)$ is the correlation length obtained with the so-called "second moment method" [128, 129, 130] in a finite system of size L. The finite size scaling variable $z = \xi(L)/L$ measures the size of the system in physical units. We have performed Monte Carlo simulations in both frameworks, with our cluster algorithm for the 2-d $SU(3)$ quantum ferromagnet, and with a usual Metropolis algorithm for the Wilsonian $CP(2)$ model. The results are presented in figure 4.2. Up to small scaling violations, the agreement between the two data sets confirms that the D-theory formulation provides a valid regularization of 2-d

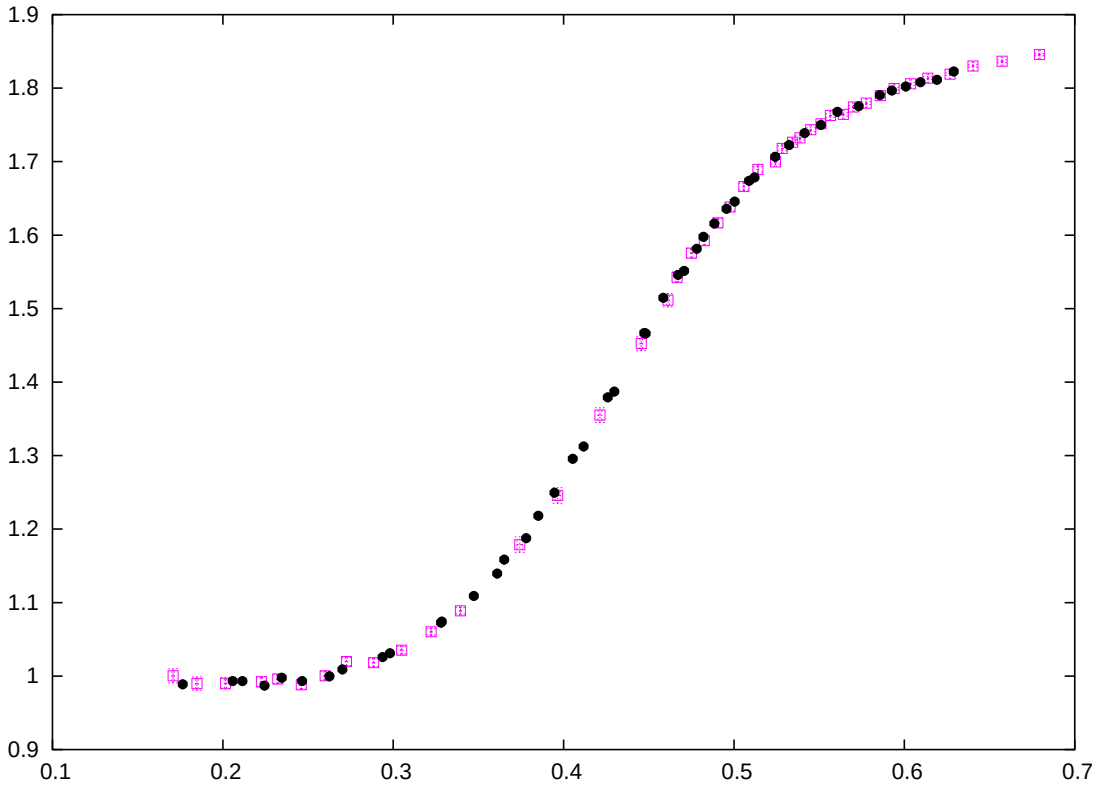

Figure 4.2: *Monte Carlo data for the universal finite-size scaling function $F(z)$ of the 2-dimensional $CP(2)$ model at $\theta = 0$. The black points represent D-theory data from an $SU(3)$ quantum ferromagnet at $\beta J = 5.5$ and 6, while the pink open squares correspond to data obtained with the standard Wilson lattice field theory at $1/g^2 = 2.25$ and 2.5.*

$CP(N-1)$ models. This proves both the spontaneous symmetry breaking scenario and the dimensional reduction mechanism. Remarkably, thanks to the cluster algorithm, the D-theory framework allows calculations that are much more accurate than the ones using the Wilson approach. In particular, critical slowing down is almost completely removed close to the continuum limit.

4.4 $CP(N-1)$ Models at $\theta = 0, \pi$ as an $SU(N)$ Quantum Spin Ladder

As stressed earlier, we would like to demonstrate the efficiency of the D-theory formulation in the context of the $CP(N-1)$ models. In this section, we will show that $SU(N)$ quantum spin ladders with an odd number of chains yield the $CP(N-1)$ models at $\theta = \pi$. In contrast to Wilson's formulation, no sign problem arises and an efficient cluster algorithm is used to investigate the θ-vacuum effects. We will present several results from numerical

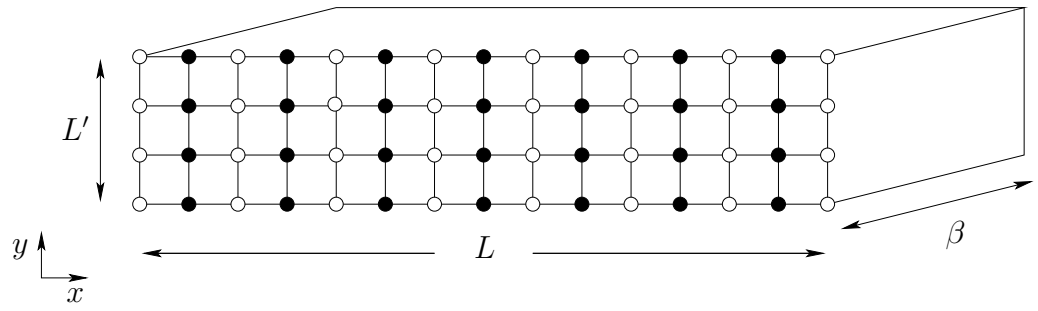

Figure 4.3: *Spin ladder geometry: The open circles belong to sublattice A, while the filled circles form sublattice B. As before, β is the inverse temperature of the quantum system.*

simulations, which confirm the existence of the conjectured first order phase transition with spontaneous breaking of the charge conjugation symmetry at $\theta = \pi$ with $N \geq 3$.

4.4.1 $SU(N)$ quantum spin ladders

Quantum spin ladders are interesting systems which have been studied in detail in the past. In particular, Haldane's conjecture has been generalized to quantum spin ladders in [131]. The ladders consisting of an odd number of transversely coupled spin 1/2 chains are gapless, while they have a mass-gap for an even number of chains [132, 133, 134]. Moreover, as one increases the even number of coupled chains, the mass-gap decreases exponentially. In the limit of a large even number of coupled spin chains, one approaches the continuum limit of the 2-d classical $O(3)$ model, which is equivalent to $CP(1)$ [135]. More recently, quantum spin ladders placed in a external uniform magnetic field have been studied with a powerful meron-cluster algorithm [28]. The corresponding quantum field theory is a $(1+1)$-d $O(3)$ model with a chemical potential. Such field theories are usually very difficult to simulate due to the notorious complex action problem.

As for the $SU(N)$ ferromagnet, we use generalized quantum spins T_x^a which generate an $SU(N)$ symmetry. Again they obey the relations (4.12). The spins are located on the sites x of a square lattice $L' \times L$ with lattice spacing a. We consider $L \gg L'$ and we use periodic boundary conditions. This is illustrated in figure 4.3 where we have a quantum spin ladder consisting of $n = L'/a$ transversely coupled spin chains of length L. The x-direction of size L corresponds to the spacial dimension of the 2-dimensional target $CP(N-1)$ model, while the extra y-dimension of finite extent L' will ultimately disappear via dimensional reduction. In contrast to the ferromagnetic case, here the β direction is the Euclidean time direction of the target theory. We consider nearest-neighbor couplings which are antiferromagnetic along the chains of length L and ferromagnetic between different chains. Therefore, we decompose the lattice into two sublattices A and B with even and odd sites along the x-direction, respectively. Hence, neighboring sites along the transverse y-direction belong to the same sublattice. Since one has both ferro- and antiferromagnetic

couplings, the spin variables transform differently whether they are on sublattices A or B. Indeed, the spins T_x^a on sublattice A transform in the fundamental representation $\{N\}$ of $SU(N)$ while the ones on sublattice B are in the antifundamental representation $\{\overline{N}\}$. They are thus described by the conjugate generators $-T_x^{a*}$. With these fundamental variables, one can write the following quantum spin ladder Hamiltonian

$$H = -J \sum_{x \in A} [T_x^a T_{x+\hat{1}}^{a*} + T_x^a T_{x+\hat{2}}^a] - J \sum_{x \in B} [T_x^{a*} T_{x+\hat{1}}^a + T_x^{a*} T_{x+\hat{2}}^{a*}], \tag{4.35}$$

where $J > 0$ and $\hat{1}$ and $\hat{2}$ are unit-vectors in the spatial x- and y- direction, respectively. Note that, in the case of $SU(2)$, the $\{2\}$ and $\{\overline{2}\}$ representation are unitarily equivalent. One can always transform T_x^a into $-T_x^{a*}$ by a unitary transformation. Finally, by construction the system has a global $SU(N)$ symmetry, i.e.

$$[H, T^a] = 0, \tag{4.36}$$

with the total spin given by

$$T^a = \sum_{x \in A} T_x^a - \sum_{x \in B} T_x^{a*}. \tag{4.37}$$

The total spin satisfies the $SU(N)$ algebra $[T^a, T^b] = i f_{abc} T^c$. The system is also C-invariant. For a quantum spin ladder, charge conjugation corresponds to replacing each spin state q_x by $q_{x+\hat{1}}$ (which is the conjugate of $\bar{q}_{x+\hat{1}}$). In terms of the generators T_x^a, it corresponds to shift them by one lattice spacing and make the substitution $T^a \to T^{a*}$. As before, this Hamiltonian evolves the system in an extra dimension of size β, but here this dimension corresponds to the Euclidean time of the 2-d $CP(N-1)$ target model and will therefore not disappear via dimensional reduction. Nevertheless, the quantum partition function at temperature $T = 1/\beta$ is given by the usual formula

$$Z = \mathrm{Tr} \exp(-\beta H). \tag{4.38}$$

4.4.2 Low-energy effective theory and dimensional reduction

A priori it is not obvious that the $(2+1)$-dimensional quantum spin ladder system provides a viable regularization of the 2-dimensional $CP(N-1)$ field theory. As a necessary prerequisite, the quantum spin ladder does have the global $SU(N)$ symmetry of $CP(N-1)$ models. Moreover, it is also invariant under the charge conjugation C. Of course, another natural choice would have been a 2-dimensional $SU(N)$ antiferromagnetic spin ladders, with antiferromagnetic couplings in all directions. This type of system also has the right symmetry properties. However, it has been demonstrated that there is no Néel ground state and thus no spontaneous symmetry breaking for $N \geq 5$ in 2-dimensional $SU(N)$ quantum antiferromagnets [136]. Hence a major ingredient of D-theory, the existence of massless modes, is missing. Instead, in order to access any value of N, we consider $SU(N)$ quantum spin ladders with both ferro- and antiferromagnetic couplings.

In the infinite volume limit (both $L, L' \to \infty$) and at zero temperature, one can show that the system undergoes spontaneous symmetry breaking from $SU(N)$ to $U(N-1)$. This can be done using the coherent state techniques of [137]. In that paper, Read and Sachdev confirm an earlier result of Arovas and Auerbach [138, 139]. They prove that a square lattice $SU(N)$ antiferromagnet undergoes spontaneous symmetry breaking for a large symmetric representation n of $SU(N)$ if $N < \kappa n$, where κ is a numerical constant. The generalization to the spin ladder case is almost straightforward. Only the sublattices A and B have to be defined differently. The $SU(N)$ symmetric representation, determined in that paper by the number of boxes n of the corresponding Young tableau, is in our case simply the number of coupled spin chains in the y-direction. The $SU(2)$ spin ladder case is discussed in detail in [135].

In our context, spontaneous symmetry breaking arises for a large number of coupled chains. Again, the choice of the $SU(N)$ spin representation (here $\{N\}$ and $\{\overline{N}\}$) has an effect on the breaking pattern. Due to the symmetry breaking, there are massless Goldstone bosons governing the low-energy physics of the system. These spin-waves are described by fields in the coset space $SU(N)/U(N-1) = CP(N-1)$. Again, the matrix field $P(x,y,t)$ is the Hermitean $N \times N$ projector matrix with $P^2 = P$ and $\mathrm{Tr}P = 1$. Using chiral perturbation theory, the lowest order terms in the Euclidean effective action for the Goldstone bosons are given by

$$\begin{aligned} S[P] &= \int_0^\beta dt \int_0^L dx \int_0^{L'} dy \ \mathrm{Tr}\Big[\rho_s'\partial_y P \partial_y P + \rho_s\Big(\partial_x P \partial_x P + \frac{1}{c^2}\partial_t P \partial_t P\Big) \\ &\quad - \frac{1}{2a}\,(P\partial_x P \partial_t P - P\partial_t P \partial_x P)\Big]. \end{aligned} \tag{4.39}$$

Here ρ_s and ρ_s' are spin stiffness parameters for the x- and y-direction, respectively, and c is the spin-wave velocity. By construction, the action is invariant under global $SU(N)$ transformations

$$P'(x) = \Omega P(x) \Omega^\dagger, \tag{4.40}$$

with $\Omega \in SU(N)$. The last term in (4.39) is purely imaginary and is related to the topological charge which has been introduced in chapter 3. Its exact form is

$$Q[P] = \frac{1}{2i\pi}\int_0^\beta dt \int_0^L dx \ \mathrm{Tr}(P\partial_x P \partial_t P - P\partial_t P \partial_x P). \tag{4.41}$$

We have seen before that Q is an integer in the second homotopy group $\pi_2[CP(N-1)] = \mathbb{Z}$, and thus y-independent. Therefore, the integration over y in (4.39) can be performed trivially, this yields the term $i\theta Q[P]$ where the vacuum angle is given by

$$\theta = \frac{L'\pi}{a} = n\pi. \tag{4.42}$$

Here a is the lattice spacing of the quantum spin ladder and $L'/a = n$ is the number of transversely coupled spin chains. Thus, the vacuum angle is trivial for even n, while for

odd n it is equivalent to $\theta = \pi$.

The dimensional reduction process is similar to the cases presented before. The infinite $(2+1)$-d system has massless Goldstone bosons, but once the y-direction is compactified to a finite extent L', the Hohenberg-Mermin-Wagner-Coleman theorem forbids the existence of massless excitations. Consequently, the Goldstone bosons pick up a mass $m = 1/\xi$ non-perturbatively and thus have a finite correlation length ξ. Using the asymptotic freedom formula (4.29) for the $CP(N-1)$ model, one obtains

$$\xi \propto \exp(4\pi/Ng^2). \tag{4.43}$$

Again, g^2 is the coupling constant of the target theory. It can be identified with the parameters of (4.39) when one considers $\xi \gg L'$. The system hence undergoes dimensional reduction to the 2-dimensional $CP(N-1)$ field theory with the action

$$S[P] = \int_0^\beta dt \int_0^L dx \ \mathrm{Tr}\left[\frac{c}{g^2}\left(\partial_x P \partial_x P + \frac{1}{c^2}\partial_t P \partial_t P\right) - \frac{n}{2}(P\partial_x P \partial_t P - P\partial_t P \partial_x P)\right]. \tag{4.44}$$

The coupling constant of the dimensionally reduced theory is hence given by

$$\frac{1}{g^2} = \frac{L'\rho_s}{c}. \tag{4.45}$$

Using this relation (4.43) becomes

$$\xi \propto \exp(4\pi L'\rho_s/cN) \gg L', \tag{4.46}$$

which is indeed exponentially large in L'. This confirms the scenario of dimensional reduction which is already well-known from quantum antiferromagnets [46, 47]. It has also been discussed for $SU(2)$ quantum spin ladders in [135]. In the D-theory context, it has been shown in [28] that the dimensional reduction of ladder systems yields a 2-d $O(3) = CP(1)$ model at non-zero chemical potential. Here, we have extended this construction, which allows us to simulate the $CP(N-1)$ models reliably both at $\theta = 0$ and π.

4.4.3 A first order phase transition at $\theta = \pi$ for $N > 2$

In what follows, we would like to present numerical results on the existence of a first order phase transition at $\theta = \pi$ with spontaneous symmetry breaking of the charge conjugation symmetry C. This confirms the long standing conjecture proposed by Seiberg and Affleck. To achieve this, we use the D-theory formulation which has the advantage to be formulated in terms of discrete degrees of freedom instead of continuum classical fields. In particular, the quantum partition function (4.38) of the $SU(N)$ quantum spin ladder can be written as a path integral using a basis of discrete $SU(N)$ spin states $q \in \{u, d, s, ...\}$ on sublattice A and $\bar{q} \in \{\bar{u}, \bar{d}, \bar{s}, ...\}$ on sublattice B. In the case of $SU(2)$, this corresponds to the usual

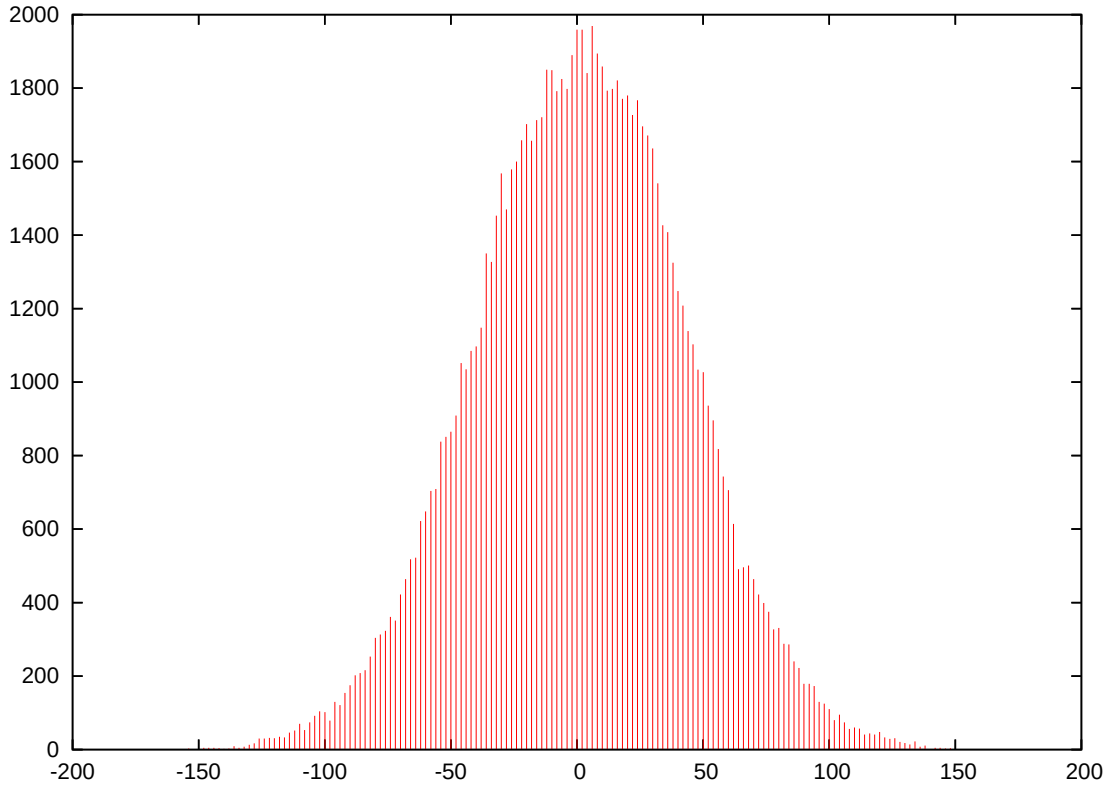

Figure 4.4: *Probability distribution of the order parameter* $Q[q, \bar{q}]$ *for the* $CP(1)$ *model at* $\theta = \pi$ *with* $L = 180a$, $n = 3$ *and* $\beta J = 7$.

"up" $\uparrow$ and "down" $\downarrow$ spins. Full details about the algorithmic setup will be given in the next chapter. We simulate this quantum system using a very efficient single loop-cluster algorithm. Remarkably, no sign problem arises at non-trivial vacuum angle and the no-go theorem, which in the Wilson's context forbids the existence of efficient cluster algorithms already at $\theta = 0$, is evaded.

In order to determine the order of the phase transition, we consider an order parameter which "measures" whether there is only one phase (second order phase transition with intact C symmetry) or a jump between to coexisting phases (first order phase transition with C-breaking). A natural quantity that suggests itself as an order parameter is the topological charge $Q[P]$, which has the property to be C-odd, i.e.

$$Q[{}^{C}P] = Q[P^{*}] = -Q[P]. \tag{4.47}$$

This is clear from the relations (3.15) and (4.41). Note that C is explicitly broken for $\theta \neq 0, \pi$. However, it is not broken explicitly at $\theta = 0, \pi$ because the Boltzmann weight

$$\exp(i\theta Q[P]) = (-1)^{Q[P]} \tag{4.48}$$

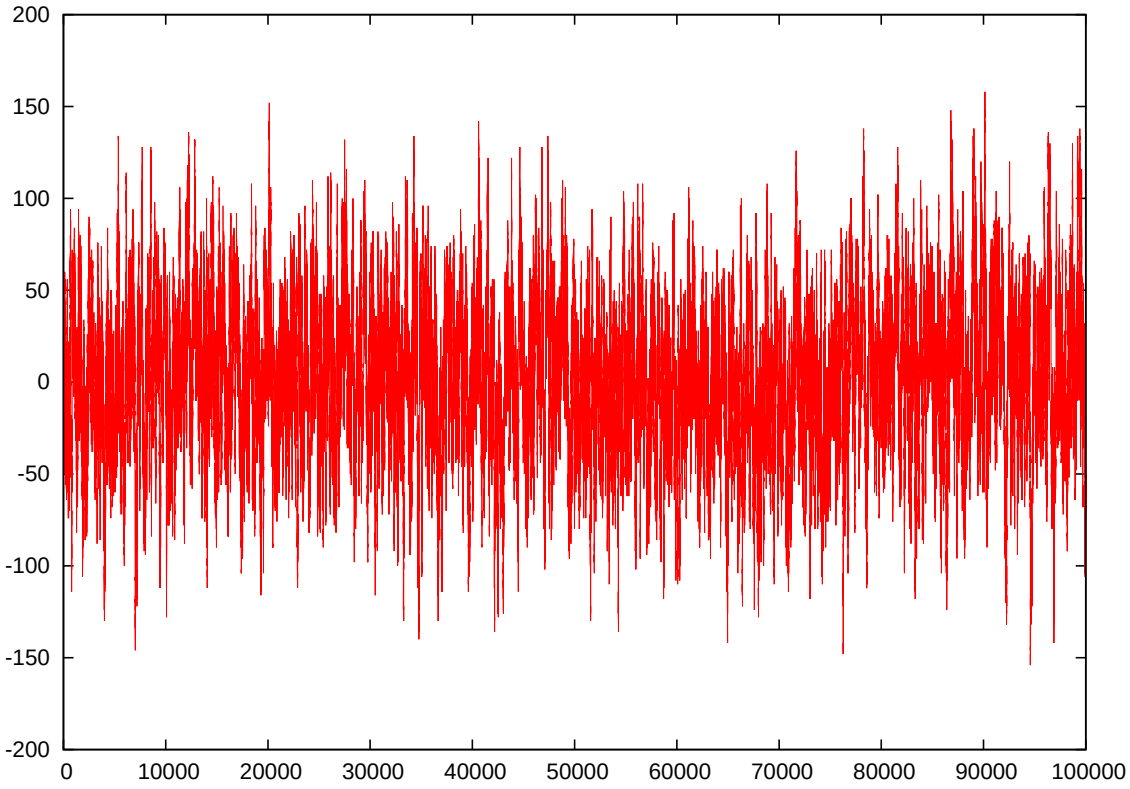

Figure 4.5: *Monte Carlo time histories of the order parameter $Q[q, \bar{q}]$ for the $CP(1)$ model at $\theta = \pi$ with $L = 180a$, $n = 3$ and $\beta J = 7$. One observes large fluctuations of the order parameter, which is characteristic of a second order phase transition.*

is then C-invariant. Unfortunately, the topological charge is defined only in the framework of the target theory. In the discrete spin system, one has to define another order parameter, which is also C-odd. In the basis of quantum spin states $(q, \bar{q})$ we define this alternative order parameter $Q[q, \bar{q}]$ by counting the number of spin flips in a configuration. The order parameter $Q[q, \bar{q}]$ receives a contribution $+1$ if a pair of nearest neighbor spins $q_x \bar{q}_{x+\hat{1}}$ along the x-direction flips to another state $q'_x \bar{q}'_{x+\hat{1}}$, at some moment in time. On the other hand, a spin flip from $\bar{q}_x q_{x+\hat{1}}$ to $\bar{q}'_x q'_{x+\hat{1}}$ contributes -1 to $Q[q, \bar{q}]$. As for the topological charge in the target theory, this term changes sign under charge conjugation while the partition function remains invariant. Again, in the quantum spin ladder system, charge conjugation corresponds to replacing each spin state q_x by $q_{x+\hat{1}}$ (which is the conjugate of $\bar{q}_{x+\hat{1}}$).

We have used a single-cluster algorithm to simulate $SU(N)$ quantum spin ladders. Let us present our numerical results. In figure 4.4, for the $CP(1)$ model at $\theta = \pi$, we observe that the values of the order parameter $Q[q, \bar{q}]$ are symmetrically distributed around zero. This is also shown in figure 4.5. One notes large fluctuations of the order parameter around zero which is characteristic of a second order phase transition. This is an expected result

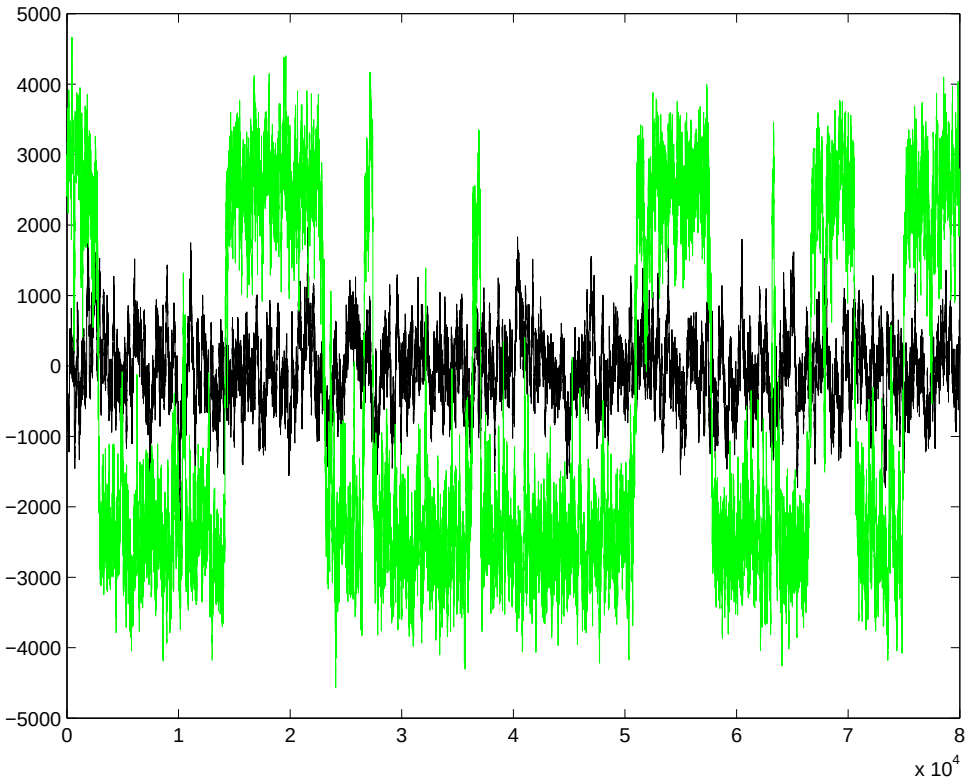

Figure 4.6: *Monte Carlo time history of the order parameter $Q[q,\bar{q}]$ for the $CP(3)$ model, which corresponds to an $SU(4)$ quantum spin ladder, at $\theta = 0$ ($n = 4$, $L = 180a$, $\beta J = 50$, dark curve) and $\theta = \pi$ ($n = 3$, $L = 200a$, $\beta J = 80$, green curve).*

since we know from [66], that the phase transition has to be second order for the 2-d $CP(1)$ model at $\theta = \pi$. We have then used our cluster algorithm to investigate higher values of N with different numbers n of coupled spin chains. In figure 4.6, we show Monte Carlo histories for $SU(4)$ quantum spin ladders with $n = 3$ and 4 which correspond to a $CP(3)$ model at $\theta = \pi$ and $\theta = 0$, respectively. For $n = 3$, one clearly observes a first order phase transition with spontaneous C-breaking. For $n = 4$, one only has a single phase, which is C-symmetric. Figure 4.7 shows the probability distribution of the order parameter $Q[q,\bar{q}]$ for an $SU(5)$ ladder system with $n = 7$. This corresponds to a $CP(4)$ model at $\theta = \pi$. Again, due to the double peak structure, we observe a first order phase transition with two coexisting phases. This is a typical signature for this phenomenon. At this point, our results confirm the conjectured θ-vacuum structure of the $CP(N-1)$ models. In order to demonstrate that we approach the continuum limit of an asymptotically free theory, we have also determined the correlation length $\xi(n)$ in the $CP(2)$ case, as a function of n. The correlation length is defined using the second moment method and the number of chains $n = L'/a$ controls the coupling $1/g^2 = L'\rho_s/a$. Note that the lattice spacing a is set to one. One obtains, $\xi(2) = 4.82(4)a$, $\xi(4) = 17.6(2)a$ and $\xi(6) = 61(2)a$,

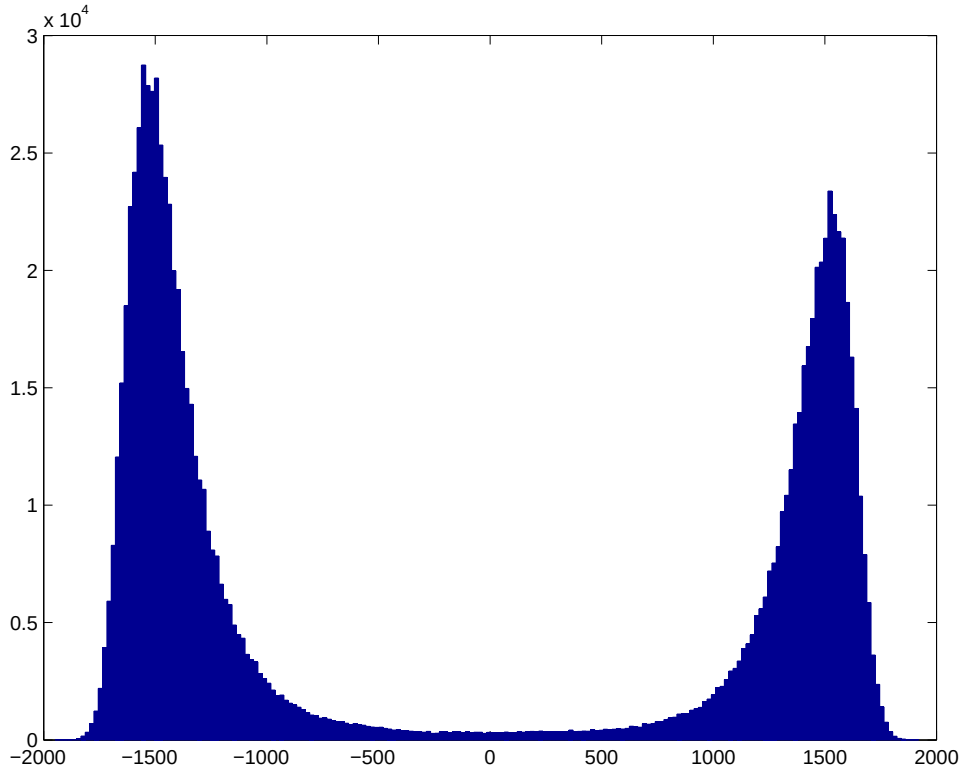

Figure 4.7: *Probability distribution of the order parameter $Q[q, \bar{q}]$ for the $CP(4)$ model at $\theta = \pi$ ($n = 7$, $L = 40a$, $\beta J = 6$). Due to limited statistics the two peak are sampled unevenly.*

which indeed shows an exponential increase of the correlation length characteristic for an asymptotically free theory. This also confirms that for $n \to \infty$ (in the infinite volume limit), the correlation length is diverges. Massless modes of the spontaneous symmetry breaking $SU(N) \to U(N-1)$ hence reappear thus supporting the spontaneous symmetry breaking scenario.

4.5 $CP(N-1)$ Models at $\theta = 0, \pi$ as an Antiferromagnetic $SU(N)$ Quantum Spin Chain

Of course, a quantum spin ladder with $n = 1$ corresponds to an antiferromagnetic quantum spin chain. In this section, we would like to show that $SU(N)$-symmetric antiferromagnetic chains of quantum spins in higher $SU(N)$ representations are related to $CP(N-1)$ models at $\theta = 0$ and π. This formulation is, however, not completely in the spirit or D-theory, since one does not have dimensional reduction. Indeed, here the 2-d $CP(N-1)$ model arises from the $SU(N)$-symmetric 1-dimensional quantum spin chain.

4.5.1 Antiferromagnetic $SU(N)$ quantum spin chains

Antiferromagnetic quantum spin chains were intensively studied in the past. In particular, Bethe was able to find the ground state for a spin 1/2 chain. We refer to section 2.1.4 for more details on the subject. Let us now consider an antiferromagnetic $SU(N)$ quantum spin chain with the Hamiltonian

$$H = J \sum_x T_x^a \overline{T}_{x+1}^a = J \sum_x T_x^a (-T_{x+1}^{a*}), \tag{4.49}$$

where $J > 0$. Now the spins T_x^a at the even sites x (sublattice A) are generators of an $SU(N)$ symmetry with a specific representation of the group while the ones at odd sites $x + \hat{1}$ (sublattice B) are in the corresponding anti-representation of $SU(N)$. Indeed, $\overline{T}_{x+1}^a = -T_{x+1}^{a*}$ transforms in the complex conjugate representation and obeys the correct $SU(N)$ commutation relations

$$[-T_x^{a*}, -T_x^{b*}] = [if_{abc}T_x^c]^* = if_{abc}(-T_x^{c*}) \tag{4.50}$$

The conserved total spin is now given by

$$T^a = \sum_{x \in A} T_x^a - \sum_{x \in B} T_x^{a*}, \tag{4.51}$$

for which indeed we have

$$[H, T^a] = 0. \tag{4.52}$$

We now consider once again the $SU(2)$ case. This group is special because its representations are real or pseudo-real and hence the complex conjugate representation $-T_{x+1}^{a*}$ is unitarily equivalent to T_x^a. In the fundamental representation, i.e. for ordinary $SU(2)$ quantum spins $s = 1/2$, the generators $T_x^a = \frac{1}{2}\sigma_x^a$ are given in terms of Pauli-matrices, and H is unitarily equivalent to the familiar spin chain Hamiltonian

$$H = \frac{J}{4} \sum_x \vec{\sigma}_x \cdot \vec{\sigma}_{x+1}. \tag{4.53}$$

As shown in section 2.1.4, antiferromagnetically coupled spins with value s are related to the 2-d $O(3)$ model with vacuum angle $\theta = 2\pi s$. In particular, Haldane noticed that chains of integer-valued spins which have a mass-gap are described by the 2-d $O(3)$ model at vacuum angle $\theta = 0$, while chains of half-integer spins are gapless and correspond to $\theta = \pi$ [54, 55, 56]. Again, the low-energy excitations of the spin chain are described by an effective action for spins waves, which takes the form

$$S[\vec{s}] = \frac{1}{2g^2} \int d^2x \; \partial_\mu \vec{s} \cdot \partial_\mu \vec{s} - i\theta Q[\vec{s}]. \tag{4.54}$$

The coupling constant g^2 is determined by the value of the spin s. In the large s limit one finds $1/g^2 = s/2$. Hence, by increasing the size of the $SU(2)$ spin representation

one approaches the continuum limit $g^2 \to 0$ of the asymptotically free 2-d $O(3)$ model [140, 141, 142]. As before, the topological charge is given by

$$Q[\vec{s}] = \frac{1}{8\pi} \int d^2x \; \epsilon_{\mu\nu} \; \vec{s} \cdot (\partial_\mu \vec{s} \times \partial_\nu \vec{s}) \in \pi_2[S^2] = \mathbb{Z}. \tag{4.55}$$

Quantum spin chains hence provide an unconventional regularization of the 2-d $O(3)$ model at $\theta = 0$ or π. This model is equivalent to the $CP(1)$ model as one can identify

$$P(x) = \frac{1}{2}[\mathbb{1} + \vec{s}(x) \cdot \vec{\sigma}]. \tag{4.56}$$

This offers a natural generalization to higher $CP(N-1)$ models. The low-energy effective theory of an antiferromagnetic quantum spin chain can be investigated using coherent state path integral techniques [70, 137]. Once again, the choice of the $SU(N)$-representation on each site determines the space in which the low-energy fields take their values. Here, we choose a completely symmetric $SU(N)$ representation on the even sites (sublattice A), corresponding to a Young tableau with a single row and n boxes.

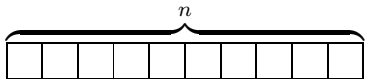

On the odd sites (sublattice B), one uses the corresponding anti-representation, i.e. the complex conjugate one, which consists of $(N-1)$ rows with n boxes.

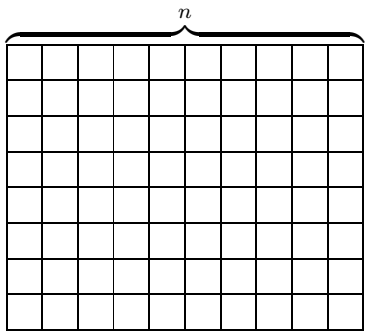

One can prove analytically that for large representations of $SU(N)$ (i.e. for large n), the low-energy physics is governed by $CP(N-1)$ fields. It should be noted that other representations with mixed symmetry (and thus with more complicated Young tableaux) in general do not lead to $CP(N-1)$ models. For example, choosing a totally antisymmetric tensor representation of $SU(N)$ with N even, i.e. the fermionic representation, one obtains the non-linear $U(N)/[U(N/2) \times U(N/2)]$ Grassmannian σ-model as the low-energy effective theory [114]. However, with our conditions, the effective action for the spin-waves is the 2-dimensional $CP(N-1)$ model described by

$$S[P] = \frac{1}{g^2} \int d^2x \; \mathrm{Tr}(\partial_\mu P \partial_\mu P) - i\theta Q[P], \tag{4.57}$$

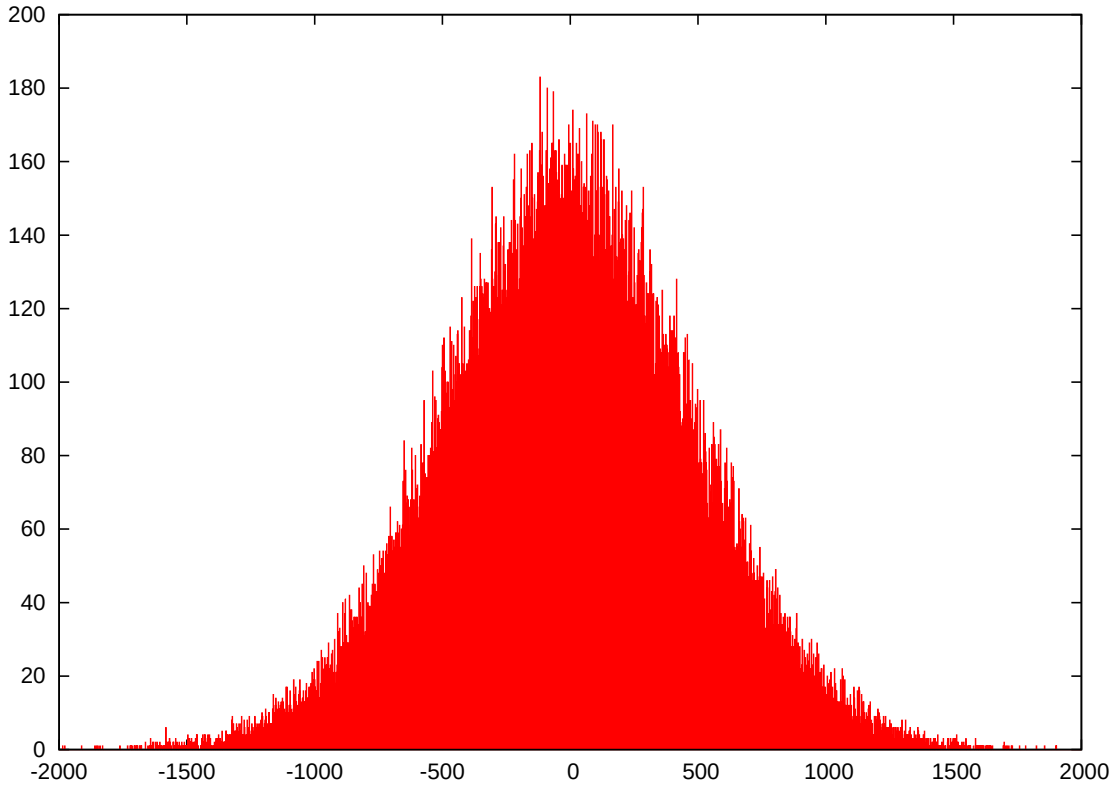

Figure 4.8: *Probability distribution of the order parameter $Q[q,\bar{q}]$ for an $SU(2)$ quantum spin chain with $n = 5$, which corresponds to a $CP(1)$ model at $\theta = \pi$. Here, $n_x = 72$, $n_t = 512$, and $\beta J = 10$. Large fluctuations of the order parameter indicate a second order phase transition.*

where $Q[P]$ is again given by

$$Q[P] = \frac{1}{2\pi i}\int d^2x\ \epsilon_{\mu\nu}\ \mathrm{Tr}(P\partial_\mu P\partial_\nu P) \in \pi_2[CP(N-1)] = \mathbb{Z}. \tag{4.58}$$

In complete analogy to the $CP(1)$ case, the size of the representation determines both the coupling constant and the vacuum angle, i.e.

$$\frac{1}{g^2} = \frac{n}{4}, \quad \theta = n\pi. \tag{4.59}$$

Note that for $SU(2)$ spin chains, $n = 2s$.

4.5.2 A first order phase transition at $\theta = \pi$ for $N > 2$

As it is illustrated in section 4.4.3, a first order phase transition occurs at $\theta = \pi$ for $CP(N-1)$ models with $N \geq 3$. The charge conjugation symmetry C (which remains

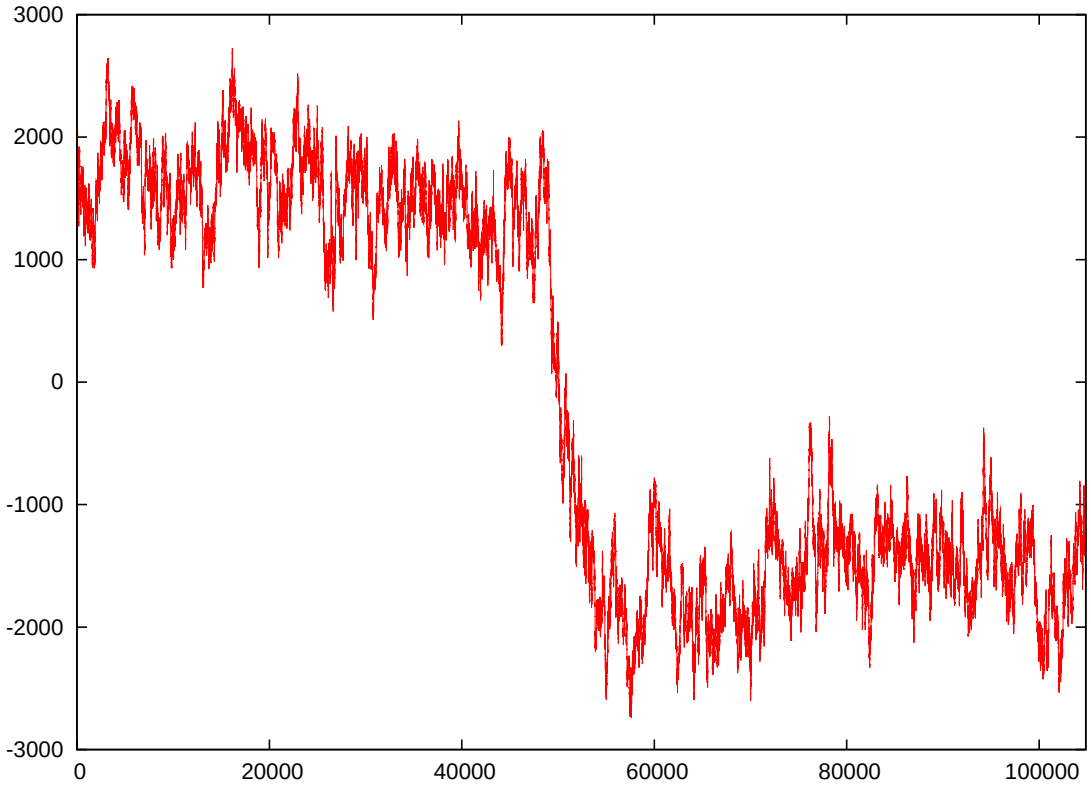

Figure 4.9: *A first order phase transition for the $SU(4)$ quantum spin chain with $n = 3$, which corresponds to a $CP(3)$ model at $\theta = \pi$. Here, $n_x = 144$, $n_t = 512$, and $\beta J = 25$.*

intact for $CP(1)$) is spontaneously broken. As before, quantum spin chains are, of course, C-invariant. Charge conjugation acts on the system in the exact same way as for quantum spin ladders. The order parameter $Q[q, \bar{q}]$ that we use here is also completely identical. We refer to the next chapter for a detailed description of $Q[q, \bar{q}]$. Here, we present numerical results for $SU(N)$ quantum spin chains with various symmetric $SU(N)$ representations. We vary the representation by changing the number n of Young tableau boxes. This demands a particular decomposition of the partition function that we will present in the next chapter. In a word, we consider spins in the symmetric $SU(N)$ representation with a Young tableau of n boxes as a direct product of n $SU(N)$ quantum spins in the fundamental representation. This direct product contains other non-symmetric representations which have to be projected out. Indeed, we need to restrict the representation on each site to a symmetric one with n Young tableau boxes. This so-called layer decomposition of the partition function is presented in detail in the next chapter. In figure 4.8, we present numerical simulations for the $CP(1)$ model at $\theta = \pi$. This corresponds to an antiferromagnetic $SU(2)$ Heisenberg chain with spin 5/2 on each site. As expected [66], we observe a second order phase transition with large fluctuations of the order parameter $Q[q, \bar{q}]$. In figure 4.9, we zoom in on a first order phase transition for the $CP(3)$ model at $\theta = \pi$. One

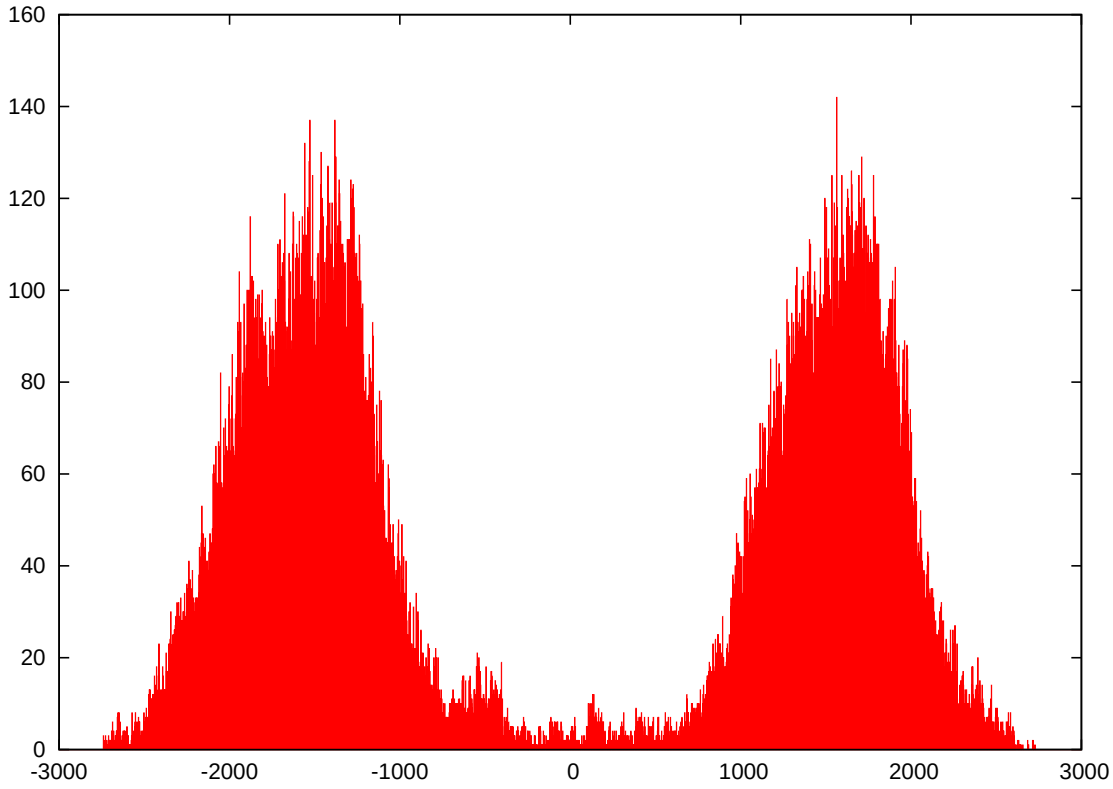

Figure 4.10: *First order phase transition at $\theta = \pi$ for the $CP(3)$ model of figure* 4.9.

clearly sees the two coexisting phases and a tunneling transition between them. This is also illustrated in figure 4.10, where we present the probability distribution of the order parameter $Q[q, \bar{q}]$. One observes a double peak structure which implies a first order phase transition. Due to limited statistics, the two peaks are not completely symmetric. Finally, in figure 4.11, we also present results for a $CP(5)$ model at $\theta = \pi$ which corresponds to an $SU(6)$ spin chain with $n = 3$. Again, one clearly sees the tunneling processes between the two phases.

4.6 Conclusions and Comments

In this chapter, we have seen that it is possible to regularize $CP(N-1)$ models with $SU(N)$-symmetric quantum spin systems in the framework of D-theory. First, an $SU(N)$ quantum ferromagnet in $(d+1)$ dimensions provides a valid regularization for the d-dimensional $CP(N-1)$ at $\theta = 0$. Indeed, at zero temperature (i.e. for an infinite extent β of the extra dimension), one has spontaneous symmetry breaking from $SU(N)$ to $U(N-1)$ and the corresponding Goldstone bosons live in the coset space $CP(N-1)$. Another ingredient of the D-theory formulation is dimensional reduction. Once β is made finite, due to asymp-

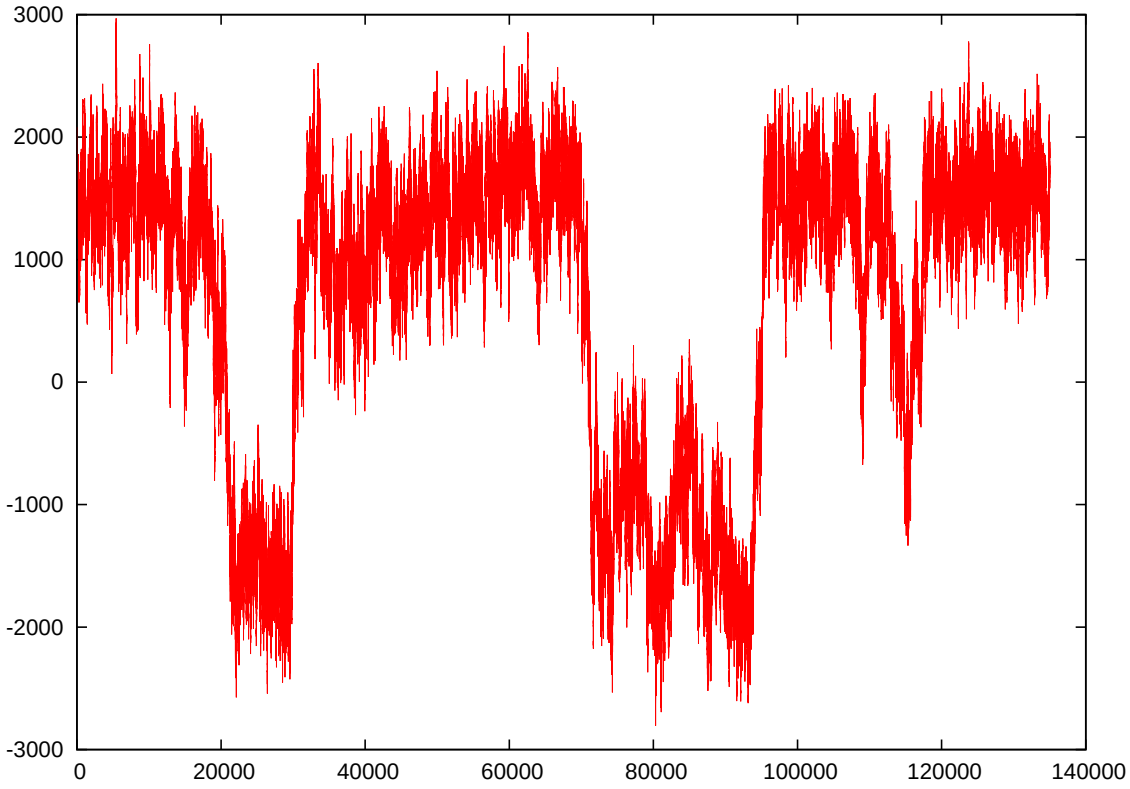

Figure 4.11: *Tunneling processes for the* $SU(6)$ *quantum spin chain with* $n = 3$*, which corresponds to a* $CP(5)$ *model at* $\theta = \pi$*. Here* $n_x = 72$*,* $n_t = 512$*, and* $\beta J = 7$*.*

totic freedom, the correlation length ξ is exponentially larger than β. Consequently, as one approaches the continuum limit, β becomes completely negligible and the system undergoes dimensional reduction to the d-dimensional target $CP(N-1)$ model at $\theta = 0$. The D-theory idea has been checked numerically with the help of an efficient cluster algorithm. One finds a remarkable agreement between the traditional Wilsonian regularization and our alternative one.

Moreover, it is also possible to simulate $CP(N-1)$ models directly at vacuum-angle $\theta = \pi$. Considering the $(2+1)$-dimensional $SU(N)$-symmetric quantum spin ladders, using coherent state path-integral techniques, one can prove that the system undergoes spontaneous symmetry breaking from $SU(N)$ to $U(N-1)$ for a large number of coupled spin chains. The dynamics of dimensional reduction is then analogous to the case of the quantum ferromagnet. Remarkably, an even number of coupled spin chains results in the 2-d $CP(N-1)$ model at $\theta = 0$, while an odd number results in the model at $\theta = \pi$. Hence, we have shown that one has a first order phase transition with C-breaking at $\theta = \pi$ for $N \geq 3$. This confirms the Seiberg-Affleck conjecture. Of course, one cannot be sure that working with a small number of coupled spin chains still leads to the right low-energy

physics. Spontaneous symmetry breaking is proved analytically only for a large number of coupled spin chains. Nevertheless, one observes the conjectured vacuum phase structure, which indicates that our formulation is indeed correct. Another important indication is the exponentially increasing correlation length $\xi(n)$ as one increases the number of chains n. This shows that for a large number of chains, the correlation length explodes. For an infinite system, $\xi(n) \to \infty$ implies massless modes and hence spontaneous symmetry breaking.

To augment our arguments, we have seen that a single $SU(N)$-symmetric quantum antiferromagnetic spin chain also provides a valid regularization of $CP(N-1)$ models both at $\theta = 0$ and π. In that case, some of the D-theory ingredients are missing. Indeed, one has no spontaneous symmetry breaking due to the Hohenberg-Mermin-Wagner-Coleman theorem, and hence no dimensional reduction. Instead, we generalized the results obtained for the quantum spin 1/2 chain to the larger group $SU(N)$. Coherent state techniques hence allow us to investigate the low-energy physics, which is described by 2-dimensional $CP(N-1)$ models with a topological term. This is strictly proved only for large representations of the group. Still, working with smaller representations, we find the conjectured phase structure: a first order phase transition for $N \geq 3$ and a second order one for $N = 2$ at $\theta = \pi$. Therefore, the considerations for large $SU(N)$ representations seem to still apply for smaller ones.

Chapter 5

Efficient Cluster Algorithms for $CP(N-1)$ Models

5.1 Introduction

In this chapter, we would like to present in some detail the algorithmic structure used to simulate our quantum spin systems. We have seen in the previous chapter that they provide a regularization of the $CP(N-1)$ models at $\theta = 0$ or π. Here, we will show how to construct efficient cluster algorithms. They are among the most powerful tools for numerical simulations of non-perturbative lattice field theories and statistical mechanics models. Interestingly, it is impossible to construct an efficient Wolff-type embedding algorithm for the $CP(N-1)$ models in Wilson's framework of lattice field theory due to a no-go theorem [123]. In the D-theory framework on the other hand, it is almost straightforward. Indeed, the algorithmic structure is relatively simple and detailed studies of the autocorrelation times show that critical slowing down in the continuum limit is almost completely eliminated. Before turning to the cluster algorithms, let us say a word about Monte Carlo simulation of physical systems.

5.1.1 The Monte Carlo method and critical slowing down

In what follows, we would like to simulate different quantum spin systems which are in general impossible to solve analytically. An exact diagonalization of the Hamilton operator is, for example, possible only for small systems, because of the huge size of the Hilbert space. Fortunately, powerful numerical methods were developed in statistical mechanics, the most accurate being the Monte Carlo method. The idea is to compute the quantum partition function by generating spin configurations numerically. Of course, the partition function is an extremely high dimensional integral, therefore a direct integration is hopeless. Instead, the Monte Carlo method give the predominance to configurations which have the largest contributions in the partition function. The Boltzmann factor $\exp(-S[\mathcal{C}^{(i)}])$ is used as the probability to generate the spin configuration $[\mathcal{C}^{(i)}]$, where $S[\mathcal{C}^{(i)}]$ is the corresponding

action. In Monte Carlo simulations one generates a sequence of configurations

$$[\mathcal{C}^{(1)}] \to [\mathcal{C}^{(2)}] \to \ldots \to [\mathcal{C}^{(N)}], \tag{5.1}$$

which form a Markow chain. An algorithm turns the spin configuration $[\mathcal{C}^{(i)}]$ into $[\mathcal{C}^{(i+1)}]$. The initial configuration is picked at random and after a number M of iterations, the system reaches an equilibrium. The configurations generated after this thermalization time are used to compute observables. The estimation of the expectation value of an observable $\mathcal{O}[\mathcal{C}]$ is performed by averaging its values over configurations of the Monte Carlo sample

$$\langle \mathcal{O}[\mathcal{C}] \rangle \approx \frac{1}{N-M} \sum_{i=M+1}^{N} \mathcal{O}[\mathcal{C}^{(i)}]. \tag{5.2}$$

This relation becomes exact as $N \to \infty$. At finite values $N - M$, one makes an error that decreases proportionally to $1/\sqrt{N-M}$. Hence, to increase the accuracy by a factor of two, one has to run the Monte Carlo algorithm four times as long. The Boltzmann weight $\exp(-S[\mathcal{C}^{(i)}])$ does not appear explicitly in the above sum. It is implicitly included, since the configurations in the Markow chain occur with probability $\exp(-S[\mathcal{C}])$.

In order to converge to the correct equilibrium distribution, the Monte Carlo algorithm has to obey ergodicity and detailed balance. Ergodicity means that starting from an initial configuration, the algorithm can in principle reach any other spin configuration. Detailed balance means that

$$\exp(-S[\mathcal{C}])w([\mathcal{C}] \to [\mathcal{C}']) = \exp(-S[\mathcal{C}'])w([\mathcal{C}'] \to [\mathcal{C}]), \tag{5.3}$$

where $w([\mathcal{C}] \to [\mathcal{C}'])$ is the transition probability for the algorithm to turn the configuration $[\mathcal{C}]$ into $[\mathcal{C}']$. In fact, a Monte Carlo algorithm is completely characterized by $w([\mathcal{C}] \to [\mathcal{C}'])$. Let us take the example of the Metropolis algorithm [11]. A new configuration $[\mathcal{C}']$ is randomly chosen in the vicinity of the old configuration $[\mathcal{C}]$. If one has

$$S[\mathcal{C}'] < S[\mathcal{C}] \Rightarrow w([\mathcal{C}] \to [\mathcal{C}']) = 1, \tag{5.4}$$

the new configuration $[\mathcal{C}']$ is accepted. On the other hand, if the new action is larger, the new configuration is accepted only with a certain probability, i.e.

$$S[\mathcal{C}'] > S[\mathcal{C}] \Rightarrow w([\mathcal{C}] \to [\mathcal{C}']) = \exp(-S[\mathcal{C}'] + S[\mathcal{C}]). \tag{5.5}$$

Otherwise the old configuration is kept. It is easy to show that this algorithm is ergodic and obeys detailed balance. This algorithm is particularly simple, but unfortunately not very efficient as the correlation length becomes large. Indeed, it turns out that successive configurations in the Markow chain are correlated with each other. The updates are only local, thus generating a new statistically independent configuration may require a large number of Monte Carlo iterations. The autocorrelation time τ of the Metropolis algorithm, which denotes the Monte Carlo time to obtain statistically independent configurations,

actually increases when one approaches a second order phase transition. This is bad news for lattice field theory or D-theory formulations, where one reaches the continuum limit by sending the correlation length ξ to infinity. In that limit, the corresponding critical slowing down is determined by

$$\tau \propto \xi^z, \tag{5.6}$$

where z is the dynamical critical exponent characterizing the efficiency of the Monte Carlo algorithm. For the Metropolis algorithm described above, one has $z \approx 2$, which leads to severe critical slowing down near the continuum limit. In lattice pure gauge theory, the best algorithm presently known has $z \approx 1$ — the so-called overrelaxation algorithm [143]. For simpler spin models as the $O(N)$ models, one can use cluster algorithms with $z \approx 0$ already in the Wilson formulation. This is not the case for the $CP(N-1)$ models, for which efficient cluster algorithms can be constructed only in the D-theory framework. In the following sections, we will show how this is possible.

5.1.2 Generalities on cluster algorithms

As shown in the previous chapter, quantum spin systems such as $SU(N)$-symmetric quantum ferromagnets, quantum antiferromagnets, and ladder systems with both couplings, lead to unconventional regularizations of the $CP(N-1)$ models in the framework of D-theory. Remarkably, within this formulation, it is almost straightforward to construct cluster algorithms which perform reliably close to the continuum limit. Indeed, cluster algorithms are among the most efficient tools for numerical simulations of lattice field theory or statistical mechanics systems. The first cluster algorithm was developed by Swandsen and Wang for discrete classical spins in the context of the Ising and Potts models [12]. This was generalized later by Wolff to $O(N)$ models formulated in terms of continuous classical spins [51, 52]. For the 2-d $O(3)$ model, the Wolff cluster algorithm has been extended to a meron-cluster algorithm which has been used to solve the complex action problem at non-zero θ-vacuum angle [66]. Cluster algorithms for quantum spin systems were first developed by Evertz et al. [50] and by Wiese and Ying for the 2-dimensional quantum antiferromagnetic Heisenberg model [38].

Cluster algorithms are very efficient because they guarantee non-trivial moves in configuration space. In contrast to local algorithms, they perform global updates of the system and detect the correlations between the quantum spins. For example, in a highly correlated system, the Metropolis step (flipping a single spin) will almost always be rejected. On the other hand, the cluster algorithm connects the spin that are correlated and can flip them with probability one. Remarkably, cluster algorithms can also be defined directly in continuous Euclidean time (no need to introduce a lattice decomposition in the β-direction), and turn out to be even more efficient [39]. We will detail the exact structure of the algorithm in the next sections. For a review on the subject, we refer to [144].

Let us now illustrate the main ideas behind cluster algorithms. We start with the simple

example of a 1-dimensional spin 1/2 Heisenberg chain with ferromagnetic coupling. The configurations are hence characterized by the spins $q(x,t)$ located on the 2-dimensional space-time lattice of sites (x,t). The spins 1/2 can be either up $u(x,t)$ or down $d(x,t)$. The cluster algorithm forms a closed loop of spins in the same quantum state on the space-time lattice. Then, it flips all the connected spins on the loop to another quantum state. In our case, a cluster with connected spins u will be flipped to spins d. It starts by picking a lattice point (x,t) at random and then grows the loop according to certain cluster rules. The probabilities of spin connections will be derived in the next sections for general $SU(N)$-symmetric spin systems. Once the updating process is done, one repeats the operation by picking up a new point at random and grows another cluster. This is performed any number of time in order to extract mean values of physical quantities.

In the following, we set up the path integral representation for d-dimensional $SU(N)$ quantum ferromagnets and for $SU(N)$ quantum spin chains with various representations of the group. In particular, we derive the Boltzmann weight of the allowed plaquette configurations. This will eventually lead to the cluster rules, which control the growth of the clusters on the space-time lattice. This set-up is then generalized to $SU(N)$ quantum spin ladder systems. In the last part of this chapter, we demonstrate the high efficiency of cluster algorithms near the continuum limit, i.e. as $\xi \to \infty$.

5.2 Path Integral Representation of $SU(N)$ Quantum Ferromagnets

Let us first construct a path integral representation of the quantum partition function

$$Z = \mathrm{Tr} \exp(-\beta H), \tag{5.7}$$

where H is the quantum Hamiltonian describing the $SU(N)$-symmetric ferromagnetic system

$$H = -J \sum_{x,\mu} T^a_x T^a_{x+\hat{\mu}}. \tag{5.8}$$

In the context of D-theory, the extent β is not the Euclidean time of the target $CP(N-1)$ model. Nevertheless, to have a clear notation, we will still denote positions in that dimension by the time parameter t. The standard way to derive a path integral representation is to discretize the β direction and insert at each time-step a complete set of basis states that spans the physical Hilbert space. Therefore, as an intermediate step, we introduce a lattice in the β direction as illustrated in figure 5.1. We use the so-called Trotter decomposition of the Hamiltonian. Indeed for a d-dimensional hyper-cubic lattice L^d with an even extent L, we decompose the Hamilton operator into $2d$ terms

$$H = H_1 + H_2 + \ldots + H_{2d}, \tag{5.9}$$

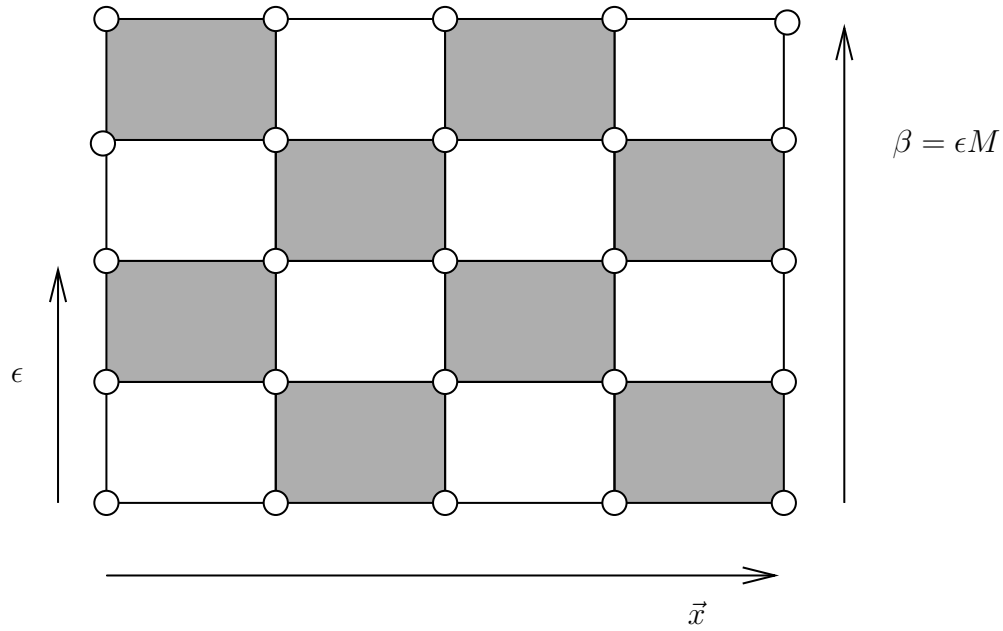

Figure 5.1: *Trotter decomposition along the extra dimension of size β. The shaded plaquettes carry the interaction. Here $\vec{x}$ is a 1-dimensional vector which denotes the physical dimensions. In D-theory, the extra dimension ultimately disappears via dimensional reduction and does hence not correpond to the Euclidean time of the target theory.*

where the independent terms are given by

$$H_i = \sum_{\substack{x=(x_1,x_2,\ldots,x_d) \\ x_i \text{even}}} h_{x,i}, \qquad H_{i+d} = \sum_{\substack{x=(x_1,x_2,\ldots,x_d) \\ x_i \text{odd}}} h_{x,i}. \tag{5.10}$$

The individual contributions $h_{x,i}$ to a given H_i commute with each other, but two different H_i do not commute. Hence, the interaction is carried only by the shaded plaquettes of figure 5.1. The individual contributions $h_{x,i}$ to equation (5.10) have the form

$$h_{x,i} = -JT^a_x T^a_{x+\hat{i}}. \tag{5.11}$$

Using the Trotter formula, one can express the partition function as

$$Z = \lim_{M\to\infty} \mathrm{Tr}[\exp(-\epsilon H_1)\exp(-\epsilon H_2)\ldots\exp(-\epsilon H_{2d})]^M. \tag{5.12}$$

We have introduced M Euclidean time-slices with the lattice spacing $\epsilon = \beta/M$ in the extra dimension. Note that the Trotterization procedure is just a technical trick. In fact, the path integral is completely well defined with a continuous extent of the extra dimension. The final result is hence independent of this decomposition. In order to obtain the path

integral representation, one inserts a complete sets of spin states $q \in \{u, d, s, \ldots\}$ between the exponential factors in (5.12). The partition function then takes the form

$$Z = \sum_{[q]} \exp(-S[q]). \tag{5.13}$$

The sum extends over configurations $[q]$ of spins $q_{(x,t)}$ on a $(d+1)$-dimensional space-time lattice of points (x,t). The Boltzmann factor has the following form

$$\begin{aligned} \exp(-S[q]) \;=\; & \prod_{p=0}^{M-1} \prod_{i=1}^{d} \prod_{\substack{x=(x_1,x_2,\ldots,x_d) \\ x_i even,\ t=2dp+i-1}} \exp\left(-S[q_{(x,t)}, q_{(x+\hat{i},t)}, q_{(x,t+1)}, q_{(x+\hat{i},t+1)}]\right) \\ & \times \prod_{\substack{x=(x_1,x_2,\ldots,x_d) \\ x_i odd,\ t=2dp+d+i-1}} \exp\left(-S[q_{(x,t)}, q_{(x+\hat{i},t)}, q_{(x,t+1)}, q_{(x+\hat{i},t+1)}]\right). \end{aligned} \tag{5.14}$$

Let us be a bit more explicit. A space-time plaquette contribution to the above expression is obtained by considering the following transfer matrix element

$$\begin{aligned} & \langle q^a_{(x,t)}, q^b_{(x+\hat{i},t)}| \exp(-\epsilon J T^a_x T^a_{x+\hat{i}})| q^c_{(x,t+1)}, q^d_{(x+\hat{i},t+1)}\rangle = \\ & \exp\{-S[q^a_{(x,t)}, q^b_{(x+\hat{i},t)}, q^c_{(x,t+1)}, q^d_{(x+\hat{i},t+1)}]\} \end{aligned} \tag{5.15}$$

The state $|q^a_{(x,t)}, q^b_{(x+\hat{i},t)}\rangle$ denotes two neighboring $SU(N)$-spins at the time-slice t in the extra dimension, and $|q^c_{(x,t+1)}, q^d_{(x+\hat{i},t+1)}\rangle$ the state a time-slice later. Here, a, b, c and d indicate the flavor of the correponding $SU(N)$-spin $q \in \{u, d, s, \ldots\}$ and run from 1 to N. We place two spins q on the sites (x,t) and $(x+\hat{i},t)$ of a shaded plaquette. They transform in the fundamental representation $\{N\}$ of $SU(N)$, and hence couple as

$$\{N\} \otimes \{N\} = \left\{\frac{N(N+1)}{2}\right\} \oplus \left\{\frac{N(N-1)}{2}\right\}. \tag{5.16}$$

In terms of Young tableaux, one gets

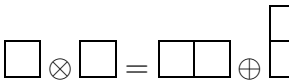

(5.17)

We now consider the basis state $|q^a_{(x,t)}, q^b_{(x+\hat{i},t)}\rangle$ with $a \in \{1, \ldots, N\}$ which has to be inserted at each time-step of the Trotter decomposition. Of course, one has

$$\sum_{a,b=1}^{N} |q^a_{(x,t)}, q^b_{(x+\hat{i},t)}\rangle\langle q^a_{(x,t)}, q^b_{(x+\hat{i},t)}| = \mathbb{1}. \tag{5.18}$$

From the relation (5.16), we see that out of the N^2 states $|q^a_{(x,t)}, q^b_{(x+\hat{i},t)}\rangle$ we can build $N(N+1)/2$ symmetric states and $N(N-1)/2$ antisymmetric ones. At a given time-slice

(for fixed time t), one can thus construct the $N(N+1)/2$ symmetric states $|ab\rangle_s$, which have the form

$$\begin{aligned} |aa\rangle_s &= |q^a_{(x,t)}, q^a_{(x+\hat{i},t)}\rangle \\ |ab\rangle_s &= \frac{1}{\sqrt{2}}\,(|q^a_{(x,t)}, q^b_{(x+\hat{i},t)}\rangle + |q^b_{(x,t)}, q^a_{(x+\hat{i},t)}\rangle), \quad a \neq b. \end{aligned} \tag{5.19}$$

The $N(N-1)/2$ antisymmetric ones are given by

$$|ab\rangle_a = \frac{1}{\sqrt{2}}\,(|q^a_{(x,t)}, q^b_{(x+\hat{i},t)}\rangle - |q^b_{(x,t)}, q^a_{(x+\hat{i},t)}\rangle). \tag{5.20}$$

Inverting these relations, one obtains the basis spin states in terms of symmetric and antisymmetric states

$$\begin{aligned} |q^a_{(x,t)}, q^a_{(x+\hat{i},t)}\rangle &= |aa\rangle_s, \\ |q^a_{(x,t)}, q^b_{(x+\hat{i},t)}\rangle &= \frac{1}{\sqrt{2}}\,(|ab\rangle_s + |ab\rangle_a), \quad a \neq b, \\ |q^b_{(x,t)}, q^a_{(x+\hat{i},t)}\rangle &= \frac{1}{\sqrt{2}}\,(|ab\rangle_s - |ab\rangle_a), \quad a \neq b. \end{aligned} \tag{5.21}$$

In order to act on these states with the Hamiltonian (5.11), we write the operator $\vec{T}_x \cdot \vec{T}_{x+\hat{i}}$ as

$$\vec{T}_x \cdot \vec{T}_{x+\hat{i}} = \frac{1}{2}(\vec{T}_x + \vec{T}_{x+\hat{i}})^2 - \frac{1}{2}\vec{T}^2_x - \frac{1}{2}\vec{T}^2_{x+\hat{i}}. \tag{5.22}$$

One recognizes the quadratic Casimir operator of $SU(N)$, which is defined as

$$C_2(\{r\}) = \vec{T}^2_{\{r\}}, \tag{5.23}$$

where $\{r\}$ denotes the representation of the group. This Casimir operator has the property to commute with all generators of $SU(N)$. In particular, for this group, depending on the representation, they are given by [145]

$$\begin{aligned} C_2(\{N\}) &= \frac{N^2-1}{2N}, \\ C_2(\{N(N+1)/2\}) &= \frac{(N-1)(N+2)}{N}, \\ C_2(\{N(N-1)/2\}) &= \frac{(N+1)(N-2)}{N}. \end{aligned} \tag{5.24}$$

Therefore, the relation (5.22) reduces to the two following expressions depending on whether the operator $(\vec{T}_x + \vec{T}_{x+\hat{i}})^2$ is in the symmetric or antisymmetric $SU(N)$ representation

$$\begin{aligned} \vec{T}_x \cdot \vec{T}_{x+\hat{i}} &= \frac{1}{2}\,C_2(\{N(N+1)/2\}) - C_2(\{N\}) = E(\{N(N+1)/2\}), \\ \vec{T}_x \cdot \vec{T}_{x+\hat{i}} &= \frac{1}{2}\,C_2(\{N(N-1)/2\}) - C_2(\{N\}) = E(\{N(N-1)/2\}), \end{aligned} \tag{5.25}$$

with

$$E(\{N(N+1)/2\}) = \frac{N-1}{2N},$$
$$E(\{N(N-1)/2\}) = -\frac{N+1}{2N}. \tag{5.26}$$

Then, using these relations and the expressions of the basis spin states (5.21) in terms of symmetric and antisymmetric states, it is easy to evaluate the transfer matrix elements (5.15). Indeed, one obtains

$$\begin{aligned}&\langle q^a_{(x,t)}, q^a_{(x+\hat{i},t)}| \exp(\epsilon J \vec{T}_x \cdot \vec{T}_{x+\hat{i}})|q^a_{(x,t+1)}, q^a_{(x+\hat{i},t+1)}\rangle \\ &= \langle aa|_s \exp(\epsilon J E(\{N(N+1)/2\}))|aa\rangle_s = \exp\left(\frac{\epsilon J(N-1)}{2N}\right).\end{aligned} \tag{5.27}$$

Hence, two spins with the same flavor can then evolve in the extra dimension through an interaction plaquette without flavor change. For two different spins ($a \neq b$), one has

$$\begin{aligned}&\langle q^a_{(x,t)}, q^b_{(x+\hat{i},t)}| \exp(\epsilon J \vec{T}_x \cdot \vec{T}_{x+\hat{i}})|q^a_{(x,t+1)}, q^b_{(x+\hat{i},t+1)}\rangle = \frac{1}{2}(\langle ab|_a + \langle ab|_s) \exp(\epsilon J \vec{T}_x \cdot \vec{T}_{x+\hat{i}}) \\ &\times (|ab\rangle_s + |ab\rangle_a) = \frac{1}{2}\left[\langle ab|_a \exp(\epsilon J E(\{N(N-1)/2\}))|ab\rangle_a\right. \\ &\left.+\langle ab|_s \exp(\epsilon J E(\{N(N+1)/2\}))|ab\rangle_s\right] = \frac{1}{2}\left[\exp\left(-\frac{\epsilon J(N+1)}{2N}\right) + \exp\left(\frac{\epsilon J(N-1)}{2N}\right)\right]\end{aligned} \tag{5.28}$$

and similarly

$$\begin{aligned}&\langle q^a_{(x,t)}, q^b_{(x+\hat{i},t)}| \exp(\epsilon J \vec{T}_x \cdot \vec{T}_{x+\hat{i}})|q^b_{(x,t+1)}, q^a_{(x+\hat{i},t+1)}\rangle = \frac{1}{2}(\langle ab|_a + \langle ab|_s) \exp(\epsilon J \vec{T}_x \cdot \vec{T}_{x+\hat{i}}) \\ &\times (|ab\rangle_s - |ab\rangle_a) = \frac{1}{2}\left[\exp\left(\frac{\epsilon J(N-1)}{2N}\right) - \exp\left(-\frac{\epsilon J(N+1)}{2N}\right)\right].\end{aligned} \tag{5.29}$$

Normalizing these relations by dividing by $\exp(\epsilon J(N-1)/2N)$ and using the relation (5.15), the plaquette contributions reduce to

$$\begin{aligned}&\exp(-S[u,u,u,u]) = \exp(-S[d,d,d,d]) = 1, \\ &\exp(-S[u,d,u,d]) = \exp(-S[d,u,d,u]) = \frac{1}{2}[1+\exp(-\epsilon J)], \\ &\exp(-S[u,d,d,u]) = \exp(-S[d,u,u,d]) = \frac{1}{2}[1-\exp(-\epsilon J)],\end{aligned} \tag{5.30}$$

where $S[u,u,u,u]$ is the contribution given by four same spins q^a on the plaquette. The flavors u and d can be permuted to other values. All other Boltzmann factors are zero. This implies several constraints on allowed configurations. The Boltzmann factor (5.14) is a product of these plaquette contributions. The allowed ones are represented in figure

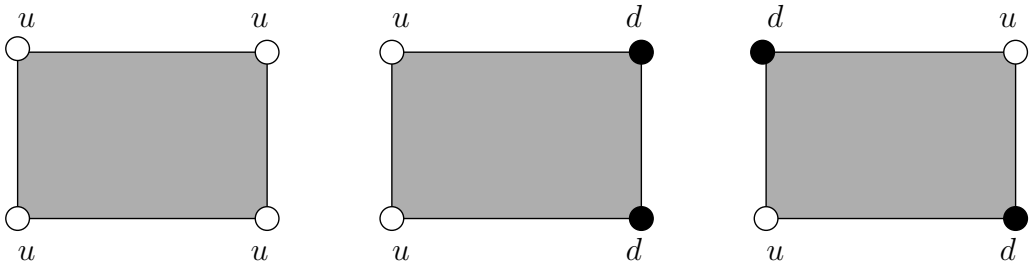

Figure 5.2: *Allowed configurations on the interaction plaquettes of the Trotter decomposition. The $SU(N)$ spins u and d can be permuted to any other spin q^a of $SU(N)$, $a = 1, \ldots, N$.*

5.2. In the following, we will consider the uniform magnetization in the 3-direction (4.19), which takes the form

$$\mathcal{M} = \sum_{x,t} [\delta_{q(x,t),u} - \delta_{q(x,t),d}]. \tag{5.31}$$

This represents one component of $T^a = \sum_x T^a_x$. One can also define the corresponding uniform susceptibility

$$\chi = \frac{1}{\beta L^d} \langle \mathcal{M}^2 \rangle, \tag{5.32}$$

where L^d is the spatial volume of the system.

5.3 Cluster Algorithm and Cluster Rules for $SU(N)$ Ferromagnetic Systems

Let us now turn to the explicit construction of clusters in our $(d+1)$-dimensional system. We will concentrate on the single-cluster algorithm, which grows one cluster and flips it with probability 1 to another quantum state. We also mention the multi-cluster algorithm. A multi-cluster algorithm first connects spins in pairs on each interaction plaquette. It identifies all resulting clusters, each spin belonging to exactly one cluster. Then, instead of flipping each cluster with probability 1 (which would be completely inefficient), it flips all clusters with a probability 1/2. Therefore, a configuration with n clusters turns into one of 2^n possible new configurations, with equal probability for each alternative. In the following, we will use a multi-cluster algorithm to investigate the efficiency of the method in the continuum limit.

The single cluster algorithm for a $(d+1)$-dimensional $SU(N)$ quantum ferromagnet is a straightforward generalization of what has been described above for the $SU(2)$ Heisenberg chain. One picks a point (x,t) randomly in the hypercubic lattice. Again, the spin located at this point participates in two plaquette interactions, one before and one after

Configurations and Break-ups	Transfer Matrix Elements
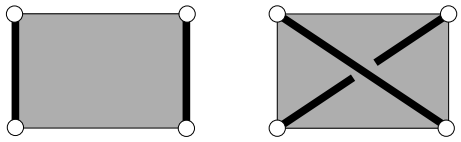	$\exp(-S[u,u,u,u]) = 1$
	$\exp(-S[u,d,u,d]) = \frac{1}{2}[1+\exp(-\epsilon J)]$
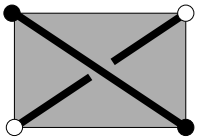	$\exp(-S[u,d,d,u]) = \frac{1}{2}[1-\exp(-\epsilon J)]$

Table 5.1: *Possible configurations for an $SU(N)$ quantum ferromagnet with the corresponding break-ups and Boltzmann weights. Again, the spins u (open circles) and d (black points) can be permuted to any other $SU(N)$ spins q^a.*

t. The choice of one of the interaction is arbitrary and one considers the other spins on that plaquette. One of the corners will be the next point of the loop. According to the path integral representation investigated in the previous section, only some plaquette configurations are allowed. This implies severe constraints on the possible growth of the loop. For configurations $C_1 = [q^a, q^b, q^a, q^b]$ with $a \neq b$, the next point is the time-like neighbor $(x, t+1)$ of (x,t) on the plaquette. For $C_2 = [q^a, q^b, q^b, q^a]$ with $a \neq b$ the next point is the diagonal neighbor $(x+\hat{i}, t+1)$. If the states are all the same, i.e. for $C_3 = [q^a, q^a, q^a, q^a]$, the next point of the loop is the time-like neighbor with probability

$$p = \frac{1}{2}\,[1+\exp(-\epsilon J)], \tag{5.33}$$

and the diagonal neighbor with probability $(1-p)$. This is illustrated in table 5.1 for the three possible configurations. The next point on the loop belongs then to another interaction plaquette for which the same process is repeated. The loop grows in this way until it finally closes. The flavor (or quantum state) is the same for all connected spins on the loop and one then flips all spins in the cluster to another randomly chosen flavor with probability 1. This is illustrated in figure 5.3, where a cluster of flavor d is flipped to another quantum state s. Note that the cluster can only evolve forward (or backward) in time, since only time-like or diagonal break-ups are allowed. As they should, the cluster

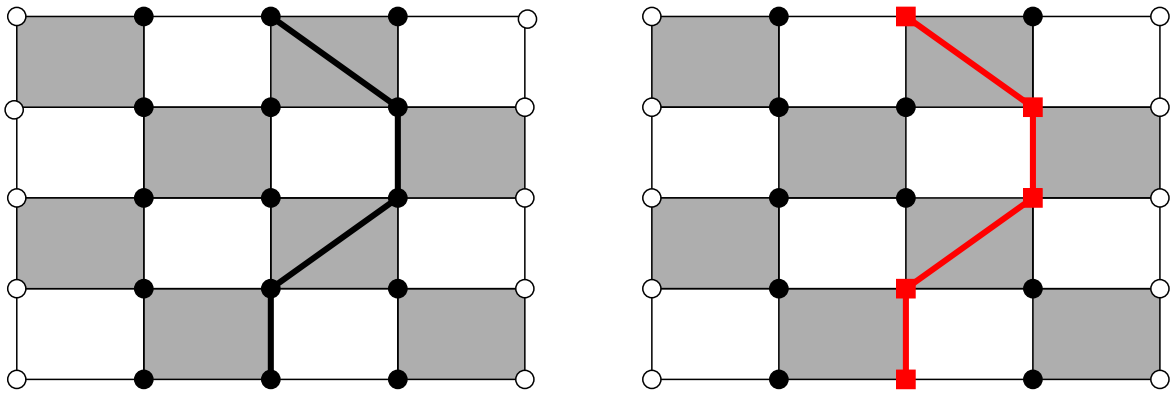

Figure 5.3: *Example of an $SU(3)$ ferromagnet. The fat black line represents a cluster of connected spins in a quantum state d. All spins in that cluster are then flipped to another flavor s, represented by the red square. Open circle represents spins in the state u.*

rules are consistent with detailed balance, i.e.

$$p(C_i)w(C_i \to C_j) = p(C_j)w(C_j \to C_i), \tag{5.34}$$

where $p(C_i) = \exp(-S[C_i])$ is the Boltzmann weight of the plaquette configuration and $w(C_i \to C_j)$ is the transition probability to go from C_i to C_j. In particular, we have

$$\begin{aligned} p(C_1)w(C_1 \to C_2) &= 0 = p(C_2)w(C_2 \to C_1), \\ p(C_1)w(C_1 \to C_3) &= p = p(C_3)w(C_3 \to C_1), \\ p(C_2)w(C_2 \to C_3) &= 1 - p = p(C_3)w(C_3 \to C_2). \end{aligned} \tag{5.35}$$

If one repeats the updating process a number of times, one can extract physical quantities such as the uniform susceptibility of equation (5.32). In particular, one can define a so-called improved estimator for this quantity. Improved estimators can be constructed using the multi-cluster algorithm briefly described above. With such an estimator, the statistics is increased by a factor 2^n, which is exponentially large in the number of clusters and hence in the physical volume. Let us illustrate this idea for the improved estimator of the uniform susceptibility. Again, χ is defined as

$$\chi = \frac{1}{\beta L^d}\langle \mathcal{M}^2 \rangle, \tag{5.36}$$

where $\mathcal{M}$ is the uniform magnetization (5.31) in the 3-direction of the $SU(N)$ space. According to the cluster rules, all spins in a cluster have the same flavor. Since all points are touched once in a multi-cluster algorithm, one has

$$\chi = \frac{1}{\beta L^d}\langle (\sum_c \mathcal{M}_c)^2 \rangle, \tag{5.37}$$

where $\mathcal{M}_\mathcal{C}$ is the cluster magnetization. Each cluster $\mathcal{C}$ has an integer winding number which is the number of times the cluster winds around the extra dimension. This quantity times β is the cluster size $|\mathcal{C}|$ (which is equal to $|\mathcal{M}_\mathcal{C}|$). Moreover, the susceptibility takes the form

$$\chi = \frac{1}{\beta L^d}\langle(\sum_\mathcal{C}\mathcal{M}_\mathcal{C})^2\rangle = \frac{1}{\beta L^d}\langle\sum_{\mathcal{C},\mathcal{C}'}\mathcal{M}_\mathcal{C}\mathcal{M}_{\mathcal{C}'}\rangle = \frac{1}{\beta L^d}\langle\sum_\mathcal{C}\mathcal{M}_\mathcal{C}^2\rangle. \tag{5.38}$$

In the second step, we have averaged over the sub-ensemble of 2^n equally probable configurations. According to the relation (5.31), the cluster changes sign under cluster flip from u to d flavors. Therefore, the term $\mathcal{M}_\mathcal{C}\mathcal{M}_{\mathcal{C}'}$ averages to zero unless $\mathcal{C} = \mathcal{C}'$. This relates the uniform susceptibility to the average $\mathcal{M}_\mathcal{C}^2$ of a multi-cluster algorithm.

Let us turn back to the single cluster algorithm where a loop is grown from a randomly chosen point and then flipped to another value of the spin. In this case, the improved estimator obtained for the multi-cluster algorithm has to be modified by the probability $|\mathcal{M}_\mathcal{C}|/L^d\beta$ to pick a single cluster of size $|\mathcal{M}_\mathcal{C}|$. Hence, the improved estimator for the single-cluster algorithm is given by

$$\chi = \frac{1}{\beta L^d}\ \langle\frac{L^d\beta}{|\mathcal{M}_\mathcal{C}|}\mathcal{M}_\mathcal{C}^2\rangle = \langle|\mathcal{C}|\rangle, \tag{5.39}$$

where the cluster size $|\mathcal{C}|$ is the sum over all displacements in the cluster, i.e.

$$|\mathcal{C}| = \frac{\epsilon}{M}\ \sum_{(x,t)\in\mathcal{C}} 1. \tag{5.40}$$

Again, M is the number of slices of separation ϵ in the extra dimension of extent β.

5.4 Path Integral Representation for $SU(N)$ Antiferromagnetic Spin Chains

The path integral representation of $SU(N)$-symmetric quantum antiferromagnetic spin chains can be set up following the same type of arguments. In full analogy with the case of an $SU(N)$ ferromagnet, we use a Trotter decomposition of the partition function and insert a complete set of basis spin states at the time-slices. One splits the Hamiltonian into two pieces because the chain is 1-dimensional. Hence, we have

$$Z = \lim_{M\to\infty}\ \mathrm{Tr}[\exp(-\epsilon H_1)\exp(-\epsilon H_2)]^M, \tag{5.41}$$

where H_1 and H_2 act on successive time-slice steps as illustrated by the shaded plaquettes in figure 5.1. The individual contributions to equation (5.10) are given by

$$h_{x,1} = -JT_x^a T_{x+\hat{1}}^{a*}, \tag{5.42}$$

with $J > 0$ and $\hat{1}$ the direction along the chain. The local contributions to the Boltzmann weight factor $\exp(-S[q, \bar{q}])$ are given by the relation

$$\begin{aligned} &\exp(-S[q^a_{(x,t)}, \bar{q}^b_{(x+\hat{1},t)}, q^c_{(x,t+1)}, \bar{q}^d_{(x+\hat{1},t+1)}]) \\ &= \langle q^a_{(x+\hat{1},t)}, \bar{q}^b_{(x+\hat{1},t)}| \exp(-\epsilon J T^a_x T^{a*}_{x+\hat{1}})|q^c_{(x,t+1)}, \bar{q}^d_{(x+\hat{1},t+1)}\rangle. \end{aligned} \tag{5.43}$$

Again $a, b, c, d \in \{1, \ldots, N\}$. In the following, we study the path integral representation for spins q and $\bar{q}$ in the fundamental and antifundamental representations, respectively. Generalization to higher $SU(N)$ spin representations will be investigate separately in section 5.6.

Let us begin by placing the fundamental representation $\{N\}$ of $SU(N)$ on each even site, and the corresponding antifundamental representation $\{\overline{N}\}$ on the odd sites of the chain. Coupling two neighboring spins results in the following decomposition

$$\{N\} \otimes \{\overline{N}\} = \{N^2 - 1\} \oplus \{1\}. \tag{5.44}$$

Indeed, a representation and its antirepresentation couple to the adjoint representation plus a singlet. In terms of Young tableaux, for example for $SU(3)$, one has

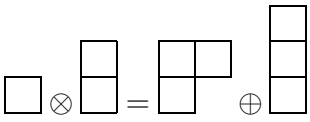

(5.45)

We can easily construct the state which transforms as a singlet under $SU(N)$ transformations as well as the ones which transform in the adjoint representation. For the singlet, one has

$$|\{1\}\rangle = \frac{1}{\sqrt{N}} \sum_a |q^a_{(x,t)}, \bar{q}^a_{(x+\hat{1},t)}\rangle, \tag{5.46}$$

where $|q^a_{(x,t)}, \bar{q}^a_{(x+\hat{1},t)}\rangle$ is the state formed by two $SU(N)$ spins $q \in \{u, d, s, \ldots\}$ and $\bar{q} \in \{\bar{u}, \bar{d}, \bar{s}, \ldots\}$, located on the neighboring sites on a plaquette interaction. It is also straightforward to build the states of the adjoint representation (think about the octet representation of $SU(3)$, for example about the state $|u_{(x,t)}, \bar{d}_{(x+\hat{1},t)}\rangle$)

$$|\{N^2 - 1\}\rangle = |q^a_{(x,t)}, \bar{q}^b_{(x+\hat{1},t)}\rangle, \quad a \neq b. \tag{5.47}$$

However, in this way, one has only $N(N-1)$ possible different states. One needs to construct $N^2 - 1 - N(N-1) = N - 1$ others. In the $SU(3)$ case, one has two states of this type, they are given by

$$\begin{aligned} |\{8\}\rangle_1 &= \frac{1}{\sqrt{2}} \left(|u_{(x,t)}, \bar{u}_{(x+\hat{1},t)}\rangle - |d_{(x,t)}, \bar{d}_{(x+\hat{1},t)}\rangle\right) \\ |\{8\}\rangle_2 &= \frac{1}{\sqrt{6}} \left(|u_{(x,t)}, \bar{u}_{(x+\hat{1},t)}\rangle + |d_{(x,t)}, \bar{d}_{(x+\hat{1},t)}\rangle - 2|s_{(x,t)}, \bar{s}_{(x+\hat{1},t)}\rangle\right). \end{aligned} \tag{5.48}$$

It is easy to generalize this result to the case of $SU(N)$, one gets

$$|\{N^2-1\}\rangle_k = \frac{1}{\sqrt{N(N-1)}}\left(\sum_{a=1}^{N}|q^a_{(x,t)},\bar{q}^a_{(x+\hat{1},t)}\rangle - N|q^k_{(x,t)},\bar{q}^k_{(x+\hat{1},t)}\rangle\right), \tag{5.49}$$

with $k=1,\ldots,N$. There are $N-1$ independent states because one of them is not linearly independent of the other ones. Indeed, they are not orthogonal, i.e.

$${}_j\langle\{N^2-1\}|\{N^2-1\}\rangle_k = -\frac{1}{N-1}, \quad j\neq k. \tag{5.50}$$

As before, we can express the basis spin states in term of this new basis, one obtains

$$\begin{aligned}
|q^a_{(x,t)},\bar{q}^b_{(x+\hat{1},t)}\rangle &= |\{N^2-1\}\rangle, \quad a\neq b.\\
|q^a_{(x,t)},\bar{q}^a_{(x+\hat{1},t)}\rangle &= \frac{1}{\sqrt{N}}\,|\{1\}\rangle - \frac{\sqrt{N-1}}{\sqrt{N}}\,|\{N^2-1\}\rangle.
\end{aligned} \tag{5.51}$$

We then write the Hamilton operator in terms of the quadratic Casimir operator $C_2(\{r\}) = \vec{T}^2_{\{r\}}$ of $SU(N)$ with the corresponding representation $\{r\}$, i.e.

$$\begin{aligned}
\vec{T}_x\cdot\vec{T}^*_{x+\hat{1}} &= \frac{1}{2}\,(\vec{T}_x+\vec{T}^*_{x+\hat{1}})^2 - \frac{1}{2}\,\vec{T}^2_x - \frac{1}{2}\,\vec{T}^{*2}_{x+\hat{1}}\\
&= \frac{1}{2}\,C_2(\{1\}\text{ or }\{N^2-1\}) - C_2(\{N\}),
\end{aligned} \tag{5.52}$$

where $C_2(\{N\}) = C_2(\{\overline{N}\})$. The relevant Casmir operators have the form [145]

$$\begin{aligned}
&C_2(\{N\}) = C_2(\{\overline{N}\}) = \frac{N^2-1}{2N},\\
&C_2(\{N^2-1\}) = N,\\
&C_2(\{1\}) = 0.
\end{aligned} \tag{5.53}$$

We can then compute the transfer matrix element between two spins $q^a,\bar{q}^b$ at the time-slice t and two others at the time-slice $(t+1)$. First, for two different spins $(a\neq b)$, one obtains

$$\begin{aligned}
&\langle q^a_{(x,t)},\bar{q}^b_{(x+\hat{1},t)}|\exp(-\epsilon J\;\vec{T}_x\cdot\vec{T}^*_{x+\hat{1}}|q^a_{(x,t+1)},\bar{q}^b_{(x+\hat{1},t+1)}\rangle = \langle\{N^2-1\}|\exp(-\epsilon J\;\vec{T}_x\cdot\vec{T}^*_{x+\hat{1}})\\
&\times|\{N^2-1\}\rangle = \exp\left(-\epsilon J\;\left[\frac{1}{2}\,C_2(\{N^2-1\}) - C_2(\{N\})\right]\right) = \exp\left(-\frac{\epsilon J}{2N}\right).
\end{aligned} \tag{5.54}$$

For four spins with the same flavor, using the second relation in (5.51), we get

$$\begin{aligned}
&\langle q^a_{(x,t)},\bar{q}^a_{(x+\hat{1},t)}|\exp(-\epsilon J\;\vec{T}_x\cdot\vec{T}^*_{x+\hat{1}}|q^a_{(x,t+1)},\bar{q}^a_{(x+\hat{1},t+1)}\rangle = \frac{1}{N}\;\exp\left(-\epsilon J\left[\frac{1}{2}\,C_2(\{1\})\right.\right.\\
&\left.\left.-\,C_2(\{N\})\right]\right) + \frac{N-1}{N}\;\exp\left(-\epsilon J\left[\frac{1}{2}\,C_2(\{N^2-1\}) - C_2(\{N\})\right]\right)\\
&= \frac{1}{N}\;\exp\left(\frac{\epsilon J(N^2-1)}{2N}\right) + \frac{N-1}{N}\;\exp\left(-\frac{\epsilon J}{2N}\right).
\end{aligned} \tag{5.55}$$

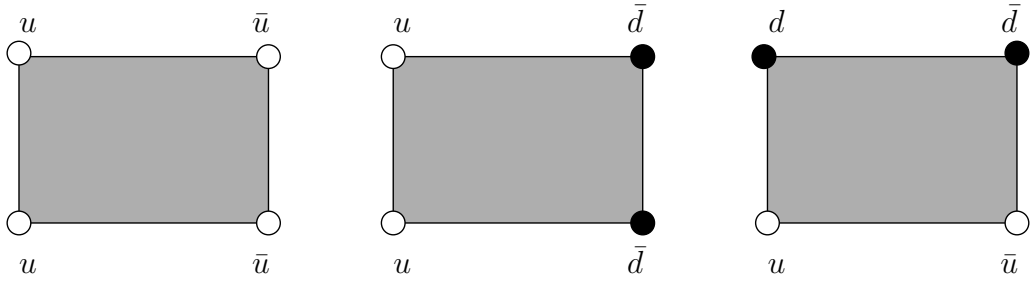

Figure 5.4: *Allowed configurations on the interaction plaquettes of the Trotter decomposition for an antiferromagnetic spin chain. The $SU(N)$ spins u, $\bar{u}$, d, and $\bar{d}$ can be permuted to any other spin q or $\bar{q}$ of $SU(N)$.*

Finally, the last non-trivial configuration is given by two spins of flavor a at the time-slice t and two other spins of flavor $b \neq a$ a time-slice later in the extra dimension. Using the relations (5.50) and (5.51), one has

$$\begin{aligned}
&\langle q^b_{(x,t)}, \bar{q}^b_{(x+\hat{1},t)}| \exp(-\epsilon J\ \vec{T}_x \cdot \vec{T}^*_{x+\hat{1}} |q^a_{(x,t+1)}, \bar{q}^a_{(x+\hat{1},t+1)}\rangle = \frac{1}{N}\ \exp\Bigg(- \epsilon J \Bigg[\frac{1}{2}\ C_2(\{1\}) \\
&- C_2(\{N\})\Bigg]\Bigg) - \ \frac{1}{N-1}\ \frac{N-1}{N}\ \exp\left(-\epsilon J\left[\frac{1}{2}\ C_2(\{N^2-1\}) - C_2(\{N\})\right]\right) \\
&= \ \frac{1}{N}\ \exp\left(\frac{\epsilon J(N^2-1)}{2N}\right) - \frac{1}{N}\ \exp\left(-\frac{\epsilon J}{2N}\right). \qquad (5.56)
\end{aligned}$$

Normalizing these relations by dividing by $\exp(-\epsilon J/2N)$, we find the Boltzmann weights for an $SU(N)$ antiferromagnet in the fundamental representation,

$$\begin{aligned}
&\exp(-S[u,\bar{u},u,\bar{u}]) = \exp(-S[d,\bar{d},d,\bar{d}]) = \frac{1}{N}[\exp(\epsilon JN/2) + N - 1], \\
&\exp(-S[u,\bar{d},u,\bar{d}]) = \exp(-S[d,\bar{u},d,\bar{u}]) = 1, \\
&\exp(-S[u,\bar{u},d,\bar{d}]) = \exp(-S[d,\bar{d},u,\bar{u}]) = \frac{1}{N}[\exp(\epsilon JN/2) - 1]. \qquad (5.57)
\end{aligned}$$

Again, the flavors of the $SU(N)$-spins can be permuted to any other values. All other combination of spins give a zero Boltzmann weight factor. The allowed ones are illustrated in figure 5.4.

5.5 Cluster Algorithm for $SU(N)$ Antiferromagnetic Systems

As for $SU(N)$ ferromagnets, we can also define a cluster algorithm for $SU(N)$ antiferromagnetic systems. Let us consider here the simplest case: spins in the fundamental

Configurations and Break-ups	Transfer Matrix Elements
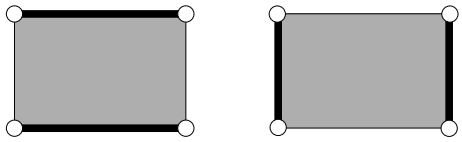	$\exp(-S[u,\bar{u},u,\bar{u}]) = \frac{1}{N}[\exp(\epsilon JN/2)+N-1]$
	$\exp(-S[u,\bar{d},u,\bar{d}]) = 1$
	$\exp(-S[u,\bar{u},d,\bar{d}]) = \frac{1}{N}[\exp(\epsilon JN/2)-1]$

Table 5.2: *Possible configurations for an $SU(N)$ quantum antiferromagnet with $n = 1$ with the corresponding break-ups and Boltzmann weights. Again, the spins $u, \bar{u}$ (open cirles) and $d, \bar{d}$ (black points) can be permuted to any other $SU(N)$ spins $q^a, \bar{q}^a$.*

representation of $SU(N)$. Generalization for higher $SU(N)$-spin representations is investigated in the next section. Here, a cluster consists of spins in the same state q^a on even lattice sites and in the conjugate state $\bar{q}^a$ on odd ones. Again, one picks up a random initial lattice site (x, t) and investigates the states of the spins on an interaction plaquette. One of the corners will be the next point on the loop. Here, only a number of configurations are allowed. Indeed, for configurations $C_1 = [q^a, \bar{q}^b, q^a, \bar{q}^b]$ or $[q^b, \bar{q}^a, q^b, \bar{q}^a]$ with $a \neq b$ the next point on the plaquette is the time-like neighbor of (x, t) on that plaquette. For configurations $C_2 = [q^a, \bar{q}^a, q^b, \bar{q}^b]$ or $[q^b, \bar{q}^b, q^a, \bar{q}^a]$ with $a \neq b$ the next point is the space-like neighbor. Finally for $C_3 = [q^a, \bar{q}^a, q^a, \bar{q}^a]$ or $[q^b, \bar{q}^b, q^b, \bar{q}^b]$ with $a \neq b$, the next point on the loop is again the time-like neighbor with probability

$$p = \frac{1}{N}\,[\exp(\epsilon JN/2) - N - 1], \tag{5.58}$$

or the space-like neighbor with probability $(1 - p)$. The new point defined in that way belongs to the next interaction plaquette and the process is then repeated until the loop eventually closes. In contrast to the ferromagnet, the cluster can grow forward in time and suddenly turns backward. The cluster rules are illustrated in table 5.2 and are consistent with detailed balance (5.34). In particular, one has

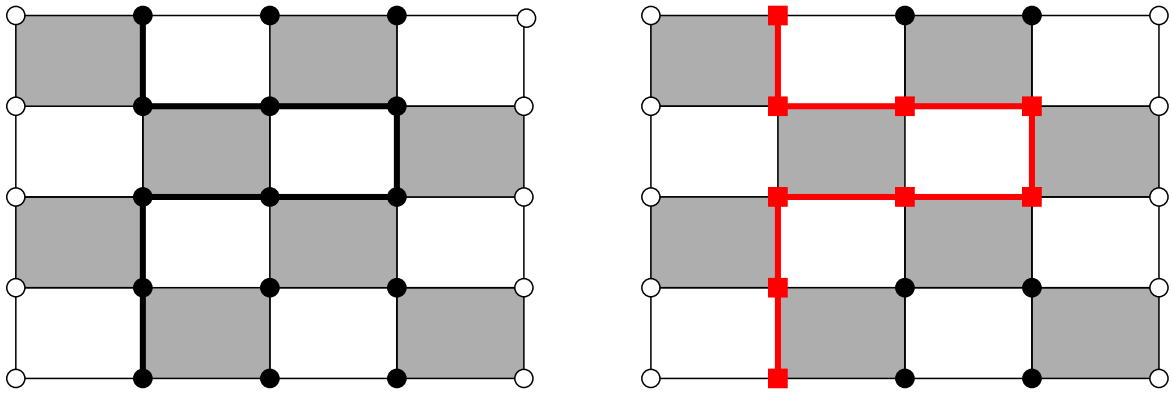

Figure 5.5: *A cluster algorithm update for an $SU(N)$ antiferromagnetic chain with the $SU(N)$ spins in the fundamental (or antifundamental) representation, i.e. $n = 1$. The open circles are in the quantum state $u, \bar{u}$. The fat black line represents a cluster of connected spins in a quantum state $d, \bar{d}$. All spins in that cluster are then flipped to another flavor $s, \bar{s}$, represented by the red squares.*

$$
\begin{aligned}
&p(C_1)w(C_1 \to C_2) = 0 = p(C_2)w(C_2 \to C_1), \\
&p(C_1)w(C_1 \to C_3) = 1 = \frac{1}{p}\, p = p(C_3)w(C_3 \to C_1), \\
&p(C_2)w(C_2 \to C_3) = \frac{1}{N}\, [\exp(\epsilon JN/2) - 1] = \frac{1}{p}\, (1-p) = p(C_3)w(C_3 \to C_2)
\end{aligned}
\tag{5.59}
$$

They have been derived according to the transfer matrix elements that we have computed in the previous section. A single cluster update is illustrated in figure 5.5. Again, note that this cluster algorithm can operate directly in continuous Euclidean time [39].

5.6 Generalization to Higher $SU(N)$ Representations for Quantum Spin Chains

In order to obtain the $CP(N-1)$ models at $\theta = 0$ or π, we have seen in the previous chapter that one needs to vary the number of Young tableau boxes of the $SU(N)$ symmetric representation on each site. Recall that we place a symmetric $SU(N)$ representation with n Young tableau boxes in a single row on each even site. On odd sites we place the corresponding antirepresentation (with $n \times (N-1)$ Young tableau boxes). This is illustrated in section 4.5. Including this extra degree of freedom implies a non-trivial algorithmic set-up. The idea is the following. We want to have a given representation with n Young tableau boxes on an even site x of the spin chain. We first couple n $SU(N)$ spins in the fundamental representation of $SU(N)$. These n quantum spins are placed on n layers on site x. Their

direct product decomposes into a direct sum of various $SU(N)$ representations. In order to keep only the completely symmetric representation, we project out the unwanted ones. This can be done by inserting a projector operator between the usual transfer matrices in the Trotter formula (5.41). It corresponds to impose an infinitely strong "ferromagnetic coupling" between the n spins to be sure to select the highest-dimensional representation (the completely symmetric one). On the odd sites the set-up is completely identical, we couple n times $SU(N)$ spins in the corresponding antirepresentation. This scheme was developed some time ago by Wiese and collaborators in order to build cluster algorithms for higher spin antiferromagnetic Heisenberg model. We will present this particular example, and then generalize the construction to $SU(3)$ with $n = 2, 3$, i.e. the 6- and 10-dimensional representation.

5.6.1 Path integral representation and layer decomposition

As emphasized above, one has first to decompose the $SU(N)$ spins in the symmetric $\{(N+n-1)!/(N-1)!\ n!\}$-dimensional representation into n $SU(N)$ spins in the fundamental $\{N\}$-dimensional representation. Here, n is the number of boxes of the corresponding Young tableau. On even sites x of the chain, we hence decompose the quantum spins as

$$T_x^a = \sum_{i=1}^{n} T_x^{a,i}, \tag{5.60}$$

where $T_x^{a,i}$ are the $SU(N)$ spins in the fundamental representation. We do the same on the odd sites and the total Hamiltonian then takes the form

$$H = -J \sum_{\langle xy \rangle} \sum_{(i,j)=1}^{n} \vec{T}_x^i \cdot \vec{T}_y^{j*}. \tag{5.61}$$

Again, $J > 0$ and $\langle xy \rangle$ denotes nearest neighbors. The Trotterization procedure is then a bit more complicated due to this extra degree of freedom. In fact, one has to add n more Trotter steps corresponding to the possibilities of interactions between the n spins on site x and the n others on site y. In order to write the quantum partition function in its Trotter decomposed form, one has to include a projector operator $\mathcal{P}$ which guarantees the desired symmetric $SU(N)$ representation on each site. The projector acts on each site, therefore we have

$$\mathcal{P} = \prod_x \mathcal{P}_x. \tag{5.62}$$

It consists in the sum over all symmetric states that one can build out of n spins in the fundamental representation of $SU(N)$. This will become clear with the following examples. This projector has to be inserted between each exponential in the Trotter formula (5.41). However, since $\mathcal{P} = \mathcal{P}^2$ and from the cyclicity of the trace, one simply has

$$Z = \lim_{M \to \infty} \mathrm{Tr}\{[\exp(-\epsilon H_1) \exp(-\epsilon H_2)]^M\ \mathcal{P}\}, \tag{5.63}$$

where we have used

$$[H, \mathcal{P}] = 0. \tag{5.64}$$

As before, we insert a complete set of spin states between the exponential factors. Remarkably, since we work with a sum of spins in the fundamental (or antifundamental) representation of $SU(N)$, the transfer matrix elements of the exponential factors are completely identical to the ones obtained before. In fact, we only need to evaluate the matrix elements of the projection operator, i.e

$$\langle q^{a,i}_{(x,t)} | \mathcal{P} | q^{b,j}_{(x,t+1)} \rangle = \prod_x \mathcal{P} \left(q^{a,1}_{(x,t)}, \ldots, q^{a,n}_{(x,t)}; q^{a,1}_{(x,t+1)}, \ldots, q^{a,n}_{(x,t+1)} \right). \tag{5.65}$$

Let us consider the following example. We want to construct a spin 1 quantum Heisenberg chain, i.e. spins in the triplet (or anti-triplet) representation of $SU(2)$. Hence, we have $n = 2s = 2$ and two spin $1/2$ places in two layers at the point (x, t). In order to keep only the symmetric representation (spin 1) and to project out the other (spin 0), we write the projector $\mathcal{P}$ as a sum over the symmetric states

$$\mathcal{P}_x = |1,1\rangle\langle 1,1| + |1,0\rangle\langle 1,0| + |1,-1\rangle\langle 1,-1|, \tag{5.66}$$

where

$$\begin{aligned} |1,1\rangle &= |uu\rangle_{(x,t)}, \\ |1,0\rangle &= \frac{1}{\sqrt{2}} \left(|ud\rangle_{(x,t)} + |du\rangle_{(x,t)} \right), \\ |1,-1\rangle &= |dd\rangle_{(x,t)}. \end{aligned} \tag{5.67}$$

Note that the antisymmetric state $|0,0\rangle = (|ud\rangle_{(x,t)} - |du\rangle_{(x,t)})/\sqrt{2}$ has been left out. In that case, the transfer matrix in the basis $\{|uu\rangle, |ud\rangle, |du\rangle, |dd\rangle\}$ at the site (x, t) is given by

$$\mathcal{P} = \begin{pmatrix} 1 & 0 & 0 & 0 \\ 0 & \frac{1}{2} & \frac{1}{2} & 0 \\ 0 & \frac{1}{2} & \frac{1}{2} & 0 \\ 0 & 0 & 0 & 1 \end{pmatrix}. \tag{5.68}$$

We now consider the case of a spin in the sextet representation of $SU(3)$. Again, $n = 2$ and on each even site x we have two $SU(3)$ spins in the fundamental representation. Out of these, we can build six symmetric states and hence construct the projection operator.

These states are

$$\begin{aligned}
|1\rangle &= |uu\rangle_{(x,t)}, \\
|2\rangle &= |dd\rangle_{(x,t)}, \\
|3\rangle &= |ss\rangle_{(x,t)}, \\
|4\rangle &= \frac{1}{\sqrt{2}}\,(|ud\rangle_{(x,t)} + |du\rangle_{(x,t)}), \\
|5\rangle &= \frac{1}{\sqrt{2}}\,(|us\rangle_{(x,t)} + |su\rangle_{(x,t)}), \\
|6\rangle &= \frac{1}{\sqrt{2}}\,(|ds\rangle_{(x,t)} + |sd\rangle_{(x,t)}).
\end{aligned} \tag{5.69}$$

As before $\mathcal{P}$ is defined as

$$\mathcal{P}_x = \sum_{k=1}^{6} |k\rangle\langle k|, \tag{5.70}$$

which, in the basis $\{|uu\rangle, |ud\rangle, |du\rangle, |dd\rangle, |ds\rangle, |sd\rangle, |ss\rangle, |us\rangle, |su\rangle\}$, gives a 9×9 transfer matrix of the form

$$\mathcal{P} = \begin{pmatrix}
1 & 0 & 0 & 0 & 0 & 0 & 0 & 0 & 0 \\
0 & \frac{1}{2} & \frac{1}{2} & 0 & 0 & 0 & 0 & 0 & 0 \\
0 & \frac{1}{2} & \frac{1}{2} & 0 & 0 & 0 & 0 & 0 & 0 \\
0 & 0 & 0 & 1 & 0 & 0 & 0 & 0 & 0 \\
0 & 0 & 0 & 0 & \frac{1}{2} & \frac{1}{2} & 0 & 0 & 0 \\
0 & 0 & 0 & 0 & \frac{1}{2} & \frac{1}{2} & 0 & 0 & 0 \\
0 & 0 & 0 & 0 & 0 & 0 & 1 & 0 & 0 \\
0 & 0 & 0 & 0 & 0 & 0 & 0 & \frac{1}{2} & \frac{1}{2} \\
0 & 0 & 0 & 0 & 0 & 0 & 0 & \frac{1}{2} & \frac{1}{2}
\end{pmatrix}. \tag{5.71}$$

Generalizations to higher N and n are straightforward. The transfer matrix is $(N^n \times N^n)$-dimensional. For example, in the decuplet representation of $SU(3)$ ($n = 3$), $\mathcal{P}$ is 27-dimensional. On the diagonal, one has six (3×3)-blocks with entries $1/3$, one (6×6)-block with entries $1/6$ and three times 1. This corresponds to the ten symmetric states that one can built out of three $SU(3)$ spins in the fundamental representation.

5.6.2 Cluster rules

To summarize, one needs to consider different symmetric $SU(N)$ representations on each site in order to simulate $CP(N-1)$ models at $\theta = 0$ or π. This is done by introducing layers in an unphysical direction. Indeed, in order to build an $SU(N)$ spin in a certain symmetric representation on a site x, we place a number of $SU(N)$ spins in the fundamental representation on layers at that point which couple to different $SU(N)$ representations.

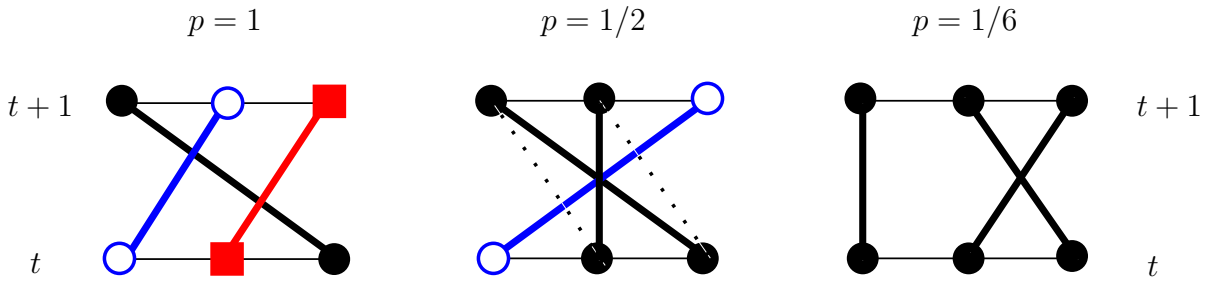

Figure 5.6: *Example of the layer break-ups in the case of* $SU(3)$ *with* $n = 3$. *The spins are in two successive time-slices at the even site* x. *The open blue circles are spin* u, *the filled black ones are spin* d, *and the red squares are spin* s. *The probabilities of each connection are indicated. In the first case, we have only one possibily of connection. In the second configuration, the dashed line represents the other possible connection which have the same probability* $1/2$. *Finally, there are six possible connections in the third case, we draw only one of them.*

We then use a projector operator $\mathcal{P}$ to select the symmetric ones. Formally, the cluster can evolve as well in this unphysical dimension, and the transfer matrix (5.65) determines the break-ups probabilities. In the plane of points (x, t), everything is as described in section 5.5. In this unphysical dimension however, the spins on n layers at the time-slice t can be connected with any other of the n spins on the layers at the time-slice $(t + 1)$. Let us illustrate this with a few examples. We consider the case of the triplet representation of $SU(2)$, where we place two spins $1/2$ on two layers on an even site x. They can be in the states u or d. In the unphysical dimension and in the β direction the cluster rules are the following. If one has a configuration $[ud; ud]$ the next point on the loop is the point forward in time, because the flavor has to be always conserved in a cluster. For a configuration $[ud; du]$, the next point is the diagonal one. For $[uu; uu]$, there are two possibilities with both a probability $1/2$. This has a natural generalization to higher $SU(N)$ with any symmetric representation. Let us investigate the case of the decuplet representation of $SU(3)$. As illustrated in figure 5.6, at an even site x one has three spins in the fundamental representation of $SU(3)$ on a layer. They can be in the flavor states u, d, and s. Recall that in all cases the flavor state has to be conserved. Some of the allowed configurations are presented in figure 5.6. Depending on the flavors of the spins at t and $(t + 1)$, there is a number of connection configurations. They all have the same probabilistic weight p. The cluster rules are the following. When the loop reaches a spin on the layer, one has to investigate the layer configuration in the next time-slice. If there is only one spin in the same state, it will be the next point of the loop with probability 1. With two spins in the same state, one has an equal probability $1/2$ to choose one or the other in the next time-slice. If the three spins are in the same flavor state one has a probability $1/3$ to reach any of these spins. This construction is straightforward to generalize to higher N and n.

To investigate the vacuum structure of $CP(N-1)$ models, we have used an order parameter $Q[q,\bar{q}]$. As described in section (4.4.3), this order parameter is C-odd. It is defined by counting the number of spin flips in a configuration. $Q[q,\bar{q}]$ receives a contribution $+1$ if a pair of nearest neighbor spins $q_x\bar{q}_{x+\hat{1}}$ along the x-direction flips to another state $q'_x\bar{q}'_{x+\hat{1}}$, at some moment in time. On the other hand, a spin flip from $\bar{q}_x q_{x+\hat{1}}$ to $\bar{q}'_x q'_{x+\hat{1}}$ contributes -1 to $Q[q,\bar{q}]$. Hence, the layer construction has no effect on that parameter. It is defined in this way for all $SU(N)$ representations. When programming such system, one should carefully implement the periodic boundary conditions along the antiferromagnetic chain. An odd number of sites in a chain would lead to frustration. This would have dramatic effects on the efficiency of the algorithm. Indeed, it is extremely difficult to deal with frustrated systems.

5.7 Path Integral Representation and Cluster Rules for $SU(N)$ Spin Ladders

In the previous chapter, we haved used quantum spin ladder systems to simulate $CP(N-1)$ models at non-trivial vacuum angle. Being a model with both ferro- and antiferromagnetic couplings, the path integral representation of the quantum partition function is very similar to what has been presented in detail above. Recall that we are in $(2+1)$ dimensions. The quantum ladder Hamiltonian

$$H = -J\sum_{x\in A}[T^a_x T^{a*}_{x+\hat{1}} + T^a_x T^a_{x+\hat{2}}] - J\sum_{x\in B}[T^{a*}_x T^a_{x+\hat{1}} + T^{a*}_x T^{a*}_{x+\hat{2}}], \tag{5.72}$$

is a sum of four terms that we denote, respectively, by $H_1,\ldots,H_4$. Two of them (H_1,H_3) describe the antiferromagnetic interaction, while the two others (H_2,H_4) describe the ferromagnetic one. Using the Trotter decomposition, one can write the partition function Z as

$$Z = \lim_{M\to\infty} \mathrm{Tr}\,[\exp(-\epsilon H_1)\exp(-\epsilon H_2)\exp(-\epsilon H_3)\exp(-\epsilon H_4)]^M, \tag{5.73}$$

where we have introduced M slices in the β-direction with spacing $\epsilon = \beta/M$. As before, one can insert a complete set of basis states between the exponential factors and then use the results obtained for the cases of ferro- and antiferromagnetic systems. Since we are working with the fundamental representation $\{N\}$ of $SU(N)$ on even sites and with the antifundamental $\{\overline{N}\}$ on odd sites, one does not need to introduce layer decompositions.

Therefore, one hence gets the following transfer matrix elements

$$\begin{aligned}
\langle q_x^a, q_y^a | \exp(-\epsilon h_2) | q_{x'}^a, q_{y'}^a \rangle &= \exp\left(\frac{\epsilon J(N-1)}{2N}\right), \\
\langle q_x^a, q_y^b | \exp(-\epsilon h_2) | q_{x'}^a, q_{y'}^b \rangle &= \frac{1}{2}\left[\exp\left(\frac{\epsilon J(N-1)}{2N}\right) + \exp\left(-\frac{\epsilon J(N+1)}{2N}\right)\right], \quad a \neq b \\
\langle q_x^a, q_y^b | \exp(-\epsilon h_2) | q_{x'}^b, q_{y'}^a \rangle &= \frac{1}{2}\left[\exp\left(\frac{\epsilon J(N-1)}{2N}\right) - \exp\left(-\frac{\epsilon J(N+1)}{2N}\right)\right], \quad a \neq b \\
\langle q_x^a, \bar{q}_y^a | \exp(-\epsilon h_1) | q_{x'}^a, \bar{q}_{y'}^a \rangle &= \frac{1}{N}\ \exp\left(-\frac{\epsilon J}{2N}\right)\ \left[\exp\left(\frac{\epsilon J}{2N}\right) + N - 1\right], \\
\langle q_x^a, \bar{q}_y^a | \exp(-\epsilon h_1) | q_{x'}^b, \bar{q}_{y'}^b \rangle &= \frac{1}{N}\ \exp\left(-\frac{\epsilon J}{2N}\right)\ \left[\exp\left(\frac{\epsilon J}{2N}\right) - 1\right], \quad a \neq b \\
\langle q_x^a, \bar{q}_y^b | \exp(-\epsilon h_1) | q_{x'}^a, \bar{q}_{y'}^b \rangle &= \exp\left(-\frac{\epsilon J}{2N}\right), \quad a \neq b.
\end{aligned} \tag{5.74}$$

Here, x and y denote the nearest neighbors at the time-slice t, while x' and y' are the neighboring sites a time-slice later. The transfer matrix elements for h_3 and h_4 can be obtained by substituting $h_1 \to h_3$ and $h_2 \to h_4$ with $q \leftrightarrow \bar{q}$.

The cluster rules follow from the above relations. A cluster grows according to these rules and eventually closes. Again, one flips the cluster to another quantum state of $SU(N)$. As presented in the previous chapter, this ladder system provides an unconventional regularization of $CP(N-1)$ models. We have investigated the vacuum structure with the help of the order parameter $Q[q, \bar{q}]$ described in the previous section. Again, one must have an even site extent in the antiferromagnetic direction to make sure that one does not have a frustrated system.

5.8 Efficiency of the Cluster Algorithm in the Continuum Limit

In this section, we like to show that our algorithm is remarkably efficient close to the continuum limit. Indeed, critical slowing down is almost completely eliminated. As emphasized in the beginning of this chapter, Monte Carlo simulations become very difficult close to a second order phase transition, i.e. when the correlation length becomes large. In particular, the autocorrelation time τ (the number of Monte Carlo steps to generate a statistically independent configuration) grows as

$$\tau \propto \xi^z, \tag{5.75}$$

and so behaves the relative statistical error. The efficiency of an algorithm is hence characterized by its dynamical critical exponent z. For $CP(N-1)$ models in the Wilson

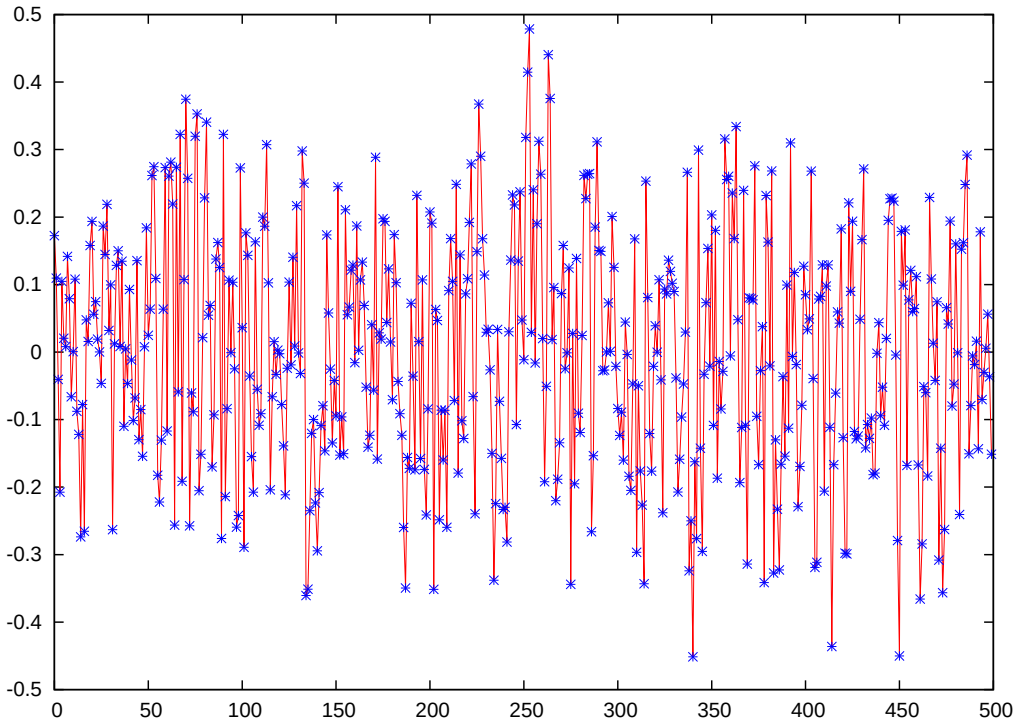

Figure 5.7: *History of the magnetization of an $SU(3)$ ferromagnet on a 320^2 lattice at $\beta J = 6.75$ as a function of the Monte Carlo time (measured in units of sweeps with the multi-cluster algorithm).*

formulation, due to a no-go theorem, no efficient Wolff-type embedding cluster algorithm can be constructed [123]. Numerical studies have shown no improvement over a local Metropolis algorithm [100]. The local Metropolis algorithm is not particularly efficient with a critical exponent $z \approx 2$. Still, a rather efficient multigrid algorithm does exist with a critical exponent $z \approx 0.2$ [101, 102], but it works only at $\theta = 0$. This algorithm is, at a first sight, not easy to implement. Our cluster algorithm, on the other hand, has the advantage to be almost straightforward to program.

In order to test the efficiency of our method, we have considered the cluster algorithm for an $SU(N)$ ferromagnet which regularizes the $CP(N-1)$ model at $\theta = 0$. We have then determined the autocorrelation time. More precisely, we have considered the integrated autocorrelation time which measures the area under the exponential fall-off of the autocorrelation function. Here, we will not treat the case of the spin ladder system or the antiferromagnetic spin chain. Remarkably, such systems can regularize the model also at $\theta = \pi$. In that context, the simulations suffer from "supercritical slowing down". Due to the first order phase transition, there is slowing down during the tunneling processes. We use here a multi-cluster algorithm for a $(2+1)$-dimensional $SU(3)$ ferromagnet in discrete

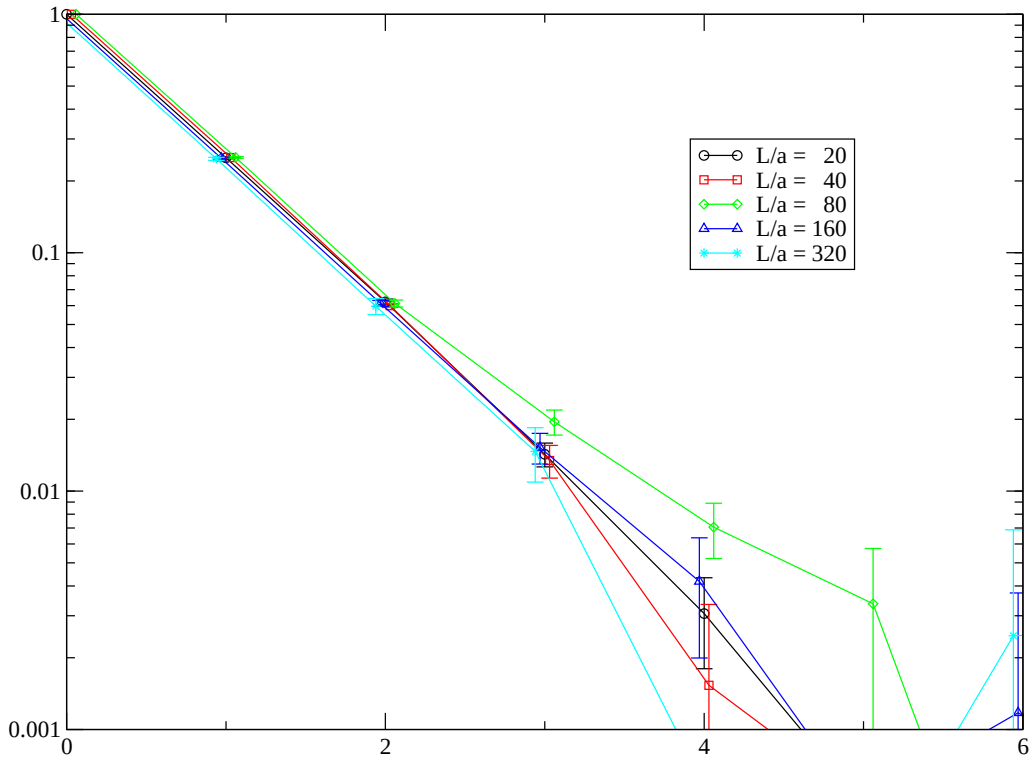

Figure 5.8: *Autocorrelation functions of the magnetization of an $SU(3)$ ferromagnet as a function of the number of sweeps with the multi-cluster algorithm. In order to increase visibility, some points have been slightly displaced.*

Euclidean time (the extra dimension of extent β). This is a convenient choice since a multi-cluster algorithm allows a natural definition of a Monte Carlo sweep — all points are touched once by a cluster. Of course, a similar study would have been possible for a single cluster algorithm defined both in continuous or discrete Euclidean time. However, one then grows only one cluster at a time and only a variable number of sites is touched depending on the cluster size. Therefore, the definition of a sweep in that context may be rather unclear. Here, we use an $SU(3)$ quantum ferromagnet and investigate the integrated autocorrelation times $\tau_{\mathcal{M}}$ of the uniform magnetization and τ_{χ} of the corresponding susceptibility. These quantities are defined in relations (5.31) and (5.32). The integrated autocorrelation time is defined as

$$\tau_{int} = \frac{1}{2} + \sum_{t=1}^{\infty} \frac{C(t)}{C(0)}, \tag{5.76}$$

where $C(t)$ is the autocorrelation function which is an exponentially decreasing function [146]. Again, τ_{int} represents the area the autocorrelation function. For example, in case of

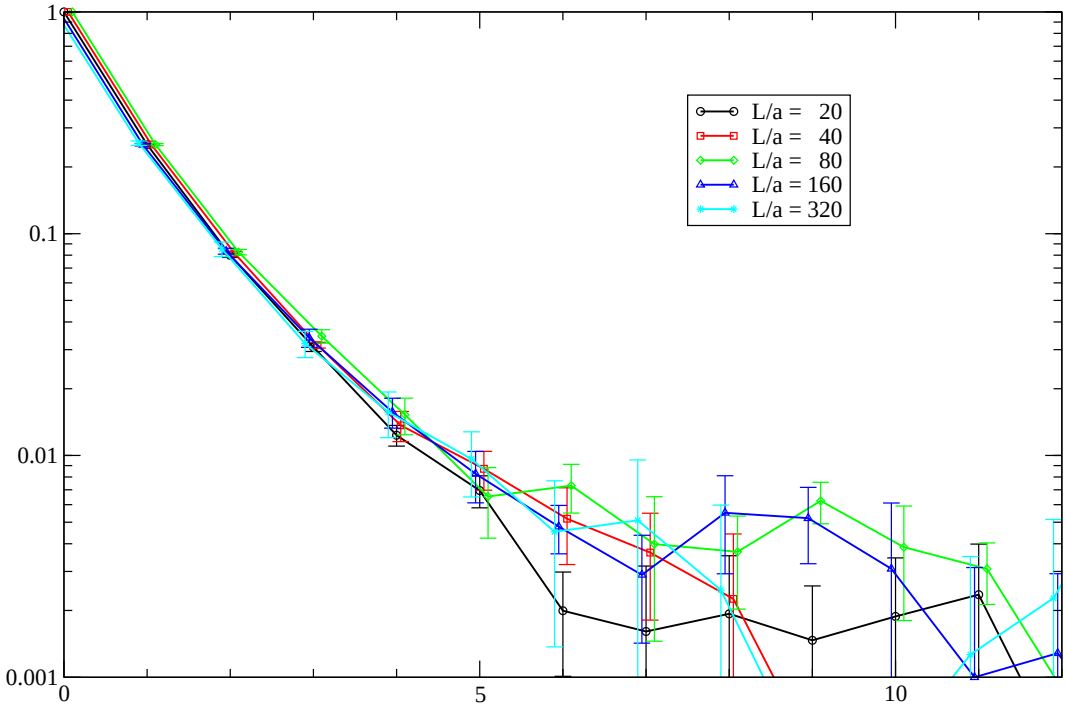

Figure 5.9: *Autocorrelation functions of the susceptibility of an $SU(3)$ ferromagnet as a function of the number of sweeps with the multi-cluster algorithm. In order to increase visibility, some points have been slightly displaced.*

the uniform magnetization, the autocorrelation function is given by

$$C_{\mathcal{M}}(t) = \langle \mathcal{M}(s)\mathcal{M}(s+t)\rangle - \langle \mathcal{M}\rangle^2, \tag{5.77}$$

where s and t are Monte Carlo times. In figure 5.7, we present a Monte Carlo history of the magnetization (5.31). One observes no correlations between successive Monte Carlo sweeps. The points are indeed uniformly distributed around zero. This already indicates that autocorrelations are very much suppressed. We have then analyzed the autocorrelation functions for the magnetization and the susceptibility which are illustrated in figures 5.8 and 5.9. The results for the integrated autocorrelation times are collected in table 5.3. In order to estimate the dynamical critical exponent z of critical slowing down, we have considered several lattices with decreasing lattice spacing. The ratio $\xi(L)/L$ of the correlation length $\xi(L)$ and the lattice size L was kept fixed. $\xi(L)$ was obtained with the continuous time single cluster algorithm using the second moment method [39].

Remarkably, the autocorrelation times $\tau_{\mathcal{M}}$ and τ_{χ} do not show any dependence on the

L/a	20	40	80	160	320	640
β	4.5	5.0	5.55	6.2	6.75	7.45
$\xi(L)/a$	8.78(1)	16.76(1)	32.26(3)	64.6(1)	123.4(2)	253(1)
$\tau_{\mathcal{M}}$	0.833(3)	0.831(4)	0.836(5)	0.831(2)	0.828(2)	—
τ_{χ}	0.884(6)	0.893(7)	0.898(10)	0.898(11)	0.903(11)	—

Table 5.3: *Numerical data for the correlation length $\xi(L)$ and the integrated autocorrelation times $\tau_{\mathcal{M}}$ and τ_{χ} for an $SU(3)$-symmetric ferromagnet corresponding to a $CP(2)$ model in D-theory.*

correlation length $\xi(L)$. The critical slowing down is hence practically eliminated and our data are consistent with $z = 0$. It should be noted that, although the autocorrelation time does not scale with a power law, it could still increase as the logarithm of the correlation length. The D-theory construction hence allows us to work with really efficient cluster algorithms. This offers a way to evade the no-go theorem and allows us to build efficient cluster algorithms for $CP(N-1)$ models which can operate reliably both at $\theta = 0$ and π.

Chapter 6

Conclusions

We have seen in this thesis that D-theory provides a very rich structure. It allows to formulate quantum field theories in terms of discrete variables. Scalar fields are represented by quantum spins while gauge fields are represented by quantum link variables. Due to the quantum nature of the system, one has to deal with an extra dimension. Remarkably, we have seen that the phenomenon of dimensional reduction is completely generic. For $(d+1)$-dimensional quantum spin systems with $d \geq 2$, it occurs because of spontaneous symmetry breaking. Indeed, global symmetries of the quantum systems are spontaneously broken and the low-energy physics is governed by massless Goldstone bosons. In $(2+1)$ dimensions, as one makes the extent β of the extra-dimension finite, the Goldstone bosons pick up a small mass and the corresponding correlation length ξ is exponentially large in β. Therefore, one reaches the continuum limit by sending β to infinity. The system hence appears dimensionally reduced because the fields are essentially constant in the extra dimension due to the exponentially large correlation length. This is ensured since the target 2-dimensional quantum field theories are asymptotically free. For higher dimensions, spontaneous symmetry breaking also occurs and one directly sits in a massless phase where $\xi = \infty$. The mechanism of dimensional reduction follows naturally. In the case of non-abelian quantum link models in $(4+1)$ dimensions, the dimensional reduction process is due to the existence of a 5-dimensional massless Coulomb phase. One hence has an infinite correlation length. Once the extent of the extra dimension is made finite, asymptotic freedom predicts an exponentially large correlation length in β. As a consequence, dimensional reduction occurs again because one can average the fields in the fifth dimension resulting in the usual 4-dimensional Yang-Mills theory. The inclusion of fermions is also very natural in D-theory. One just follows Shamir's variant of Kaplan's domain wall fermion proposal. Interestingly, when the theories are dimensionally reduced, the confinement hypothesis in 4 dimensions (gluons form glueballs and are hence confined) plays the same role as the Hohenberg-Mermin-Wagner-Coleman theorem in two dimensions. It forbids the existence of free massless particles in the reduced theory.

The D-theory formulation of QCD hence rests on a solid theoretical basis but, unfortunately, it has so far not been possible to simulate such systems. The use of discrete

quantum variables normally allows to use powerful numerical techniques such as cluster algorithms. However, no efficient cluster algorithm has been developed even for the simplest quantum link models. This can be seen as a potential weakness of the formulation, but investigations are still on their way and there is good hope to find new types of algorithms which will allow precise numerical simulation in that framework as well. For 2-dimensional spin systems, the situation is far better. We have seen here that it is possible to regularize $CP(N-1)$ models with quantum $SU(N)$-symmetric systems. This offers a new way to attack non trivial problems which are not accessible with the perturbative approach or with the Wilsonian regularization. In this thesis, we have thus investigated the vacuum structure of $CP(N-1)$ models. It was not clear whether the system faces a first order phase transition with C-breaking at vacuum angle $\theta = \pi$ for not too large $N \geq 3$. Using the D-theory formulation and an efficient cluster algorithm, we have been able to perform numerical simulations reliably directly at $\theta = \pi$. This is impossible with the traditional Wilson approach due to the complex term in the action. In this way, we have been able to confirm that the phase transition is second order for $N = 2$ and first order for larger N. The quantum spin systems used here were $(2+1)$-dimensional quantum spin ladders and $(1+1)$-dimensional quantum spin chains. They both have a global $SU(N)$ symmetry and can regularize $CP(N-1)$ models both at $\theta = 0$ or π. On the other hand, $(2+1)$-dimensional $SU(N)$ ferromagnetic systems, which provide a regularization at $\theta = 0$, were also investigated in detail. In particular, we have been able to prove the perfect agreement between the Wilsonian and D-theory regularizations. This has confirmed the mechanism of spontaneous symmetry breaking from $SU(N)$ to $U(N-1)$ and the dimensional reduction scenario to the target 2-dimensional $CP(N-1)$ model.

To simulate these quantum systems, we have used highly efficient numerical simulation techniques. D-theory indeed offers a perfect framework for the use of cluster algorithms. This type of algorithms have the advantage to remove almost completely the critical slowing down near the continuum limit. Indeed, they can perform global updates of the size of the correlation length and are hence particularly efficient for highly correlated systems. They have been used in many classical or quantum spin models. Nevertheless, cluster algorithms turn out to be inefficient for $CP(N-1)$ models in the Wilson formulation. This is even proved by a no-go theorem. Remarkably, the D-theory formulation of the $CP(N-1)$ models, in terms of $SU(N)$ quantum systems, completely evades this theorem. We have shown here that, at $\theta = 0$, the dynamical critical exponent is consistent with $z = 0$. This means that successive Monte Carlo sweeps are practically not correlated. On the other hand, these algorithms are relatively simple to implement and one can simulate $CP(N-1)$ models at vacuum angle $\theta = \pi$ without any additional numerical effort.

Being able to simulate $CP(N-1)$ models at $\theta = 0$ for large correlation lengths ξ offers wide new perspectives. Indeed, it would now be possible to investigate numerically the mass-gap of the theory, which is not known analytically. In order to do so, we just have to simulate the $(2+1)$-dimensional $SU(N)$ quantum ferromagnet with our cluster algorithm. The limited power of computers will, of course, prevents simulations at very small lattice

spacing. Fortunately, one can use finite size scaling techniques to extrapolate the value of ξ to the continuum limit and hence obtain the mass-gap of the theory. Similar studies can be made as well in the large N limit, where the system is believed to simplify. The mass-gap in that limit can also be investigated. Besides the $CP(N-1)$ models, it would be interesting to see if D-theory also allows us to build efficient cluster algorithms for other field theories. For example, the $SU(N) \otimes SU(N)$ chiral models for $N \geq 3$ to which the no-go theorem also applies. As emphasized before, an important goal is to find a way to simulate more efficiently pure gauge theories. The most efficient algorithm is nowadays the overrelaxation algorithm which has a critical exponent of $z \approx 1$. Unfortunately, the D-theory formulation of pure gauge theories has so far not yielded the expected results. However, there is still good hope to construct modified cluster algorithms which would allow us to simulate gauge theories efficiently. Simulations of fermions would be the next step. Indeed, we have seen, that Shamir's version of Kalplan domain-wall fermions can be naturally included in D-theory. Hence, all ingredients of QCD are included in the D-theory formulation. The theoretical framework rests on a solid basis and we expect further algorithmic developments in the coming years.

As it was suggested by U.-J. Wiese in [147], D-theory may provide a far deeper framework for physics at ultra-short distances. Indeed, it is believed that the quantum field theory picture, and therefore the use of classical fields as basic concepts, has to be replaced at very high energies. This has already been pointed out by Dirac, who was not satisfied with the usual procedure of removing the infinities in the perturbative treatment of quantum electrodynamics [148]. Nowadays, the most discussed candidate to regularize particle physics at a fundamental level is string theory. However, deteminating the physical processes at the Planck scale is far from the scope of today's experiments. Hence, it is more a question of speculation and discrete quantum variables such as quantum links and quantum spins may also be promising candidates for the degrees of freedom of fundamental physics. Indeed, what could be more fundamental than a quantum spin? D-theory indeed provides a framework in which classical fields emerge naturally from discrete quantum variable that undergo dimensional reduction. Formulating a theory in one or more extra dimensions is not a weakness, since it is strongly believed that hidden dimensions must be present at high energies. A hint in that direction is the existence of light fermions in Nature. Indeed, without invoking extra dimensions and Kaplan's remarkable solution, one would not understand non-pertubatively why fermions can be naturally light. Of course, the D-theory formulation may well not be adapted to describe fundamental physics, one needs maybe more dimensions and a different framework. It is also not clear whether gravity or the full standard model can be regularize in the D-theory framework. Nevertheless, discrete quantum variables are interesting alternative objects which could provide new insights towards a better comprehension of fundamental physics.

Appendix A

Determination of the Low-Energy Parameters of an $SU(N)$-Symmetric Ferromagnet

In section 4.3.2, we have given values for the low-energy parameters of an $SU(N)$ quantum ferromagnetic system without justifying these results. Indeed, the uniform magnetization m and the spin stiffness ρ_s were given in terms of the microscopic parameters n and J, the number of Young tableau boxes of the corresponding symmetric $SU(N)$ representation on each site x and the ferromagnetic coupling constant, respectively. To determine these low-energy parameters, we will compute the energy-momentum dispersion relation in the microscopic theory. We will then match the coefficients with the results obtained in chiral perturbation theory [126]. We start by considering an $SU(N)$ symmetric quantum ferromagnet defined on a 2-dimensional lattice of size L^2. As before, the Hamiltonian is given by

$$H = -J \sum_{\langle xy \rangle} \vec{T}_x \cdot \vec{T}_y, \tag{A.1}$$

where $J > 0$ and $\langle xy \rangle$ denotes nearest neighbors. The quantum spins T_x^a, $a \in \{1, \ldots, N^2 - 1\}$, are in any symmetric representation of $SU(N)$, corresponding to a Young tableau with n boxes in a single row. The normalization is fixed by the relation

$$\mathrm{Tr}\left(T_x^a T_y^b\right) = \frac{1}{2}\delta^{ab}\delta_{xy}. \tag{A.2}$$

Let us begin by determining the ground state energy E_0 of such a system. As described in section 4.3.2, the vacuum state is a completely symmetric state with maximal spin projection on each site. For example, in the fundamental representation of $SU(N)$ one can choose a state $|uu\ldots u\rangle$. Here, we will simply denote this ground state by $|n\rangle$. In order to find the ground state energy, let us express (A.1) as a sum of quadratic Casimir operators of $SU(N)$

$$H|n\rangle = -J \sum_{\langle xy \rangle} \left(\frac{1}{2} \left(\vec{T}_x + \vec{T}_y\right)^2 - \frac{1}{2}\, \vec{T}_x^2 - \frac{1}{2}\, \vec{T}_y^2 \right) |n\rangle. \tag{A.3}$$

The quadratic Casimir operator for symmetric representations of $SU(N)$ with a corresponding Young tableau with n boxes in one row is given by [149]

$$C_2 = C_f \, \frac{n(N+n)}{N+1}, \tag{A.4}$$

with

$$C_f = \frac{N^2-1}{2N}, \tag{A.5}$$

the quadratic Casimir of the fundamental representation. Hence, for a ground state with all $SU(N)$ spins in the symmetric representation with n Young tableau boxes, one has

$$H|n\rangle = E_0|n\rangle = -JL^2n^2 \, \frac{(N-1)}{N}|n\rangle. \tag{A.6}$$

Here we have summed over the $2L^2$ bounds of nearest neighbors. The dispersion relation of such systems is defined by the difference $E_{\vec{p}} - E_0$, where $E_{\vec{p}}$ is the energy-spectrum of the 1-magon (or spin-wave) state. It is defined as

$$H|\vec{p}\,\rangle = E_{\vec{p}}\,|\vec{p}\,\rangle, \tag{A.7}$$

where the state with momentum $\vec{p}$ is

$$|\vec{p}\,\rangle = T^-_{\vec{p}}\;|n\rangle = \sum_x \; e^{i\vec{p}\cdot\vec{x}}\; T^-_x\;|n\rangle = \sum_x \; e^{i\vec{p}\cdot\vec{x}}|n'_x\rangle. \tag{A.8}$$

The operator T^-_x is a "lowering operator" acting on the site x which flips the $SU(N)$ spin on that site to another quantum state. It is defined in terms of non-diagonal generators of $SU(N)$. For example

$$T^-_x = \frac{1}{\sqrt{2}}\,(T^1_x - iT^2_x), \tag{A.9}$$

with T^1_x and T^2_x two non-diagonal generators of $SU(N)$. In order to act on $|\vec{p}\,\rangle$, let us split the Hamilton operator into two parts,

$$H = H_d + H_s. \tag{A.10}$$

Here, H_d is defined as a sum over all diagonal operators of $SU(N)$. Since the rank of the group is $N-1$, there are $N-1$ of them, which yields

$$H_d = -J\sum_{\langle xy\rangle}\sum_{a=1}^{N-1} \; T^a_x T^a_y. \tag{A.11}$$

On the other hand, H_s is a sum of product of shift operators of the form (A.9). Since each of them contains two generators of $SU(N)$, there are $N(N-1)/2$ terms in the following sum

$$H_s = -J\sum_{\langle xy\rangle}\sum_{b=1}^{N(N-1)/2} \; \left(T^{+,b}_x T^{-,b}_y + T^{-,b}_x T^{+,b}_y\right). \tag{A.12}$$

For example, $b = 1$ corresponds to the operator (A.9). Let us act with H_d on $|\vec{p}\,\rangle$. For that we can first study

$$H_d|n'_x\rangle = (H_r + 4H_{b'})|n'_x\rangle. \tag{A.13}$$

The generalization to $|\vec{p}\,\rangle$ is trivial. Here H_r is defined as

$$H_r|n'_x\rangle = (2L^2 - 4)E_b|n'_x\rangle, \tag{A.14}$$

where E_b is the energy of a bond defined by

$$E_b = \frac{E_0}{2L^2} = -Jn^2\ \frac{(N-1)}{2N}. \tag{A.15}$$

We have subtracted the four bonds that are connected with the site x from the total number of bonds $2L^2$. Indeed, the energy of the rest of the system is not affected by the introduction of a different spin on the site x. We now determine the energy $E_{b'}$ of a bond connected with x,

$$H_{b'}|n'_x\rangle = -J\sum_{a=1}^{N-1} T_x^a T_y^a |n'_x\rangle = E_{b'}|n'_x\rangle. \tag{A.16}$$

As emphasized before, the state $|n'_x\rangle$ consists of $L^2 - 1$ spins in the same state "up" and one in a different quantum state "down". This latter is in any symmetric representation of $SU(N)$. In particular, let us arbitrarly choose the representation with $(n-1)$ Young tableaux boxes in a single row. The above relations becomes

$$\begin{aligned} H_{b'}|n'_x\rangle &= -J\left(T_x^1 T_y^1 + \sum_{a=2}^{N-1} T_x^a T_y^a\right)|n'_x\rangle = -J\left[\frac{n}{2}\left(\frac{n}{2}-1\right) + \frac{n^2}{2}\sum_{a=2}^{N-1}\frac{1}{a(a+1)}\right]|n'_x\rangle \\ &= -J\left[\frac{n}{2}\left(\frac{n}{2}-1\right) + \frac{n^2}{2}\frac{(N-2)}{2N}\right]|n'_x\rangle. \end{aligned} \tag{A.17}$$

Here, the first term gives a contribution $n/2$ for the site y and $(n/2-1)$ for x. To illustrate this, one may think about the $SU(2)$ case, where $T^1 \propto \sigma^3$ and $n = 2s$ with s being the total spin. There, we have a spin $(s-1)$ on x and a maximal spin projection s on all other sites. Hence, as one sums over all sites and introduces the momentum $\vec{p}$, one gets

$$\sum_x e^{i\vec{p}\vec{x}} H_{b'}|n'_x\rangle = -\frac{Jn}{2}\ \left(\frac{n(N-1)}{N} - 1\right)|\vec{p}\,\rangle. \tag{A.18}$$

Let us now consider the case of H_s. Again this is a local operator one can decompose in four parts

$$H_s = H_{(x,+\hat{1})} + H_{(x,-\hat{1})} + H_{(x,+\hat{2})} + H_{(x,-\hat{2})}, \tag{A.19}$$

where $\hat{1}$ and $\hat{2}$ are the two directions on the lattice. For example, one has

$$H_{(x,+\hat{1})} = -J\sum_{b=1}^{N(N-1)/2)}\left(T^{+,b}_{(x_1,x_2)}T^{-,b}_{(x_1+1,x_2)} + T^{-,b}_{(x_1,x_2)}T^{+,b}_{(x_1+1,x_2)}\right). \tag{A.20}$$

As one acts on a state $|n'_x\rangle$ the sum reduces to the value of b which corresponds to the quantum state of the $SU(N)$ spin on site x. This yields

$$\begin{aligned} H_{(x,+\hat{1})}|n'_x\rangle &= -J\left(T^+_{(x_1,x_2)}T^-_{(x_1+1,x_2)} + T^-_{(x_1,x_2)}T^+_{(x_1+1,x_2)}\right)|n'_{(x_1,x_2)}\rangle \\ &= -JT^+_{(x_1,x_2)}T^-_{(x_1+1,x_2)}|n'_{(x_1,x_2)}\rangle = -JT^-_{(x_1+1,x_2)}T^+_{(x_1,x_2)}T^-_{(x_1,x_2)}|n_{(x_1,x_2)}\rangle \\ &= -JT^-_{(x_1+1,x_2)}T^1_{(x_1,x_2)}|n_{(x_1,x_2)}\rangle == -\frac{Jn}{2}\ |n'_{(x_1+1,x_2)}\rangle, \end{aligned} \tag{A.21}$$

We have used the relation

$$T^+_{(x_1,x_2)}T^-_{(x_1,x_2)}|n_{(x_1,x_2)}\rangle = \left[T^1_{(x_1,x_2)} - T^-_{(x_1,x_2)}T^+_{(x_1,x_2)}\right]|n_{(x_1,x_2)}\rangle = T^1_{(x_1,x_2)}|n_{(x_1,x_2)}\rangle. \tag{A.22}$$

Again, T^1 denotes the first diagonal operator of the group $SU(N)$. In the fundamental representation of the group, it is given by the matrix $diag(1,-1,0,\ldots,0)/2$. We still need to sum over all sites and consider also the momentum $\vec{p}$, i.e.

$$\begin{aligned} H_{(x,+\hat{1})}|\vec{p}\,\rangle &= \sum_{x_1,x_2} e^{ip_1x_1}e^{ip_2x_2}H_{(x,+\hat{1})}|n'_x\rangle = -\frac{nJ}{2}\sum_{x_1,x_2} e^{ip_1x_1}e^{ip_2x_2}\ |n'_{(x_1+1,x_2)}\rangle \\ &= -\frac{nJ}{2}\sum_{x'_1,x_2} e^{ip_1x'_1}e^{ip_2x_2}e^{ip_1}\ |n'_{(x'_1,x_2)}\rangle = -\frac{nJ}{2}e^{ip_1}\ |\vec{p}\,\rangle \end{aligned} \tag{A.23}$$

Therefore, the eigenvalue of the operator H_s (A.19) is given by

$$H_s|\vec{p}\,\rangle = -\frac{nJ}{2}\left(e^{ip_1} + e^{-ip_1} + e^{ip_2} + e^{-ip_2}\right)|\vec{p}\,\rangle = -Jn\left[\cos(p_1) + \cos(p_2)\right]|\vec{p}\,\rangle. \tag{A.24}$$

Putting all those contributions together, one obtains

$$H|\vec{p}\,\rangle = (H_r + 4H_{b'} + H_s)|\vec{p}\,\rangle = E_{\vec{p}}|\vec{p}\,\rangle, \tag{A.25}$$

where

$$E_{\vec{p}} = -(2L^2-4)Jn^2\ \frac{(N-1)}{2N} - 2Jn\left(\frac{n(N-1)}{N} - 1\right) - Jn\left[\cos(p_1) + \cos(p_2)\right]. \tag{A.26}$$

As a cross-check, it is clear that $E_{\vec{p}=0} = E_0$. The energy momentum dispersion relation is hence given by

$$\begin{aligned} E_{\vec{p}} - E_0 &= 2Jn^2\ \frac{(N-1)}{N} - 2Jn\left(\frac{n(N-1)}{N} - 1\right) - Jn\left[\cos(p_1) + \cos(p_2)\right] \\ &= Jn\left[2 - \cos(p_1) + \cos(p_2)\right] \\ &= Jn\left[(1-\cos(p_1)) + (1-\cos(p_2))\right]. \end{aligned} \tag{A.27}$$

For small values of $\vec{p}$, we expand $E_{\vec{p}} - E_0$ to second order and find

$$E_{\vec{p}} - E_0 \simeq Jn\left(1 - 1 + \frac{p_1^2}{2} + \mathcal{O}(p_1^4) + 1 - 1 + \frac{p_2^2}{2} + \mathcal{O}(p_2^4)\right) = \frac{Jn}{2}p^2 + \mathcal{O}(p^4), \tag{A.28}$$

where $p = |\vec{p}|$. We can then match this result to the one obtained by Leutwyler using chiral perturbation theory. Hence,

$$E_{\vec{p}} - E_0 = \frac{\rho_s}{m} p^2 = \frac{Jn}{2} p^2 \Rightarrow \frac{\rho_s}{m} = \frac{Jn}{2}. \tag{A.29}$$

From the $SU(2)$ case, it is clear that the uniform magnetization m is equal to the total spin $s = n/2$. Therefore, for $SU(N)$ one has

$$\rho_s = \frac{Jn^2}{4}, \quad m = \frac{n}{2}, \tag{A.30}$$

which proves the results of section 4.3.2.

Bibliography

[1] K. G. Wilson, *Confinement of quarks*, Phys. Rev. **D10** 2445 (1974).

[2] H. B. Nielsen and M. Ninomiya, *No go theorem for regularizing chiral fermions*, Phys. Lett. **B105** 219 (1981).

[3] L. Susskind, *Lattice fermions*, Phys. Rev. **D16** 3031 (1977).

[4] K. G. Wilson, *New Phenomena In Subnuclear Physics*, ed. A. Zichichi, (Plenum Press, New York), Part A, 69 (1977).

[5] D. B. Kaplan, *A method for simulating chiral fermions on the lattice*, Phys. Lett. **B288** 342 (1992) [hep-lat/9206013].

[6] R. Narayanan and H. Neuberger, *Infinitely many regulator fields for chiral fermions*, Phys. Lett. **B302** 62 (1993) [hep-lat/9212019].

[7] P. H. Ginsparg and K. G. Wilson, *A Remnant Of Chiral Symmetry On The Lattice*, Phys. Rev. **D25** 2649 (1982).

[8] P. Hasenfratz and F. Niedermayer, *Perfect lattice action for asymptotically free theories*, Nucl. Phys. **B414** 785 (1994) [hep-lat/9308004].

[9] M. Lüscher, *Abelian chiral gauge theories on a lattice with exact gauge invariance*, Nucl. Phys. **B549** 295 (1999) [hep-lat/9811032].

[10] M. Lüscher, *Weyl fermions on the lattice and the nonabelian gauge anomaly*, Nucl. Phys. **B568** 162 (2000) [hep-lat/9904009].

[11] N. Metropolis, A. W. Rosenbluth, M. N. Rosenbluth, A. H. Teller and E. Teller, *Equation of state calculations by fast computing machines*, J. Chem. Phys. **21** 1087 (1953).

[12] R. H. Swendsen and J.-S. Wang, *Nonuniversal critical dynamics in Monte Carlo simulations*, Phys. Rev. Lett. **58** 86 (1987).

[13] M. Lüscher, *Lattice QCD and the Schwarz alternating procedure*, JHEP **0305** 052 (2003) [hep-lat/0304007].

[14] A. Hasenfratz, *Dynamical simulations with smeared link staggered fermions*, Nucl. Phys. Proc. Suppl. **119** 131 (2003) [hep-lat/0211007].

[15] I. Montvay and G. Münster, *Quantum fields on a lattice*, Cambridge Monographs On Mathematical Physics, Cambridge University Press (1994).

[16] H. J. Rothe, *Lattice Gauge Theories: An Introduction*, World Scientific Lecture Notes in Physics, 59 (1997).

[17] M. Lüscher, *Advanced lattice QCD*, published in Les Houches, "Probing the standard model of particle interactions", Part 2, 229 (1997).

[18] M. Creutz, *Aspects of chiral symmetry and the lattice*, Rev. Mod. Phys. **73** 119 (2001) [hep-lat/0007032].

[19] S. Chandrasekharan and U.-J. Wiese, *An introduction to chiral symmetry on a lattice*, Prog. Part. Nucl. Phys. **53** 373 (2004) [hep-lat/0405024].

[20] S. Chandrasekharan and U.-J. Wiese, *Quantum link models: A discrete approach to gauge theories*, Nucl. Phys. **B492** 455 (1997) [hep-lat/9609042].

[21] D. Horn, *Finite matrix models with continuous local gauge invariance*, Phys. Lett. **100B** 149 (1981).

[22] P. Orland and D. Rohrlich, *Lattice gauge magnets: Local isospin from spin*, Nucl. Phys. **B338** 647 (1990).

[23] R. Brower, S. Chandrasekharan and U.-J. Wiese, *QCD as a quantum link model*, Phys. Rev. **D60** 094502 (1999) [hep-th/9704106].

[24] B. Schlittgen and U.-J. Wiese, *Low-energy effective theories of quantum spin and quantum link models*, Phys. Rev. **D63** 085007 (2001) [hep-lat/0012014];

B. Schlittgen and U.-J. Wiese, *Quantum spin formulation of the principal chiral model*, Nucl. Phys. Proc. Suppl. **83** 718 (2000) [hep-lat/0005020].

[25] R. Brower, S. Chandrasekharan, S. Riederer and U.-J. Wiese, *D-theory: Field quantization by dimensional reduction of discrete variables*, Nucl. Phys. **B693** 149 (2004) [hep-lat/0309182].

[26] B. B. Beard, M. Pepe, S. Riederer and U.-J. Wiese, *Study of $CP(N-1)$ θ-vacua by cluster simulation of $SU(N)$ quantum spin ladders*, Phys. Rev. Lett **94** 010603 (2005) [hep-lat/0406040];

B. B. Beard, M. Pepe, S. Riederer and U.-J. Wiese, *Study of the 2-d $CP(N-1)$ models at $\theta = 0$ and π*, Nucl. Phys. Proc. Suppl. **140** 805 (2005) [hep-lat/0409074].

[27] B. B. Beard, R. J. Birgeneau, M. Greven and U.-J. Wiese, *Square-lattice Heisenberg antiferromagnet at very large correlation lengths*, Phys. Rev. Lett. **80** 1742 (1998) [cond-mat/9709110].

[28] S. Chandrasekharan, B. Scarlet and U.-J. Wiese, *From spin ladders to the 2-d $O(3)$ model at non-zero density*, Comput. Phys. Commun. **147** 388 (2002) [hep-lat/0110215];

S. Chandrasekharan, B. Scarlet and U.-J. Wiese, *Meron-Cluster Simulation of Quantum Spin Ladders in a Magnetic Field*, [cond-mat/9909451].

[29] J. J. Sakurai, *Modern quantum mechanics*, Revisited edition, Addison-Wesley Publishing Company (1994).

[30] Y. Shamir, *Chiral fermions from lattice boundaries*, Nucl. Phys. **B406** 90 (1993) [hep-lat/9303005].

[31] H. Harari, *A schematic model Of quarks and leptons*, Phys. Lett. **B86** 83 (1979).

[32] O. Bär, R. Brower, B. Schlittgen and U.-J. Wiese, *Quantum link models with many rishon flavors and with many colors*, Nucl. Phys. Proc. Suppl. **106**, 1019 (2002) [hep-lat/0110148].

[33] M. Troyer and U.-J. Wiese, *Computational complexity and fundamental limitations to fermionic quantum Monte Carlo simulations*, Phys. Rev. Lett. **94** 170201 (2005) [cond-mat/0408370].

[34] J. Cox and K. Holland, *Meron cluster algorithms and chiral symmetry breaking in a (2+1)-d staggered fermion model*, Nucl. Phys. **B583** 331 (2000) [hep-lat/0003022].

[35] B. B. Beard, M. Pepe, S. Riederer and U.-J. Wiese, *An efficient cluster algorithm for $CP(N-1)$ models*, Talk given by SR at the 23nd International Symposium on Lattice Field Theory (Lattice 2005), Dublin, Ireland, 25-30 Jul 2005, PoS **LAT2005** 113 (2005) [hep-lat/0510041];

B. B. Beard, M. Pepe, S. Riederer and U.-J. Wiese, *Efficient cluster algorithm for $CP(N-1)$ models*, To be published in Comp. Phys Commun. [hep-lat/0602018].

[36] U.-J. Wiese, *Quantum spins and quantum links: The D-theory approach to field theory*, Prog. Theor. Phys. Suppl. **131** 483 (1998);

U.-J. Wiese, *Quantum spins and quantum links: The D-theory approach to field theory*, Nucl. Phys. B (Proc. Suppl.) **73** 146 (1999) [hep-lat/9811025].

[37] T. Barnes, *The 2d Heisenberg antiferromagnet in high T_c superconductivity: A review of numerical techniques and results*, Int. J. Mod. **C2** 659 (1991).

[38] U.-J. Wiese and H. P. Ying, *A Determination of the low-energy parameters of the 2-d Heisenberg antiferromagnet*, Z. Phys. **B93** 147 (1994) [cond-mat/9212006].

[39] B. B. Beard and U.-J. Wiese, *Simulations of discrete quantum systems in continuous Euclidean time*, Nucl. Phys. Proc. Suppl. **53** 838 (1997) [cond-mat/9602164].

[40] J. Goldstone, A. Salam and S. Weinberg, *Broken Symmetries*, Phys. Rev. **127** 965 (1962).

[41] J. Gasser and H. Leutwyler, *Chiral Perturbation Theory To One Loop*, Annals Phys. **158** 142 (1984).

[42] J. Gasser and H. Leutwyler, *Chiral Perturbation Theory: Expansions In The Mass Of The Strange Quark*, Nucl. Phys. **B250** 465 (1985).

[43] P. Hasenfratz and H. Leutwyler, *Goldstone Boson Related Finite Size Effects In Field Theory And Critical Phenomena With $O(N)$ Symmetry*, Nucl. Phys. **B343** 241 (1990).

[44] N. D. Mermin and H. Wagner, *Absence Of Ferromagnetism Or Antiferromagnetism In One-Dimensional Or Two-Dimensional Isotropic Heisenberg Models*, Phys. Rev. Lett. **17** 1133 (1966).

[45] S. R. Coleman, *There Are No Goldstone Bosons In Two-Dimensions*, Commun. Math. Phys. **31** 259 (1973).

[46] P. Hasenfratz and F. Niedermayer, *The Exact Correlation Length Of The Antiferromagnetic $D = (2+1)$ Heisenberg Model At Low Temperatures*, Phys. Lett. **B268** 231 (1991).

[47] S. Chakravarty, B. I. Halperin, and D. R. Nelson, *Two-dimensional quantum Heisenberg antiferromagnet at low temperatures*, Phys. Rev. **B39** 2344 (1989).

[48] P. Hasenfratz, M. Maggiore and F. Niedermayer, *The Exact Mass Gap Of The $O(3)$ And $O(4)$ Nonlinear Sigma Models In $D = 2$*, Phys. Lett. **B245** 522 (1990).

[49] P. Hasenfratz and F. Niedermayer, *The exact mass gap of the $O(N)$ σ-model for arbitrary $N \geq 3$ in $d = 2$*, Phys. Lett. **B245** 529 (1990).

[50] H. G. Evertz, G. Lana and M. Marcu, *Cluster algorithm for vertex models*, Phys. Rev. Lett. **70** 875 (1993) [cond-mat/9211006].

[51] U. Wolff, *Collective Monte Carlo Updating For Spin Systems*, Phys. Rev. Lett. **62** 361 (1989).

[52] U. Wolff, *Asymptotic Freedom And Mass Generation In The O(3) Nonlinear Sigma Model*, Nucl. Phys. **B334** 581 (1990).

[53] H. Bethe, *On The Theory Of Metals. 1. Eigenvalues And Eigenfunctions For The Linear Atomic Chain*, Z. Phys. **71** 205 (1931).

[54] F. D. M. Haldane, *Continuum Dynamics Of The 1-D Heisenberg Antiferromagnetic Identification With The $O(3)$ Nonlinear Sigma Model*, Phys. Lett. **A93** 464 (1983).

[55] F. D. M. Haldane, *Nonlinear Field Theory Of Large Spin Heisenberg Antiferromagnets. Semiclassically Quantized Solitons Of The One-Dimensional Easy Axis Néel State*, Phys. Rev. Lett. **50** 1153 (1983).

[56] F. D. M. Haldane, *"θ-physics" and quantum spin chains (abstract)*, J. Appl. Phys. **57** 3359 (1985).

[57] E. H. Lieb, T. Schultz and D. Mattis, *Two Soluble Models Of An Antiferromagnetic Chain*, Annals Phys. **16** 407 (1961).

[58] I. Affleck and E. H. Lieb, *A Proof Of Part Of Haldane's Conjecture On Spin Chains*, Lett. Math. Phys. **12** 57 (1986).

[59] I. Affleck, T. Kennedy, E. H. Lieb and H. Tasaki, *Rigorous Results On Valence Bond Ground States In Antiferromagnets*, Phys. Rev. Lett. **59** 799 (1987).

[60] I. Affleck, T. Kennedy, E. H. Lieb and H. Tasaki, *Valence Bond Ground States In Isotropic Quantum Antiferromagnets*, Commun. Math. Phys. **115** 477 (1988).

[61] R. Botet, R. Jullien and M. Kolb, *Finite-size-scaling study of the spin-1 Heisenberg-Ising chain with uniaxial anisotropy*, Phys. Rev. **B28** 3914 (1983).

[62] J. B. Parkinson and J. C. Bonner, *Spin chains in a field: Crossover from quantum to classical behavior* Phys. Rev. **B32** 4703 (1985).

[63] M. P. Nightingale and H. W. J. Blöte, *Gap of the linear spin-1 Heisenberg antiferromagnet: A Monte Carlo calculation*, Phys. Rev. **B33** 659 (1986).

[64] U. Schollwöck and T. Jolicoeur, *Haldane Gap and Hidden Order in the $S = 2$ Antiferromagnetic Quantum Spin Chain*, Europhys. Lett. **30** 493 (1995) [cond-mat/9501115].

[65] Y. J. Kim, M. Greven, U.-J. Wiese and R. J. Birgeneau, *Monte Carlo Study of Correlations in Quantum Spin Chains at Non-Zero Temperature*, Eur. Phys. J. **B4** 291 (1998) [cond-mat/9712257].

[66] W. Bietenholz, A. Pochinsky and U.-J. Wiese, *Meron cluster simulation of the theta vacuum in the 2-d $O(3)$ model*, Phys. Rev. Lett. **75** 4524 (1995) [hep-lat/9505019].

[67] I. Affleck, *Field Theory Methods And Quantum Critical Phenomena*, in Fields, Strings, and Critical Phenomena, Proceedings of the Les Houches Summer School, Session XLIX, edited by E. Brezin and J. Zinn-Justin (North Holland, Amsterdam, 1988), p. 563.

[68] S. P. Novikov, *The Hamiltonian Formalism And A Many Valued Analog Of Morse Theory*, Usp. Mat. Nauk **37N5** 3 (1982); Sov. Math. Dokl. **24** 222 (1981).

[69] E. Witten, *Nonabelian Bosonization In Two Dimensions*, Commun. Math. Phys. **92** 455 (1984).

[70] A. Auerbach, *Interacting electrons and quantum magnetism*, Springer-Verlag New York, Inc. (1994).

[71] H. Georgi, *Lie Algebras in Particle Physics, From Isospin to Unified Theories*, Second edition, Frontiers in Physics (1999).

[72] F. A. Berezin and M. S. Marinov, *Particle Spin Dynamics As The Grassmann Variant Of Classical Mechanics*, Annals Phys. **104** 336 (1977).

[73] P. Coleman, E. Miranda and A. Tsvelik, *Possible realization of odd frequency pairing in heavy fermion compounds* [cond-mat/9302018].

[74] R. Slansky, *Group Theory For Unified Model Building*, Phys. Rept. **79** 1 (1981).

[75] H.-Q. Ding and M. S. Makivić, *Kosterlitz-Thouless transition in the two-dimensional quantum XY model*, Phys. Rev. **B42** 6827 (1990).

[76] K. Harada and N. Kawashima, *Universal Jump in the Helicity Modulus of the Two-Dimensional Quantum XY Model*, Phys. Rev. **B55** R 11949 (1997) [cond-mat/9702081].

[77] K. Harada and N. Kawashima, *Kosterlitz-Thouless transition of quantum XY model in two dimensions*, J. Phys. Soc. Jpn. **67** 2768 (1998) [cond-mat/9803090].

[78] J. Balog, S. Naik, F. Niedermayer and P. Weisz, *Exact Mass Gap of the Chiral $SU(n) \times SU(n)$ Model*, Phys. Rev. Lett. **69** 873 (1992).

[79] T. H. Hollowood, *The exact mass-gaps of the principal chiral models*, Phys. Lett. **B329** 450 (1994) [hep-th/9402084].

[80] K. Holland, P. Minkowski, M. Pepe and U.-J. Wiese, *Exceptional confinement in $G(2)$ gauge theory*, Nucl. Phys. **B668** 207 (2003) [hep-lat/0302023].

[81] M. Pepe, *Confinement and the center of the gauge group*, PoS **LAT2005** 017 (2005) [hep-lat/0510013].

[82] M. Creutz, *Confinement And The Critical Dimensionality Of Space-Time*, Phys. Rev. Lett. **43** 553 (1979) [Erratum-ibid. **43** 890 (1979)].

[83] B. B. Beard, R. C. Brower, S. Chandrasekharan, D. Chen, A. Tsapalis and U.-J. Wiese, *D-theory: Field theory via dimensional reduction of discrete variables*, Nucl. Phys. Proc. Suppl. **63** 775 (1998) [hep-lat/9709120].

[84] A. M. Polyakov, *Quark Confinement And Topology Of Gauge Groups*, Nucl. Phys. **B120** 429 (1977).

[85] M. Gopfert and G. Mack, *Proof Of Confinement Of Static Quarks In Three-Dimensional $U(1)$ Lattice Gauge Theory For All Values Of The Coupling Constant*, Commun. Math. Phys. **82** 545 (1981).

[86] V. A. Rubakov and M. E. Shaposhnikov, *Do We Live Inside A Domain Wall?*, Phys. Lett. **B125** 136 (1983).

[87] V. Furman and Y. Shamir, *Axial symmetries in lattice QCD with Kaplan fermions*, Nucl. Phys. **B439** 54 (1995) [`hep-lat/9405004`].

[88] M. Nyfeler, M. Pepe and U.-J. Wiese, *A new efficient cluster algorithm for the Ising model*, PoS **LAT2005** 112 (2005) [`hep-lat/0510040`].

[89] A. D'Adda, M. Lüscher and P. Di Vecchia, *A $1/N$ Expandable Series Of Nonlinear σ Models With Instantons*, Nucl. Phys. **B146** 63 (1978).

[90] H. Eichenherr, *$SU(N)$ Invariant Nonlinear Sigma Models*, Nucl. Phys. **B146** 215 (1978) [Erratum-ibid. **B155** 544 (1979)].

[91] V. L. Golo and A. M. Perelomov, *Solution Of The Duality Equations For The Two-Dimensional $SU(N)$ Invariant Chiral Model*, Phys. Lett. **B79** 112 (1978).

[92] E. Witten, *Instantons, The Quark Model, And The $1/N$ Expansion*, Nucl. Phys. **B149** 285 (1979).

[93] S. Coleman, *Aspects of Symmetry*, Selected Erice Lectures, Cambridge University Press (1985).

[94] A. V. Manohar, *Large N QCD*, Published in "Les Houches 1997, Probing the standard model of particle interactions, Pt. 2" 1091-1169 (1997) [`hep-ph/9802419`].

[95] G. Munster, *The $1/N$ Expansion And Instantons In $CP(N-1)$ Models On A Sphere*, Phys. Lett. **B118** 380 (1982);

G. Munster, *A Study Of $CP(N-1)$ Models On The Sphere Within The $1/N$ Expansion*, Nucl. Phys. **B218** 1 (1983).

[96] M. Campostrini and P. Rossi, *$CP(N-1)$ models in the $1/N$ expansion*, Phys. Rev. **D45** 618 (1992) [Erratum-ibid. **D46** 2741 (1992)].

[97] B. Berg and M. Lüscher, *Computation Of Quantum Fluctuations Around Multi - Instanton Fields From Exact Green's Functions: The $CP(N-1)$ Case*, Commun. Math. Phys. **69** 57 (1979).

[98] M. Lüscher, *Does The Topological Susceptibility In Lattice Sigma Models Scale According To The Perturbative Renormalization Group?*, Nucl. Phys. **B200** 61 (1982).

[99] D. Petcher and M. Lüscher, *Topology And Universality In The Lattice $CP(2)$ Model*, Nucl. Phys. **B225** 53 (1983).

[100] K. Jansen and U.-J. Wiese, *Cluster algorithms and scaling in $CP(3)$ and $CP(4)$ models*, Nucl. Phys. **B370** 762 (1992).

[101] M. Hasenbusch and S. Meyer, *Testing accelerated algorithms in the lattice $CP(3)$ model*, Phys. Rev. **D45** 4376 (1992).

[102] M. Hasenbusch and S. Meyer, *Multigrid acceleration for asymptotically free theories*, Phys. Rev. Lett. **68** 435 (1992).

[103] A. C. Irving and C. Michael, *Finite size effects and scaling in lattice $CP(N-1)$*, Phys. Lett. **B292** 392 (1992) [hep-lat/9206003].

[104] N. Schultka and M. Muller-Preussker, *The Topological susceptibility of the lattice $CP(N-1)$ model on the torus and the sphere*, Nucl. Phys. **B386** 193 (1992) [hep-lat/9207013].

[105] P. Goddard and D. I. Olive, *New Developments In The Theory Of Magnetic Monopoles*, Rept. Prog. Phys. **41** 1357 (1978).

[106] G. Morandi, *The Role of Topology in Classical and Quantum Physics*, Berlin, Germany: Springer (1992).

[107] J. Zinn-Justin, *Chiral anomalies and topology*, Lect. Notes Phys. **659** 167 (2005) [hep-th/0201220].

[108] U.-J. Wiese *The Standard Model of Particle Physics*, Lecture Notes, Bern University.

[109] F. Lenz, *Topological concepts in gauge theories*, Lect. Notes Phys. **659** 7 (2005) [hep-th/0403286].

[110] R. D. Peccei and H. R. Quinn, *Constraints Imposed By CP Conservation In The Presence Of Instantons*, Phys. Rev. **D16** 1791 (1977).

[111] R. D. Peccei and H. R. Quinn, *CP Conservation In The Presence Of Instantons*, Phys. Rev. Lett. **38** 1440 (1977).

[112] S. R. Coleman, *More About The Massive Schwinger Model*, Annals Phys. **101** 239 (1976).

[113] N. Seiberg, *Theta Physics At Strong Coupling*, Phys. Rev. Lett. **53** 637 (1984).

[114] I. Affleck, *Critical Behavior Of $SU(N)$ Quantum Chains And Topological Nonlinear Sigma Models*, Nucl. Phys. **B305** 582 (1988).

[115] I. Affleck, *Nonlinear sigma model at $\theta = \pi$: Euclidean lattice formulation and solid-on-solid models*, Phys. Rev. Lett. **66** 2429 (1991).

[116] U.-J. Wiese, *Numerical Simulation Of Lattice Theta Vacua: The 2-D $U(1)$ Gauge Theory As A Test Case*, Nucl. Phys. **B318** 153 (1989).

[117] R. Burkhalter, M. Imachi, Y. Shinno and H. Yoneyama, *$CP(N-1)$ models with Theta term and fixed point action*, Prog. Theor. Phys. **106** 613 (2001) [hep-lat/0103016].

[118] M. Asorey and F. Falceto, *Vacuum structure of $CP(N)$ sigma models at $\theta = \pi$*, Phys. Rev. Lett. **80** 234 (1998) [hep-th/9712126].

[119] V. Azcoiti, G. Di Carlo, A. Galante and V. Laliena, *New proposal for numerical simulations of theta-vacuum like systems*, Phys. Rev. Lett. **89** 141601 (2002) [hep-lat/0203017].

[120] M. Imachi, Y. Shinno and H. Yoneyama, *$CP(N-1)$ model with the theta term and maximum entropy method*, Nucl. Phys. Proc. Suppl. **140** 659 (2005) [hep-lat/0409145].

[121] S. Olejnik and G. Schierholz, *On the existence of a first order phase transition at small vacuum angle theta in the $CP(3)$ model*, Nucl. Phys. Proc. Suppl. **34** 709 (1994) [hep-lat/9312019].

[122] J. C. Plefka and S. Samuel, *Monte Carlo studies of two-dimensional systems with a Theta term*, Phys. Rev. **D56** 44 (1997) [hep-lat/9704016].

[123] S. Caracciolo, R. G. Edwards, A. Pelissetto and A. D. Sokal, *Wolff type embedding algorithms for general nonlinear sigma models*, Nucl. Phys. **B403** 475 (1993) [hep-lat/9205005].

[124] A. Tsapalis, *Correlation functions from quantum cluster algorithms: Application to $U(1)$ quantum spin and quantum link models*, Nucl. Phys. Proc. Suppl. **73** 742 (1999) [hep-lat/9810001].

[125] P. Kopietz and S. Chakravarty, *Low-temperature behavior of the correlation length and the susceptibility of a quantum Heisenberg ferromagnet in two dimensions*, Phys. Rev. **B40** 4858 (1989).

[126] H. Leutwyler, *Nonrelativistic effective Lagrangians*, Phys. Rev. **D49** 3033 (1994) [hep-ph/9311264].

[127] A. B. Zamolodchikov and A. B. Zamolodchikov, *Factorized S-Matrices In Two Dimensions As The Exact Solutions Of Certain Relativistic Quantum Field Models*, Annals Phys. **120** 253 (1979).

[128] J. K. Kim, *An Application of finite size scaling to Monte Carlo simulations*, Phys. Rev. Lett. **70** 1735 (1993).

[129] J. K. Kim, *Asymptotic scaling of the mass gap in the two-dimensional $O(3)$ nonlinear sigma model: A Numerical study*, Phys. Rev. **D50** 4663 (1994).

[130] S. Caracciolo, R. G. Edwards, A. Pelissetto and A. D. Sokal, *Asymptotic scaling in the two-dimensional $O(3)$ sigma model at correlation length 10^5*, Phys. Rev. Lett. **75** 1891 (1995) [hep-lat/9411009].

[131] E. Dagotto and T. M. Rice, *Surprises on the Way from 1D to 2D Quantum Magnets: the Novel Ladder Materials*, Science **271** 618 (1996) [cond-mat/9509181].

[132] D. V. Khveshchenko, *Singlet pairing in the double-chain $t-J$ model* Phys. Rev. **B50** 380 (1994) [cond-mat/9401012].

[133] S. R. White, R. M. Noack and D. J. Scalapino, *Resonating Valence Bond Theory of Coupled Heisenberg Chains*, Phys. Rev. Lett. **73** 886 (1994) [cond-mat/9403042].

[134] G. Sierra, *The Non-Linear Sigma Model and Spin Ladders*, J. Phys. **A29** 3299 (1996) [cond-mat/9512007].

[135] S. Chakravarty, *Dimensional Crossover in Quantum Antiferromagnets*, Phys. Rev. Lett. **77** 4446 (1996) [cond-mat/9608124].

[136] K. Harada, N. Kawashima, and M. Troyer, *Néel and Spin-Peierls ground states of two-dimensional $SU(N)$ quantum antiferromagnets*, Phys. Rev. Lett. **90** 117203 (2003) [cond-mat/0210080].

[137] N. Read and S. Sachdev, *Some features of the phase diagram of the square lattice $SU(N)$ antiferromagnet*, Nucl. Phys. **B316** 609 (1989).

[138] D. P. Arovas and A. Auerbach, *Functional integral theories of low-dimensional quantum Heisenberg models*, Phys. Rev. **B38** 316 (1988).

[139] D. P. Arovas and A. Auerbach, *Spin Dynamics in the Square-lattice Antiferromagnet* Phys. Rev. Lett. **61** 617 (1988).

[140] I. Affleck, *The Quantum Hall Effect, Sigma Models At Theta = Pi And Quantum Spin Chains*, Nucl. Phys. **B257** 397 (1985).

[141] I. Affleck, *Quantum spin chain and the Haldane gap*, J. Phys.: Condens. Matter **1** 3047 (1989).

[142] E. Fradkin and M. Stone, *Topological terms in one- and two-dimensional quantum Heisenberg antiferromagnets*, Phys. Rev. **B38** 7215 (1988).

[143] M. Creutz, *Overrelaxation And Monte Carlo Simulation*, Phys. Rev. **D36** 515 (1987).

[144] M. Troyer, F. Alet, S. Trebst and S. Wessel, *Non-local updates for quantum Monte Carlo simulations*, AIP Conf. Proc. **690** 156 (2003) [physics/0306128].

[145] M. E. Peskin and D. V. Schroeder, *An Introduction to quantum field theory*, Westview Press (1995).

[146] A. Pelissetto, *Introduction to the Monte Carlo Method*, Lecture given at the 2^{nd} National Seminar of Theoretical Physics, Parma (1992).

[147] U.-J. Wiese, *The status of D-theory*, PoS **LAT2005** 281 (2005) [hep-lat/0510042]; U.-J. Wiese, *D-theory: A quest for nature's regularization*, Nucl. Phys. Proc. Suppl. **153** 336 (2006).

[148] P. A. M. Dirac, *The Inadequacies Of Quantum Field Theory*, printed in "Paul Adrien Maurice Dirac: Reminiscences about a great Physicist", eds. B. N. Kursunoglu and E. P. Wigner, Cambridge University Press (1987).

[149] B. Lucini and M. Teper, *Confining strings in $SU(N)$ gauge theories*, Phys. Rev. **D64** 105019 (2001) [hep-lat/0107007].

Curriculum Vitæ

Personal Data

Name	Riederer, Stéphane Jean
Date of birth	April 27, 1978
Place of birth	Lausanne, Switzerland
Nationalities	Swiss, Canadian
Marital status	Single
Present address	Institute for Theoretical Physics Bern University Sidlerstrasse 5 CH-3012 Bern E-mail: `riederer@itp.unibe.ch`

Schools

1987-1994	Schools in Lausanne
1994-1997	Gymnasium in Lausanne
1997	Matura Typus C (University entrance exam)

University

1997-2002	Lausanne University, Studies in Physics
2002	Lausanne University, M.Sc. in Theoretical Physics *Fluctuations vectorielles d'une corde abélienne en six dimensions* (supervised by Dr. M. Giovannini)
2003-2006	Bern University, Ph.D. in Theoretical Physics *D-theory Formulation of Quantum Field Theories and Application to $CP(N-1)$ Models* (supervised by Prof. Dr. U.-J. Wiese)

Other Activities

2005	XXIII International Symposium on Lattice Field Theory, Dublin, Ireland